UNIVERSITY OF GHANA

MODELING OF KUNSU ORE BODY IN THE KUMASI BASIN NORTHWEST OF KUMASI, GHANA

By

ABDUL-AZIZ ABDUL-RASHID

(10506994)

THIS THESIS IS SUBMITTED TO THE UNIVERSITY OF GHANA, LEGON IN PARTIAL FULFILLMENT OF THE REQUIREMENT FOR THE AWARD OF MASTER OF PHILOSOPHY GEOLOGY DEGREE

JULY 2018

DECLARATION

This is to certify that this thesis is the result of research carried out by Abdul-Aziz Abdul-Rashid towards the award of Master of Philosophy Degree in Geology from the Department of Earth Science, University of Ghana, under the supervision of Prof. Johnson Manu and Prof. Sandow M. Yidana.

....

Abdul-Aziz Abdul-Rashid Date

(Student)

....

Prof. Johnson Manu Date

(Principal Supervisor)

....

Prof. Sandow M. Yidana Date

(Co-Supervisor)

ABSTRACT

Available data consisting of geochemical assay dataset soil, trenches and drill holes assays from previous exploration works was used to model and determine the orientation of the gold prospect at Kunsu. The main aim of this study was to use available data from previous exploration works on Kunsu property to model and determine the orientation of the gold deposit and also compare previous trench assay results with re-trenching assays. To accomplish the aims of this study, the preferred fast and reliable Interpolation Kriging techniques related to Leapfrog Geo and Arcmap softwares in the mining and exploration industries were used to generate two and three-dimensional geological models of Kunsu gold prospect. Interpolation kriging technique aided a better understanding of the dataset used to model Kunsu gold prospect and its attributes in a form of model images and maps (prediction). Interpretation of the model shows that Kunsu ore body trends in line with the regional geological structural direction of Ghana, which is northeast-southwest along strike. Re-trenching assay values also did confirm previous trench assay results and did indicate extension of gold mineralization across strike. The study area has delineated promising areas for further exploration works that could enhance the mine potential of the concession.

DEDICATION

This work is dedicated to Almighty Allah. Secondly to my late parents, Mr. Abdul-Aziz and Madam Talahatu Yahaya. To my sweetheart, Raihanat Abdul-Kareem, my daughter, Rashida Kadara Abdul-Rashid, my entire family, friends, love ones and my enemies as well. Not forgetting the two most special people in my life in the persons of Mr. Alhaji Yakubu Iddrisu and Nana Frimponmaa II.

TABLE OF CONTENTS

TABLE OF FIGURES

LIST OF TABLES

LIST OF APPENDICES

ACKNOWLEDGMENTS

First and foremost, my profound gratitude goes to Almighty God for bring me this far and also for the bounty strength he bestowed on me making this research a successful one. My second thank goes to the Chief Consultant of Geoman Consult Ltd in the person of Alhaji Yakubu Iddrisu, who is a father to me and has being of great help in this work. I would also like to sincerely thank my supervisor, Prof. J. Manu for his motivation, encouragement, criticism, contributions, support, and fatherly love that he showed to me throughout the period of this work. I am really grateful. I am highly honoured to have Prof. Sandow M. Yidana as my co-supervisor and for taking part of his precious time and his readiness to listen to me any time I approached him. This work would not have been possible without the supports and financial assistance from Dr. Charles D. Jebuni (Director of Wononou Investment Limited). I am also grateful to Prof. P.M. Nude and the entire staff and master's students (Department of Earth Science) for their support and contribution for making this work a success. I cannot end without acknowledging the Senior Consultant, Mr. J. Asare and Mr. Mohammed Amin all of Minright Consult Limited. Last but not the least my appreciation goes to my family most especially to my late parents and to all my love ones not forgetting Nana Frimponmaa II, Founder and Chief Executive Officer of Caring Kids International). God bless you all.

CHAPTER ONE

INTRODUCTION

1.1 BACKGROUND

Ore deposits are formed as a result of crustal evolution within the earth. Hence, it is important to understand the geological settings prior to modeling of mineral prospects deposits. Three-dimensional modeling has gained recognition since 1970's, when geologists and mine engineers began to build three-dimensional (3D) geological models of ore bodies in order to visualize and interpret deposits (Zhu et al., 2011). Two and three-dimensional models are very important in mineral exploration development and also for mine designs. The models aid in designing mining pits, quantify mineral deposits and the selection of the mining methods for the extraction of ores (Jon, 2011). Currently, modeling is widely applied in mineral exploration and mining industries for better understanding of mineral deposits. Gold is used in manufacturing industry for electrical appliances, jewelries, watches and automobile. For this reason, gold is in rising demand worldwide. Therefore, it is important to prospect for more economic gold deposits to meet this increasing demand worldwide.

In Ghana, the Birimian has been a focus of commercial gold exploration since the 1900's (Griffis et al., 2002). Many gold deposits have been discovered in the Birimian of Ghana. Mining companies such as Newmont Ghana Gold Limited, Tarkwa Goldfields Limited, Asanko Gold Inc. and many more are all located within the Birimian formation of Ghana. Activities of the mining and exploration companies provide job opportunities and rural development within their working communities.

In order to mine and extract gold, there is the need to explore, estimate and characterize the mineral deposit which is an important aspect in the exploration and mining industries. This enables the geologists and mining engineers to plan well. There are many scientific techniques used in modeling and estimating mineral deposits and these techniques are employed to ensure effective and reliable understanding of mineral deposits. These techniques are also applicable in various fields including environmental, hydrogeology, engineering, geotechnical and geophysical studies.

Geostatistics is generally used in the analysis and interpretation of data obtained by limited sampling of an ore body under study (Zhang et al., 2011). Geostatistical methods and techniques useful in ore body modeling include Simple Kriging, Co-kriging, Ordinary kriging, Universal Kriging, Indicator Kriging and Block Kriging. The choice of the techniques depends on the size of the data and intended purpose of the models. The most widely technique in the mineral exploration and mining industries for modeling, interpreting and quantifying spatial correlation is the Ordinary Kriging/Interpolation that uses mathematical formula to model mineral deposits (Lefohn et al., 2005).

Ordinary Kriging is selected for this study based on the characteristics of the dataset and desired spatial model to be estimated. Interpolation Kriging technique is a spatial estimation method where the error variance is minimal and it is based on the configuration of the data and on the variogram, hence is homoscedastic (Yamamoto, 2005). To model an object in 3D, it is proper to use geostatistical techniques that projects image in 3D format and this is achieved by implementing interpolation techniques. Interpolation techniques provide fast and reliable results for interpreting models of mineral deposits.

In recent times, exploration and mining companies have adopted geostatistical techniques to fast track interpretation of data at early stage exploration works. However, these techniques do not point out directly the total characteristics of mineral deposits but rather gives much information about the deposits and requires the technical knowledge and experience of the end user.

In Ghana, most local investors within the mineral exploration and mining industries do not apply these techniques but rather adopts the traditional methods in small and large-scale mining. This is as a result of lack of local expertise and cost involved in acquiring geostatistical-modeling software. Nonetheless, it is very important to apply these techniques for a comprehensive and thorough understanding of the deposits being explored and mined in the country.

Newmont Ghana Gold Limited conducted exploration works on Kunsu concession using several exploration methods and techniques such as soil geochemical surveys, drilling and Induced Polarization, resistivity and chargeability geophysical surveys to enable delineation of the Kunsu ore body. The exploration works yielded good intercepts from the trenches and drilled holes with assay results outlining mineralization zones at 8.7 metres grading 0.4 grams gold/ton and 60.5 metres grading 0.118 grams gold/ton from the trenches and with recorded drilled holes intercepts at 36 metres grading 4.0 grams gold/ton and 18 metres 8.4 grams gold/ton both in oxides and bedrock respectively (Newmont, 2013).

1.2 PROBLEM STATEMENT AND JUSTIFICATION

Newmont Ghana Gold Limited in a joint venture agreement with Wononou Investment Ltd. drilled on Kunsu concession based on good soil and trench geochemical anomalies and geophysical data of which out of 36 Reverse Circulation (RC), 7 Diamond Drill (DD) and 265 Aircore (AC) drilled holes resulted in good intercepts. However, the ore body could not be outlined or delineated even though some of the drilled holes gave intercepts at 36 metres grading 4.0 grams gold/ton, 18 metres grading 8.4 grams gold/ton, 8 metres grading 2.5 grams gold/ton and 10 metres grading 0.9 grams gold/ton. For these reasons, there is the need for careful study of the Kunsu ore body using geostatistical techniques on the trench and drill holes' dataset to model the ore body.

Furthermore, the trench dataset can also be helpful in defining drill hole targets which can be used to intercept any other in-situ ore bodies. Secondly, modeling using trench and drill holes' geochemical assay datasets could aid future exploration drill hole targets. Finally, combining trench, drill hole assays dataset and regolith map will help classify the regolith regimes of mineralized zones to ascertain zones of residual and transported areas.

1.3 AIM AND OBJECTIVES OF THE STUDY

This study seeks to use all available data gathered from previous exploration works of the study area (Kunsu property) to model the gold deposit so as to

- Generate 2D and 3D model of the ore body using soil and drilled hole's geochemical dataset.
- Determine the parameters of ore body (orientation of the ore body).
- Compare re-trenching assay results with the previous trench assay results.

- Suggest or recommend areas for further exploration to enhance the potentials of the project to development stage.

1.4 STUDY AREA

1.4.1 Location and Accessibility

The study area is within the Kumasi basin located between the prominent Sefwi gold belt on the western margin and the Ashanti gold belt on the eastern margin of the basin. The size of the area is approximately 137.06 sq.km. The location is bounded by latitudes 6°45'00" N and 6° 44'00" N and longitudes 2°00'00" W and 1°52'00" W. The area spans between two districts namely Atwima Mponua and Ahafo-Ano south districts, both in the Ashanti Region of Ghana. The study area (Kunsu property) in figure 1.1 is situated relative to some major gold deposits within the Birimian terrane of western Ghana and approximately 40 km north west of Kumasi township and 240 km northwest of Accra, the capital of Ghana. The area (Kunsu) can be access off the main Kumasi-Sunyani road onto a third class road at Mankraso along the Tepa road.

The study area (Kunsu property) in figure 1.1 is situated relative to some major gold deposits within the Birimian terrane of western Ghana.

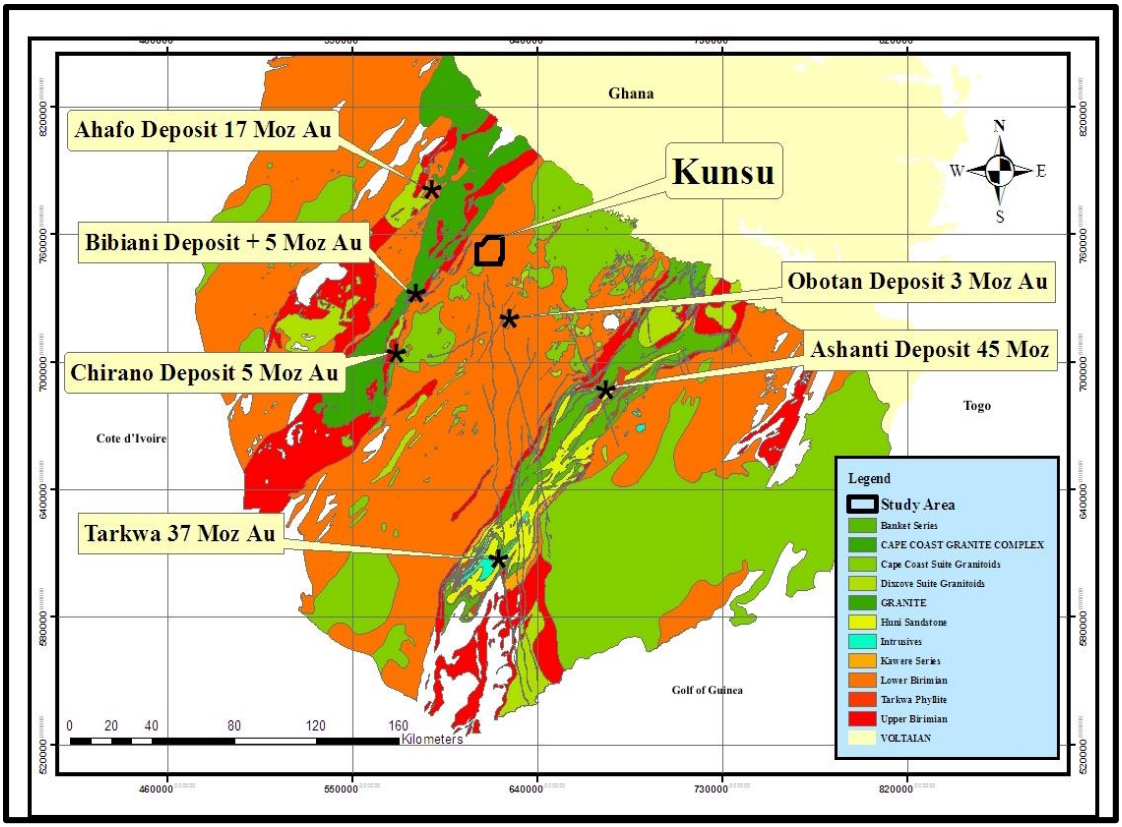

Figure 1.1 Location map of the study area (Kunsu) with respect to major gold occurrences within the Birimian of southern Ghana (Ghana Geological Survey).

1.4.2 Drainage, Vegetation and Climate

The area features a dismembered plateau with elevations in the range 225-300 m above sea level (ASL) and also a number of rounded and flat-topped hills that crest at elevations of 400-460 m above sea level (Griffis et al., 2002).

The area experiences two climatic seasons with the dry season extending from November to February followed by the rainy wet season from May to October with peaks in May to June and September to November with an average annual rainfall between 1500- 2000mm. The area is virtually within the Ofin River drainage basin (Miller et al., 2015).

Daily minimum and maximum temperatures are in the range of 20-35°C. The area features considerable primary forest, which is preserved in most parts as forest reserves. The economic activity in the area is centered on cash and food crop farming and on extensive commercial and industrial businesses in Kumasi (Griffis et al., 2002).

CHAPTER TWO

LITERATURE REVIEW

2.1 GEOCHEMICAL SURVEY

Geochemical sampling methods involve the collection and analyzing of various types of geological materials (such as soils, stream sediments and rocks). For decades these methods have been some of the most productive and successful methods used in mineral exploration discovery of mineral deposits across the world. For these reasons, many known ore bodies or mineral deposits would probably not have been discovered without geochemical sampling (Rose et al., 1979).

Even after discovery of mineral deposit, geochemical sampling still plays a key role in the delineation of mineralization. For example, geochemical sampling of soils is often employed to outline general distribution of mineralization at shallow depths where outcrops of bedrock are minimal or absent and it is also employed in the drill core sampling (NSM Mining, 2013).

Bulk Leach Extractable Gold also called **BLEG** is a geochemical sampling or analytical method used to explore for gold and other mineral deposits. The test is conducted using large quantity of sample (between 2 and 3 kg), which is digested or leached with cold sodium cyanide (NaCN) solution for one to several days. The gold is dissolved through formation of a cyanide complex, which is concentrated through the solvent exchange process into an organic solvent and subsequently analyzed for its content or concentration (Pride, 2014).

Gold values in BLEG are lower than total assays such as those of fire assays, as it analyzes only the fine grained gold fraction and largely ignores coarser and nugget gold (NSM Mining, 2013).

2.1.1 Soil geochemical analysis

Soil geochemical surveying is one aspect of exploration technology featuring several specialties. The main aim is to detect the presence of metals or mineral deposit in this case gold within the topsoil of the earth. Soil surveys are used extensively in geochemical prospecting and have resulted in the discovery of a number of ore bodies (Govett, 1983).

Generally, soil surveys are of a detailed nature and are run over a closely grid spaced. Soils are sampled at a particular horizon, analyzed for gold and values of the metal contents are plotted and contoured (Pride, 2014). Under favorable conditions, the highest values are centered over a deposit, but more generally the dispersion pattern is a train or a fan that require careful interpretation to locate its source. To ascertain high values, metal contents are centered over the mineral deposit as shown in figure 2.1 would require trenching technique.

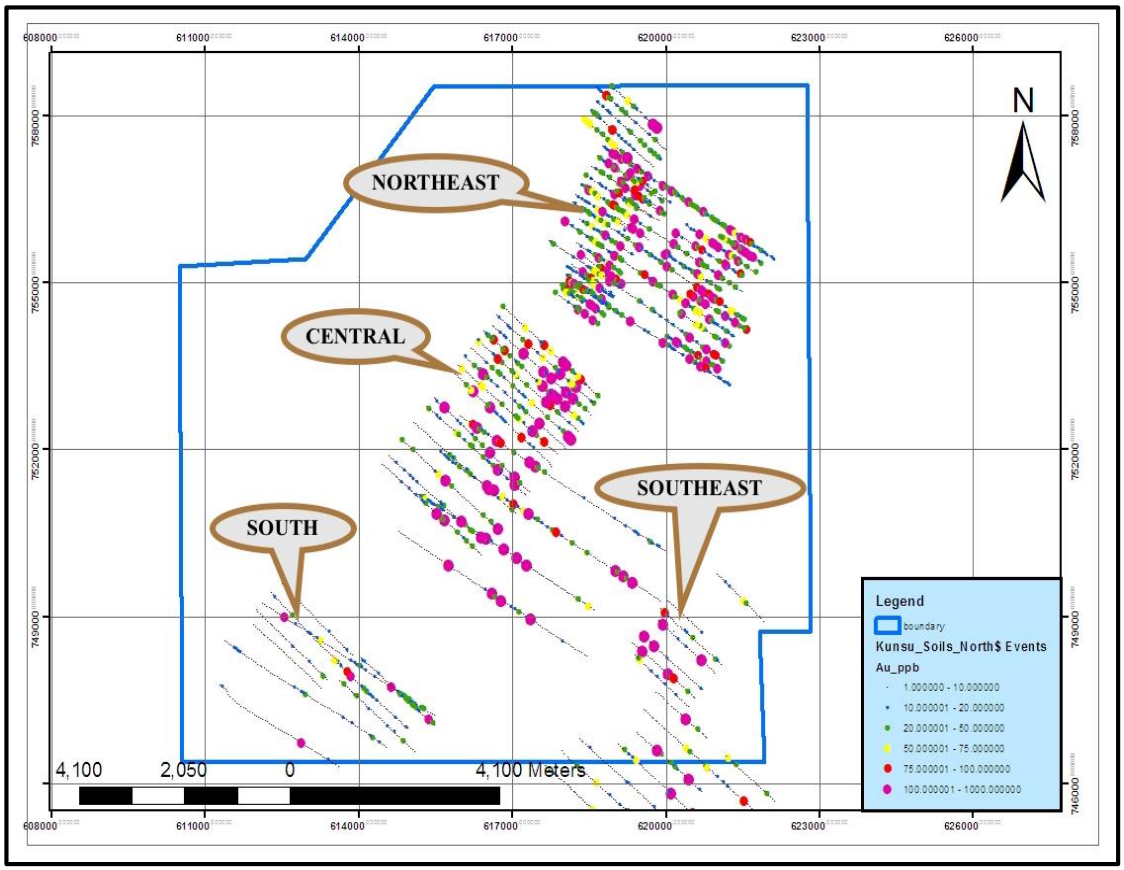

Figure 2.1 Soil geochemical results over the study area for gold (Newmont, 2013).

2.1.2 Trenching

Several ore types are weathered easily at the surface and these layers have to be removed in order to have good information on mineralogy and lithology. Preliminary trenching and pitting may be done with the objective of providing initial information to geologists in order to improve upon the initial parameters estimated for the trenching sampling program.

The main aim of trenching is to expose the earth surface to enable sampling from a more reliable depth (saprolite) to test for mineralization beyond the topsoil. Trenching provides vital information of the soil profile of the area being explored and aid in geological mapping of the soil profile and geological structures like foliation, joints and folds for a convincing choice of the azimuth and dip for drilling and for other related exploration and mining purposes.

2.2 REGOLITH MAPPING

Regolith is everything between fresh rock and fresh air and comprises the land surface of the earth and all planetary bodies with a solid surface. Regolith terrain mapping is the description of landscape that captures the landforms, materials of which it is made of and any secondary lithification. It is a useful tool for soil mapping, environmental geology, geomorphological mapping, regolith studies, planetary exploration, land systems mapping, groundwater studies, and mineral exploration (Taylor and Eggleton, 2001).

Regolith mapping is essential at all stages of exploration, as the rapid landscape changes during weathering, erosion, transportation, deposition and lateralization and they do have implications for geochemical gold exploration. The changes can enhance local redistribution of surface regolith materials that may cause surface geochemical expressions to be misleading thereby influencing decisions in mineral exploration activities. It can also cause mixed geochemical patterns of high, weak, subtle and discontinuous signals or anomalies. Therefore, to be able to interpret the regolith effectively of an area one must understand the regolith environment (Arhin, 2013).

In view of this, Newmont carried out a regolith mapping exercise to outline the regolith regimes covering the entire property except areas that were difficult to access. Areas of residual regime were matched with high-grade soil geochemical anomalies. Several SOFTWARE PRODUCTS are available for generating regolith maps but Arc GIS is used for the 2D model regolith map for this project.

High gold assays do not imply mineralization, likewise low gold assay does not mean dead zone, since the regolith of the terrain can hinder the dispersion pattern of an ore body. A clear case is the Subika gold deposit on the Sefwi gold belt in Ghana, which

was discovered with one-point soil anomalous trend. Figure 2.2 showing regolith map of Kunsu concession.

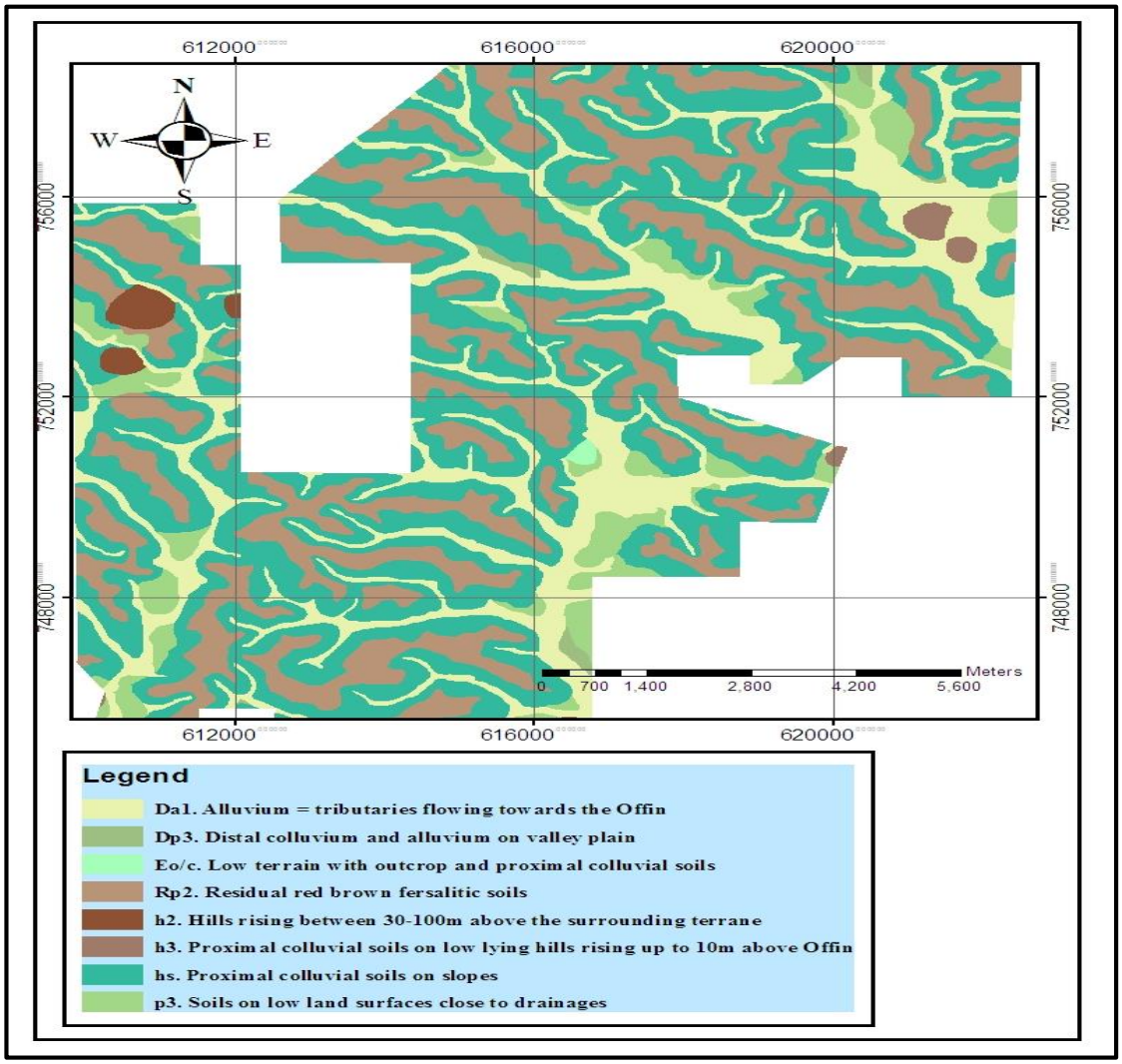

Figure 2.2: Regolith map of study area (Kunsu Concession) showing different soil regimes (Newmont, 2013)

High gold assays can be displaced through detrital dispersion and transported sediments can also mask potential mineralization (Arhin, 2013). It is therefore appropriate to accord equal weights of importance to anomalies that relate to mineralization zone of different regolith regimes. The regolith map is used in the interpretation of geochemical data for geochemical surface target generation.

2.3 GEOPHYSICAL SURVEY

Geophysical techniques are used extensively to locate hidden targets (geological structures) that are conductive and resistive in nature. Resistivity and Induced Polarization (IP) surveys are used extensively in mineral, geothermal, groundwater exploration, environmental investigations and also have other several applications in hydrocarbon exploration and secondary recovery (Sarma, 2014).

The ground resistivity is related to various geological parameters such as the mineral and fluid content, porosity and degree of water saturation in the rock. It adds meaningful understanding to results of other common exploration survey methods for easy interpretations of geochemical surveys. IP surveys may be done as follow-up to a controlled source of electric magnetotelluric (CSEM) survey (in which an induced, controlled source of electric energy is used to measure the magnetotelluric fields). Controlled source of electric magnetotelluric provides better resolution and deeper information than IP (Sarma, 2014). Thus, it is often used for reconnaissance studies of larger geographical areas to locate large structures such as faults, folds, contacts, joints, ore bodies and resistive anomalies often followed by selective IP investigation in order to prioritize drill targets.

The primary objectives of IP and resistivity surveys are to delineate discrete resistors and chargeable bodies potentially associated with gold mineralization as related to the style of mineralization within the area. These are achieved by measuring density, apparent resistivity and chargeability distribution. Clay minerals also show moderate IP effect, variations in subsurface moisture content, porosity, permeability, and soil or rock type which all affect resistivity measurements. Changes in imaged resistivity and chargeability can also be used to infer changes in geology.

2.4 EXPLORATORY DRILLING

The most expensive part of the exploration sequence is drilling. Drilling is done using drill Rig, which is designed in different forms specifically for a particular drilling techniques such as Aircore, Reverse circulation and Diamond drill (Reedman, 1979). Drilling techniques provides excellent information and accurate samples of mineral deposit, rock types, mineral type and geological structures than soils and trenches (Roger, 2010).

Each technique has its advantages and disadvantages, in terms of the depth to which it can drill, the type of sample returned, the costs involved and penetration rates achieved. There are two basic types of drilling, which are Diamond and Reverse circulation drilling. Diamond drilling is much slower than reverse circulation (RC) drilling due to the hardness of the ground being drilled (Roger, 2010). The purpose of drilling is to test for mineralization and confirm geological structures that are outlined from geophysical investigation within the oxides and bedrock.

2.5 EXPLORATION STATUS OF THE STUDY AREA

Between 2010 and 2013, Newmont Ghana Gold Limited through a joint venture agreement with Wononou Investment Limited conducted exploration works on Kunsu concession. Exploration methods such as soil geochemistry survey including trenching, geophysical survey and exploration drilling were conducted on Kunsu.

Bulk leach extractable gold **BLEG** program constituting 37 sample points were carried out to define potential prospect areas. Soil geochemistry sampling program of 3600 soil samples were collected as a follow up to the BLEG field work. Soil geochemical results defined a mineralization trend in the northeast-southwest direction. Approximately

2000 m length trenches spacing at 200 m and 400 m were conducted to test for mineralization beyond the topsoil (Newmont, 2013).

An initial Aircore drilling PROGRAM substituted for trenching of 260 holes covering a total of 5000 m in depth were completed with some intercepting mineralized zones. SUBSEQUENT DRILLING PROGRAMS comprising 38 reverse circulation (RC) and 7 diamond drill holes focused mainly on the northeastern corner of Kunsu were also completed. Field and laboratory Quality Assurance Quality Control (QAQC) measures to monitor accuracy, contamination, precision and accuracy were appropriately applied (Newmont, 2013).

2.6 GEOSTATISTICAL ANALYSIS

Geoscientists often face interpolation and estimation problems when analyzing sparse data from field observations. Geostatistics is an invaluable tool used to characterize spatial or temporal phenomena. Geostatistics which originated from the mining and petroleum industries can be successfully applied in solving cases or issues concerning expensive operations such as interpretations of sparse data in space in mineral exploration, grade control and mineral resource estimation (Garrett, 2001).

Presently, geostatistics is extended to many other fields of earth sciences, such as hydrogeology, hydrology, meteorology, oceanography, geochemistry, geography, soil sciences and forestry. Geostatistics provide descriptive tools such as semivariogram, mean, standard deviation, variance, skewness and kurtosis to characterize the spatial pattern of the data being used in the field of earth science (Howarth, 1984).

The key step in geostatistical data analysis is to verify three data features: dependency,

stationarity, and distribution. If data is independent, it makes little sense to analyze them geostatistically. If data is not stationary, they need to be made so, usually by data de-trending and data transformation. Geostatistics works best when input data is Gaussian. If not, data has to be made to be close to Gaussian distribution.

Geostatistical analyst provides exploratory data analysis tools to accomplish these tasks (dependency, stationarity, and distribution). With information on dependency, stationarity, and distribution it has paved the way to proceed to the modeling step of the geostatistical data analysis, kriging.

The most important step in kriging is modeling spatial dependency and semivariogram. Geostatistical analyst provides six kriging models, validation and cross-validation diagnostics for selecting the best model. Geostatistical analyst produces four output maps; prediction, prediction standard errors, probability, and quantile. Each output map produces a different view of the data. The best means of statistically grouping data is by graphical examination using histograms and box plots (Howarth, 1984).

An important contribution of geostatistics is the assessment of the uncertainty about un-sampled values, which usually takes the form of a map of the probability of exceeding critical values, such as regulatory thresholds in soil anomalies. This uncertainty assessment is combined with expert knowledge in decision-making for further exploration works such as trenching and drilling. Continued examination and quantitative vigor of the procedure provide a vehicle for integrating qualitative and quantitative understanding by allowing the data to speak for themselves (Rouhani et al.1996).

2.6.1 GEOSTATISTICS IN EXPLORATION AND MINING INDUSTRIES

In early exploration stages, exploratory spatial data analysis (ESDA) aids discovering potential outliers and outlining groups of correlated variables. Variography provides better understanding of the geometrical configuration of the mineralization which serves as a guide for designing optimal drilling patterns and Kriging in order to build model and estimate resource of mineral deposits.

Kriging has two distinct tasks; quantifying the spatial structure of the data and producing a prediction. Quantifying the spatial data structure, known as variography, is fitting a spatial-dependence model to the data. To make a prediction for an unknown value for a specific location, kriging uses the fitted model from variography, the spatial data configuration, and the values of the measured sample points around the prediction location (Yamamota, 2005).

Many methods are associated with geostatistics but they are all in the kriging family. Ordinary, simple, universal, probability, indicator, and disjunctive kriging along with the multivariate versions in Co-kriging is available in Geostatistical Analyst (Lefohn et al., 2005).

Kriging is a moderately quick interpolator that can be exact or smoothed depending on the measurement error model. It is very flexible and allows the user to investigate graphs of spatial autocorrelation. Kriging uses statistical models that allow a variety of map outputs. The flexibility of Kriging requires a lot of decision making. Kriging assumes data comes from a stationary stochastic process or collection of random variables that are ordered in space and/or time such as elevation measurements. Some methods, such as ordinary, simple, and universal kriging, assume normally distributed data.

Cokriging is the multivariate equivalent to kriging that uses multiple data sets and very flexible interpolation method, allowing the user to investigate graphs of cross-correlation and auto-correlation. Co-kriging also uses either semivariograms or covariances.

2.6.2. SEMIVARIOGRAM AND COVARIANCE

Semivariogram and covariance both measure the strength of statistical correlation as a function of distance. Semivariogram and covariance functions quantify the assumption that things nearby tend to be more similar than things that are farther apart. Semivariogram and covariance curves are used to predict empirical data and incorporate knowledge of the phenomenon in the model. To fit a model, directional autocorrelation of data is explored; the sill, range, and nugget are the important characteristics of the model.

If two locations, si and sj, are close to each other in terms of the distance measure of d(si, sj), they are expected to be similar, so the difference in their values, z(si) - z(sj), will be small. As si and sj get farther apart, they become less similar, so the difference in their values, z(si) - z(sj), will become larger. This can be seen in figure 2.3, which shows the anatomy of a typical semivariogram.

The semivariogram is defined as $\boldsymbol{\gamma(si,sj) = 1/2\ var(z(si) - z(sj)),}$ where **var** is the variance.

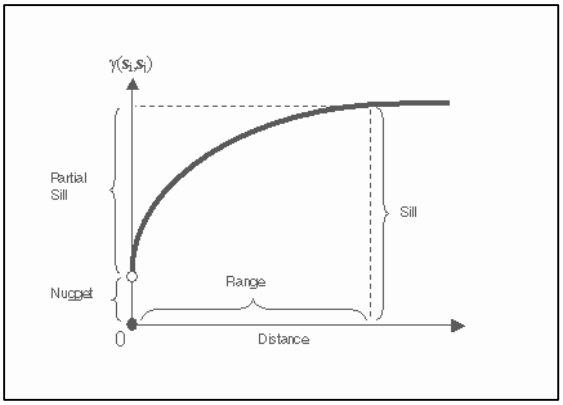

Figure 2.3: The anatomy of a typical semivariogram

The semivariogram can be thought of as a dissimilarity function, the fact is, variance of the difference increases with distance. The height semivariogram reaches when it levels off is called the sill. It is often composed of two parts, a discontinuity at the origin, called the nugget, and the partial sill. The sill is made up of the nugget plus partial sill. The nugget is simply the sum of measurement error and microscale variation and, since either component can be zero, the nugget can be composed wholly of one or the other. The distance at which the semivariogram levels off to the sill is called the range.

Covariance is a scaled version of correlation. Therefore, when two locations, si and sj, are close to each other, they are expected to be similar, and their covariance (correlation) will be large as si and sj get farther apart, they become less similar, and their covariance becomes zero. This can be seen in the figure 2.4. Covariance function decreases with distance, so it can be thought of as a similarity function. The covariance function is defined to be **c(si, sj) = cov(z(si), z(sj)),** where **cov** is the covariance.

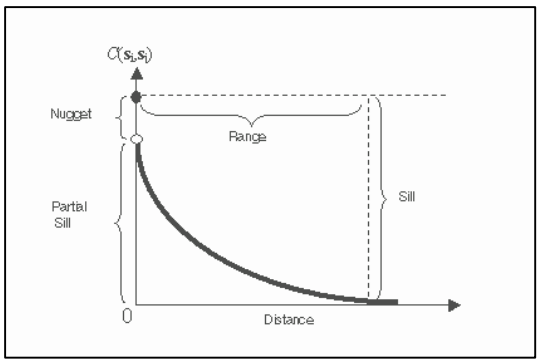

Figure 2.4: The anatomy of a typical covariance.

2.6.3 MODELING

The actual value of a mineral deposit is unknown until its attributes such as, size shape or geometry and other characteristics are determined. Ore body shape and size determination were problematic, complicated, time-consuming and prone to errors until the introduction of modeling software like Leapfrog, MineSight, Surpac and Vulcan. Technological advancement in software modelling has provided more reliable computational methods capable of developing models more accurate to true representation in relatively shorter timeframes. However, the basis for accurate modeling still remains dependent on the quality of the data and a good understanding and interpretation by the end user.

Spatial modeling which is building a mathematical model that fits with the spatial statistics variograms/covariances of one or several correlated variables is the second step of a geostatistical approach. Spatial model is based on the data itself, through the experimental curves, that also integrates additional knowledge on the variable such as geological features through the choices of the geoscientist when building the model. A model may be monovariate or multivariate, and may be composed of one or more nested spatial structures each of them with its own ranges and directions of anisotropy. It is therefore, a single mathematical function that describes either simple or complex spatial

structures.

Modeling deals with the interpretation of mineral deposit in 2D and 3D. Mineral deposit models are essential in exploration and mining industries and serve as a guide in exploration and mining activities. Models aid visualizing and understanding of mineral deposits to help geologists and engineers to plan towards subsequent exploration and mining activities. The same models are used for different purposes such as local or global estimation, simulations for uncertainty assessment and many more.

The initial stage of any modeling project is to produce a set of drill-hole sections from the drill-hole database for validation. Validation of dataset is usually automated, meaning the software does the validation as applied in Leapfrog Geo software. The geological models are constructed in blocks to enhance the resources estimation of the deposit and minimize dilution of the ore body. The shapes of the models are representation of the ore bodies and the volumes they occupy that can assist resource geologist in estimation of ore body (Osterholt1 et al., 2009). Typically, the shapes are given either by a three-dimensional enclosed solid or by a series of surfaces.

The shapes are generated by wireframing strings of points on section or plan using the drill holes' assays, or by triangulation of a series of points and strings into a digital terrain model, more commonly termed as surface. Surfaces may also be interpolated from the raw data by a number of surface-fitting techniques (Glacken and Snowden, 2001). Modern mining software has advanced to a level that major packages provides moderate to excellent tools for defining the three-dimensional shapes and for filling them with blocks (Glacken and Snowden, 2001).

According to Osterholt et al. (2009), a holistic view of geological uncertainty requires

capturing the uncertainty about the key factors controlling the grade-tonnage distribution of a prospective target which involves development of the geology and grade scenarios. To build 3D geological models representations of stationary domains requires volume and grade models to populate volumes with the relevant grade estimates. Leapfrog software provides significant advantages compared to most existing geological modeling software packages. Its innovative application of new interpolation and modeling techniques allows exploration and mine geologists to rapidly view, model and interpret lithology, alteration and assay data from drill holes. Leapfrog software models also highlight structural controls on the continuity of mineralization and can be used to improve near-mine, exploration drill targeting and domain construction for resource estimation.

At the Feasibility stage, models are used to evaluate the impact of selective mining unit (SMU) dimensions on the reserves. Geostatistical conditional Simulations may be used to assess the uncertainty associated with the reserves evaluation. The simulations provide a range of potential reserves for the ore body's tonnage, metal quantity and recovered grade. Estimation of local Confidence Intervals can be used for the Classification of resources into Measured, Indicated & Inferred categories.

In Production, Grade Control is improved by optimizing the pattern of production sampling. As the development goes on, selective mining unit or Stope grades are re-evaluated with the local production sampling information. Updated grade models are used for short-term, medium-term or even long-term mine planning to minimize the grade variability at the plant. Actual grades sampled at the plant are compared with the grades predicted in the resource model for a reconciliation exercise.

CHAPTER THREE

GEOLOGY

3.1 REGIONAL GEOLOGY

West Africa region features a wide variety of geological terranes with a complicated geological history (Griffis et al., 2002). In broad terms, the geographical region features a West African Craton (WAC) of older Precambrian rocks surrounded by younger Precambrian and Phanerozoic units. Man Shield referred to the southern part of the West African craton and Reguibat shield to the northern part of the craton. The oldest Precambrian rocks are Archean in age (>2500 Ma) and believed to be limited along the coastal region extending from western Côte d'Ivoire which stretches across Liberia, Sierra Leone and into southern Guinea as (Griffis et al., 2002) stated in gold deposits in Ghana.

Research indicates that the geology of the Archean core of the WAC has not yet been studied in detail and it appears the WAC is similar to major Archean shield areas in most parts of the world (Griffis et al., 2002). West African Craton consist of highly metamorphosed mafic to felsic gneisses and migmatites representing old basement and wedged into the basement rocks are narrow greenstone belts of less metamorphosed supracrustal rocks with extensive tholeiitic basalts and sequences of metasediments that include turbidites, conglomerates and extensive banded iron formation (Zitzmann et al., 1997).

The West African Craton has been duly identified as a zone of major crustal growth (Feybesse et al., 2006; Taylor et al., 1992). Within the greenstone belts of the WAC, there are some intermediate to felsic volcanic units and widespread late-stage intrusive complexes (mafic to granitic in composition).

There are two primitive thermotectonic events in the WAC, 2750-2900 Ma episode (Griffis et al., 2002) called the Liberian event metamorphosed all the supracrustal rocks including the surrounding basement. The other event took place earlier than the Liberian episode is known as Leonian event (greater than 3000 Ma) with evidence based on limited data but its extent is not well established as yet. (Griffis et al., 2002). The Archean cratonic area also hosts quite widespread diamond-bearing kimberlites of Mesozoic age. Alluvial diamonds from these intrusions have been mined quite extensively in Guinea and Sierra Leone.

The WAC also host Paleoproterozoic metasediments, metavolcanics and associated intrusive complexes and covers Ghana, Côte d'Ivoire, Burkina Faso, southern Mali, northern Guinea and the SW corner of Niger. The Birimian consist of rocks of Paleoproterozoic. The metasediments and metavolcanics are collectively refered to as the Birimian and were affected by a major 2.1 Ga tectono-thermal event known as the Eburnean (Taylor et al., 1992).

Inliers in parts of western Mali and eastern Senegal confirm that the Paleoproterozoic units probably underlie large areas in northern Burkina Faso and Mali where they are covered by un-metamorphosed Infra-cambrian Paleozoic sediments (Taylor et al., 1992). The Voltain Basin in northern and eastern Ghana is also believed to be underlain by the Birimian.

The Birimian generally trends northeast, parallel and evenly spaced by volcanic belts and intervening sedimentary basins. The metasediments consist of isoclinally folded, dacitic volcaniclastics, wackes and argillites (Leube et al., 1990) intruded by extensive, late-kinematic 'basin type' granitoid which vary from tonalite to peraluminous granite (Davis et al., 1994). In the West African region there are widespread occurrence of

mainly flat-lying neoproterozoic to Paleozoic sediments and the prominent mobile belts that correlate with the Pan-African (approximately 550 Ma) orogenic events.

The Neoproterozoic-Paleozoic sediments cover large areas of Mali, Mauritania, western Guinea, western Burkina Faso and eastern Ghana. The exposed units that form the stable basement of the region is marked by a well standing escarpments at the margins above the main Birimian metasediments, metavolcanics and Eburnean granitoids. These sediments are mainly flat lying except in localized areas where the Dahomeyide or the Togo tectonic belt has disrupted the Voltain units along the eastern margins of the Voltain Basin. In the northern Taoudeni Basin located between Mali and western Burkina Faso, the sediments are up to about 4000m thick (Wright et al., 1985), whereas in the deepest part of the Voltain Basin, they are estimated to be at least 5000m thick (Abouchami et al., 1990).

Several researchers suggest that the Voltain Basin has three major sedimentary sequences (Supergroups). The lowest sequence (approximately 1000 m thick) consists mainly of shallow marine clastics and minor stromatolitic carbonates deposited on fairly stable epi-continental margins of the West African cratonic block (Abouchami et al., 1990). These sediments probably span the period 1000-650 Ma (Wright et al., 1985). The sediments platform is unconformably overlain by a much thicker sequence (average 2500 m but up to about 4000 m) of deeper marine, immature clastics (greywackes), which include a distinctive sequence of glacial tillite, carbonates and finely banded cherts (silexite). In places, glacial scouring has cut down through the shallow platform sediments and left tillite sitting on basement units (Betrand-Sarfati et al., 1990).

The three distinctive supergroups interpreted by Abouchami et al., (1990) reflect an early stage of shallow marine sedimentation on a stable platform with a thickening of sediments to the east followed by the formation of a much thicker prism of deeper marine sediments also thickening towards the east and correlating with the opening of a Pan-African ocean. The Pan-African ocean closed by convergence of major crustal of the molasse sediments, which are represented by the uppermost super-group in the Voltain Basin (Abouchami et al., 1990).

3.1.1 Metavolcanic belt

The metavolcanic belt in the Birimian terrene of western Ghana consist of five main NE–SW trending volcanic belts namely, Kibi-Winneba, Ashanti, Sefwi, Bui and Bole-Navrongo belts. The only N-S trending belt is the Lawra belt in the northwestern corner of Ghana. The evenly spaced Birimian volcanic belts, whose widths are between 15 and 40 km are separated by sedimentary basins which span 60-90 km. The Birimian volcanic belts consist predominantly of metamorphosed tholeiitic lavas (basaltic flows, dolerites and gabbros) with minor volcaniclastics and calc-alkaline rocks such as andesites, dacites and rhyolites (John et al., 1999). The Birimian metalavas is composed largely of basaltic compositions with proportions of lavas to pyroclastics varying from one belt to the other. The Ashanti belt records the largest pyroclastics-lava ratio whilst the Sefwi belt records the least (Taylor et al., 1992).

3.1.2 Metasedimentary rocks

The metasedimentary rocks of the Birimian in Ghana is known as Lower Birimian and the sub-parallel NE- SW trending volcanic belts are referred to as the Upper Birimian (Griffis et al., 2002). The sediments of the Lower Birimian outcrop basically within the five main basins namely, Cape-Coast, Kumasi, Sunyani, Suhum and the Maluwe Basins. The sediments are composed of volcano-clastic rocks, turbidity related greywackes, argillitic rocks and chemical sediments. According to Aseidu et al. (2009), metagraywackes south of Kononго area are derived from mafic rocks and andesitic rocks of the volcanic belts.

In Ghana, the traditional view has been that the dominantly metasedimentary sequences (Lower Birimian) which are overlain by the more volcanic-rich sequences (Upper Birimian). Others authors in the Francophone countries like Côte d'Ivoire also suggest the opposite age relationship between the Lower Birimian and the Upper Birimian (Roddaz et al., 2007).

The metasedimentary rocks have also been intruded by 'basin-type' granitoids. The Birimian rocks in the basins generally exhibit up to greenschist facies regional metamorphism (Griffis et al., 2002). The metasedimentary succession can be divided into four main groups as volcaniclastic rocks, turbidite-related wackes, argillitic rocks and chemical sediments (Leube et al., 1990).

3.1.3 Granitoids

The Birimian sedimentary basins and volcanic belts are intruded largely by intrusive rocks. The two main types of intrusive rocks recognized in the Birimian terrane of Ghana are the 'Cape Coast' and 'Dixcove' types. The massive K-rich 'Cape Coast' type batholiths are dominantly intermediate intrusives with biotite being the most common mafic mineral; typically, they display foliation (often gneissic) and are concentrated in areas where Birimian metasediments are widespread (Lower Birimian) (Griffis et al., 2002).

The 'Dixcove' type occurs mainly within the confines of the volcanic belts (the Upper Birimian) and are also generally of an intermediate composition although more mafic and felsic phases are not uncommon and hornblende is usually the dominant mafic mineral. The intrusive occur in quite small plutons to very large batholiths but not as extensive as the 'Cape Coast' complexes.

Wright et al., (1985) described the 'Cape Coast' complex granitoids as large concordant syntectonic batholithic granite compared to the typically unfoliated and largely undeformed 'Dixcove type. The belt type granitoids are about 60–90 m.y. older than the "Cape Coast" type (Hirdes et al., 1992).

3.1.4 Tarkwaian sediments

The Tarkwaian Group consists of a distinctive sequence of metasediments occurring within a broad band along the interior of the Ashanti and the Bui Belts representing erosional products of the Birimian referred as molasses sediments. The Tarkwaian Group consists of a variety of sandstones, conglomerates and argillites (phyllites). In Tarkwa district, the sequence is in the order of 2500m thick whereas in the Bui belt

comparable the units are about 9000m thick. The units host economic paleoplacer gold deposits in quartz-pebble conglomerates.

The Tarkwaian sediments have been deposited in long narrow intramontane grabens, which formed as the result of rifting, preferentially, in the central portions of the five Birimian volcanic belts (Leube et al., 1990) with the exception of the Sefwi belt where the Tarkwaian is at the eastern margin. There is no evidence that the individual Tarkwaian depositories are ever linked. There is controversy on the relationships between the Tarkwaian and the underlying Birimian units in that many of the early workers in the region believed the contact to be an angular unconformity. The degree of metamorphism of the Tarkwaian is believed to be considerably less than that of the Birimian and the styles and timing of folding and faulting between the Tarkwaian and the Birimian are quite distinct.

Birimian Supergroup and the Tarkwaian Group were deformed jointly in a single progressive deformation event involving compression along a NE–SW directed axis. (Hirdes et al., 1992) also suggested that the Birimian and the Tarkwaian in Ghana were all affected by the Eburnean deformation.

3.2 GEOLOGY OF STUDY AREA

Kunsu is underlain by micro folded argillites, wacke, phyllite and volcaniclastic rocks of the Kumasi Basin sediments. The entire rock assemblage is believed to be gold bearing and has been metamorphosed to lower greenschist facies (Griffis et al., 2002). The Eburnean orogeny is believed to have affected the area causing deformation of the underlying rocks (Hirdes et al., 1992). Minor exposures of north-south trending post-Birimian dolerite dykes occur at the western portion of the area. The dykes are less than 10% of the underlying rock types in the Kunsu concession. Mineralization takes the form of parallel closely spaced auriferous quartz veinlets or stockworks style of mineralization (Davis et al., 1994).

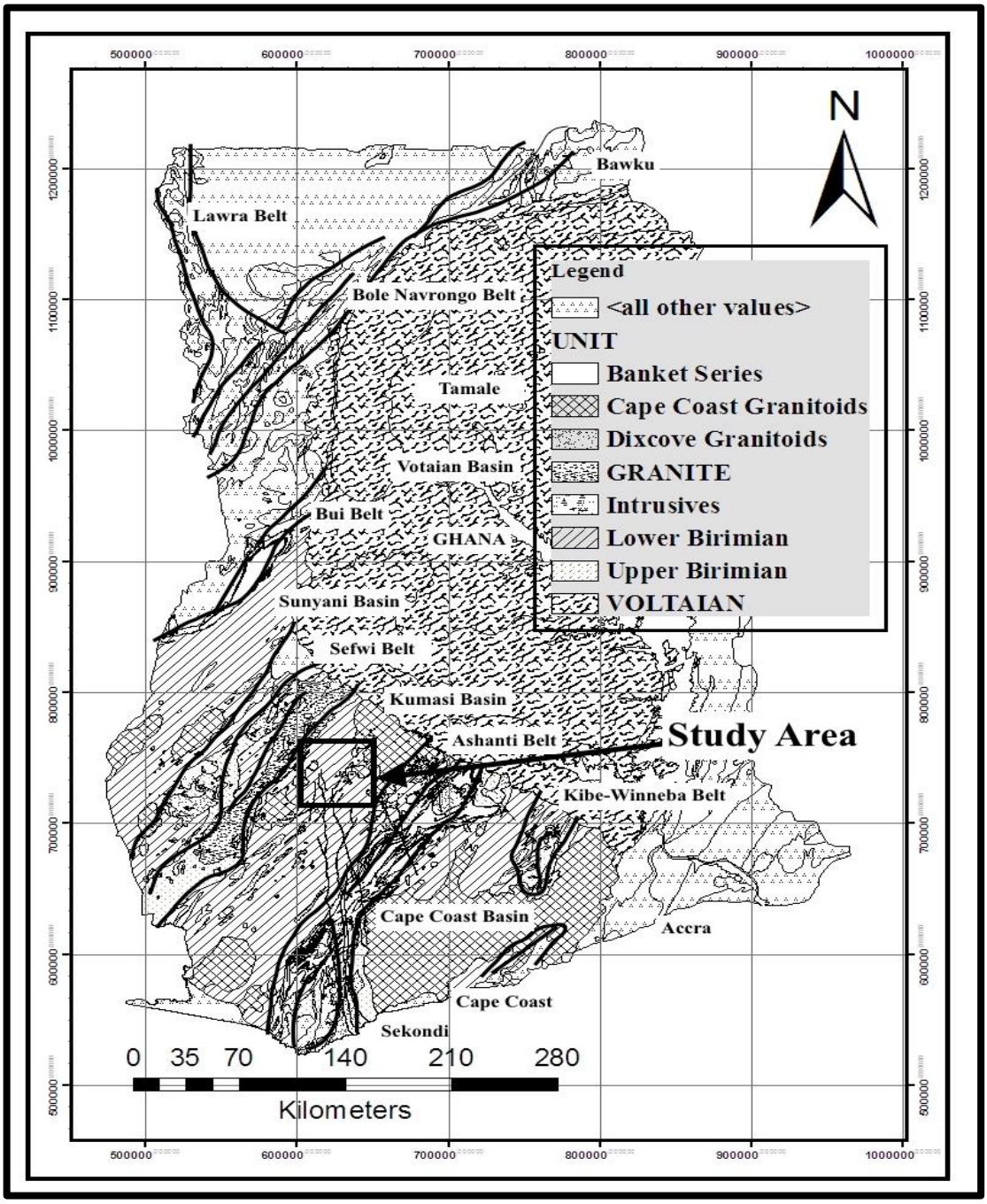

Figure 3.1: Simplified Geological map of Ghana (Agyei et al., 2009).

3.4 Gold Mineralization of Kumasi Basin

Gold deposits in this area are hosted by shear zones of the Birimian metavolcanic and metasedimentary rocks and granitoids of the Eburnean Plutonic Suite (Allibone et al., 2004); Perrouty et al., 2012). The shear zones have undergone ductile deformation (Leube et al., 1990) and host gold mineralization in the form of high grade quartz veins or stock works in fractured rock associated with brittle deformation and low grade disseminated sulphide mineralization comprising arsenopyrite and/or pyrite (Allibone et al., 2002).

The structural and geodynamic evolution of the Kumasi Basin during the Eburnean orogeny had a significant control over gold mineralization (Eisenlohr and Hirdes, 1991). Minor gold mineralization events are coincident with ductile deformation during the deformation 2 (D2) and the gold depositions were controlled and localized along NE–SW strikes and shear zones which experienced dextral dip-slip at that time marked by the development of graphitic mylonite. A later event that coincided with brittle and ductile deformation occurred during deformation four (D4) and deformation five (D5) and produced auriferous quartz veins and stock work in Birimian metasedimentary and metavolcanic rocks and Eburnean granitoids.

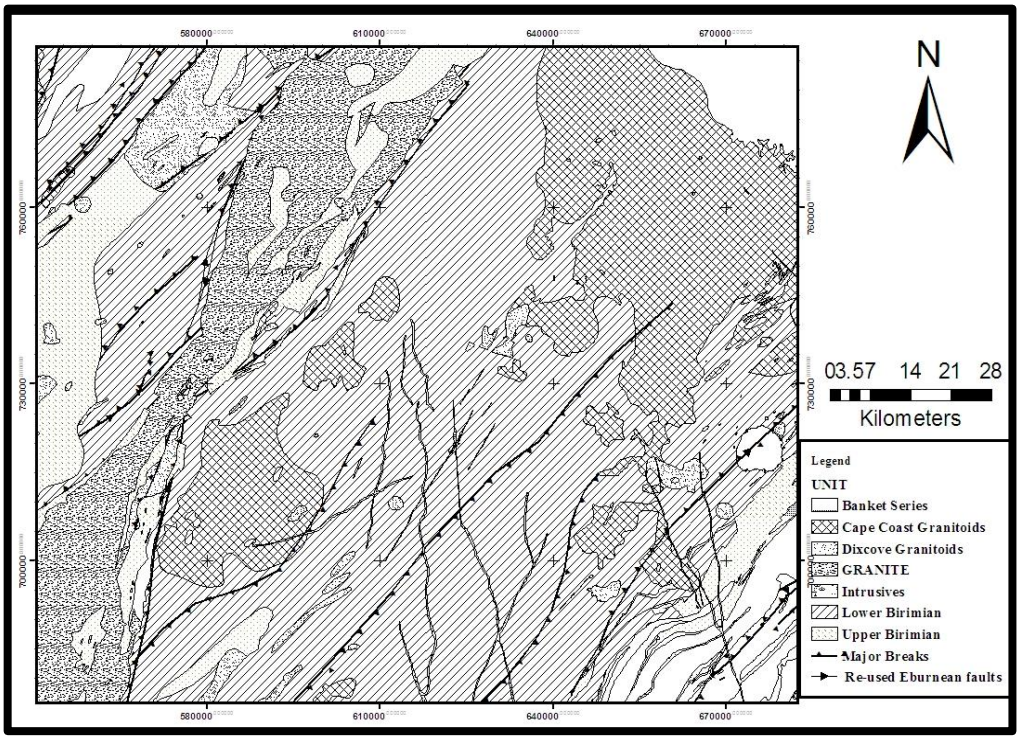

Figure 3.2: Modified Geological map of study area (Agyei et al., 2009).

Figure 3.3: Core sample of mineralized zone of drilled hole on the study area (Kunsu property); an example of stock works style of gold mineralization.

CHAPTER FOUR

METHODOLOGY

The methodology consists of three major subdivisions of work performed to achieve goals of this study, which are pre-field work, fieldwork and post-field work.

4.1 PRE-FIELD WORK

A desk study and literature review was carried out to have a knowledge of previous works performed in the study area and also have a fair idea of works conducted by other researchers. Thus, the necessary literature linked with the study area were assembled and assessed from books, scientific journals and companies who have worked on the property, surrounding areas and the Kumasi basin and the electronic data base. Acquisition of base maps and organizing field logistics were done at this stage. Secondary data from Streams sediment, soil, trenching, Aircore drilling, Reserve circulation drilling, Diamond drilling sampling and Geophysical survey were acquired from Wononou Investment Limited through Geological Management Consultancy (Geoman Consult).

4.2 FIELD WORK

The field stage entailed retrenching of the previous trenches, which had mineralized zones. The trenches were re-excavated at a length of 5 m x 1 m width x 3 m depths at a bearing of 315 degrees, as shown in figure 4.1.

Figure 4.1: Trench location on the property.

Sampling was done at an interval of 1 m from the western direction to the east at the base edge of the eastern wall of the trenches and areas of much interest duplicated for Quality Assurance Quality Control (QAQC) purposes. A total of 47 samples were taken and were sent to the ALS lab in Kumasi for gold analysis using normal fire assay method. The weights of the samples range between 2 kg to 3 kg. The walls of the trenches were mapped. The purpose of this activity was to review the previous trench works done by Newmont and to validate the trench data for this project as a Quality Control measure.

4.2.1 Trench sampling procedure

The following steps were followed during the trench sampling:

1. Trench digging was completed reaching 3 m depth where it is expected to reach the saprolitic material of the bedrock and 1m separation between each block to prevent

collapsing of the trench walls were also introduced.

2. The top edge surfaces of the trenches were cleared to avoid contamination of the samples during sampling.

3. The base edge corners of the trenches were pegged at 1 m intervals per sample point.

4. A reverse circulation sample bag was placed on the floor of the trench where the samples were taken with a geological hammer chipping off the base edge corner of the eastern wall of the trench.

5. The samples were then poured into a sample bag with the sample ID written on it as shown in figure 4.2 (A).

6. The surface of the RC sample bag was always cleaned with a duster after every sample taken to avoid contamination as illustrated in figure 4.2 (B) and step 4 was then repeated for the next sample to be taken.

7. The sample were bagged and sent to the ALS lab in Kumasi for analysis.

Figure 4.2: Sample with sample ID (A) and cleaning of RC sample bag (B)

4.3. POST-FIELD WORK

Assay results were reported in parts per million (ppm). To produce a representative and meaningful test a sample (regularly about 100 - 150 g) from a large bulk sample was taken. The grain size of the prepared sample must be so fine that the element of interest (or host mineral) can be properly liberated from the bulk matrix and distributed in the pulp to produce a homogeneous distribution to ensure sufficient representative for the following analytical methods. This is particularly important for low concentration ores such as gold where the number of mineral particles producing ore concentration is always low (Juha, 2008).

Different minerals behave differently during pulverization as most brittle minerals will easily break down to small particles while some (e.g. native gold) will just change their shape if proper sample preparation methods are not used. It is commonly accepted that poor sample preparation is next to poor sampling, which is the largest source of bias in an exploration or resource evaluation project. Sample preparation methods should therefore be selected carefully as it is for the actual analytical methods.

4.3.1 Sample preparation at the laboratory

Guidelines to sample preparation at the laboratory followed the sequence outlined below.

1. Sorting: the samples were arranged or sorted to ensure the numbering matched with the submission sheet to avoid lost samples.
2. Drying: All samples were made to dry in a drying oven at a temperature of 60^{o}C for an hour. A knife was used to test for the dryness of the samples by touching the dry samples with the knife. Samples did not stick to the knife confirming that the samples were well dried.

3. Crushing: The samples were subjected to one stage fine crushing using a Jaw Crusher (nominal particle size > 70 % < 2 mm).
4. Splitting: the crushed materials were split to two (e.g. 1 kg) splits (using rifle splitter) to reduce the sample size, one for storage and the other for pulverizing and for geochemical analysis.
5. Pulverizing: Pulverizing was done to further reduce the size of crushed samples to a finer size for higher recovery. Pulverizing always cause unavoidable contamination of wear metals at trace level from the grinding surfaces. This contamination varies depending on material of the bowl and hardness of the sample material.
6. To minimize cross contamination as a quality control, cleaning of pulverizing bowls between samples with barren quartzite was done. The Pulverizer and Jaw Crushers were frequently cleaned with compressed air and brushes between every sample. The pulverizing provided a homogenized test sample for representative subsampling directly from the bowl without any further sample handling.
7. The sample is then ready for geochemical analysis.

4.3.2 Analytical laboratory

4.3.2.1 Fire assay laboratory

1. The pulp samples were then weighed and 50 g of the pulp samples were then taken to determine the gold content.

2. Each weighed 50 g pulp samples of ore were mixed thoroughly with an appropriate amount of 200 g of flux in the crucibles.

3. The crucibles were then placed in the furnace and allowed to heat up to 1100°C for a period of sixty minutes. The crucibles were allowed to stay in the furnace until the 1100°C temperature is attained after sixty minutes if the 1100°C temperature

was not attained. The purpose was to reduce the samples to a lead buttons for the slags to settle at the top for easy separation of the slags from the lead buttons.

4. The crucibles were removed from the oven and allowed to cool to enable the removal of the lead buttons from the bottom of the mold.
5. The buttons were then pounded into a cube, breaking away the slags from buttons.
6. The buttons were kept in Cupel and placed in the cupellation furnace for up to 950°C for an hour or until when the cupel had absorbed all the lead then leaving the beads containing all of the gold, silver, and PGMs in the assay.
7. The bead containing the gold was carefully examined with a magnifying lens and was realized that the bead contains more silver and needed to be parted.
8. Each milligram (mg) weigh of the bead in weight represents 1 troy ounce of precious metals in each ton of the original ore, or: 1 mg = 1 oz/T.
9. The separation of the silver from gold was carried out at the wet laboratory and subsequently sent to the instrumentation section where the gold assay results were reported in parts per millions (ppm).

The post-field work also included the use of software for exploration methods, which includes: Arc GIS and Leapfrog Geo.

4.3.3 Data validation

An audit of the database was carried out to avoid the occurrence of unwarranted surprises or errors such as duplication of drill hole collars, erroneous entry of drill hole depth and assay values when conducting geostatistical estimation. This resulted in the careful selection of the data together with the primary acquired data from main fieldwork for this project. Errors detected were eliminated, this provided a satisfactory

basis for the use of the database in its original form to model Kunsu ore body.

Samples within the mineralized envelope were deemed 'ore' and those outside, 'waste'. Domains are defined as zones that are geologically and statistically homogenous (supported by variography and statistical analysis) (Duke and Hanna, 2001). The domains in the study were defined using grades in an iterative process of selecting mineralized intersections in each borehole using Leapfrog Geo. Mineralized domains were identified on the basis of logged samples and grade continuity (Schofield, 2011).

4.3.3.1 KEY STEPS IN EXAMINING DATA DISTRIBUTION

Histogram: Interpolation methods used to generate surfaces give the best results if the data is normally distributed (a bell-shaped curve). If data is skewed (lopsided), the data is transformed to make it normal. Thus, it is important to understand the distribution of data before creating a surface. The Histogram tool plots frequency histograms for the attributes in the dataset, enable to examine univariate (one-variable) distribution for each attribute in the dataset. To explore the distribution of the dataset the key steps below are followed.

1. Click the Geostatistical Analyst drop-down arrow, point to Explore Data, then click Histogram.
2. Click the Layer drop-down arrow and click on the data to explore.
3. Click the Attribute drop-down arrow and click Au ppm.

The distribution of the Au_ppb attribute is depicted by a histogram with the range of values separated into 10 classes. The frequency of data within each class is represented by the height of each bar.

Generally, the important features the distribution has are its central value, spread, and symmetry. As a quick check, if the mean and the median are approximately the same value, is evidence that the data may be normally distributed.

5. Click to close the dialog box.

Creating a 2D surface using Kriging in Arcmap

1. Click the Geostatistical Analyst drop-down arrow and click Geostatistical Wizard.

In the Geostatistical Wizard: Choose Input Data and Method dialog box appears.

2. Click the Input data drop-down arrow and click data to use.
3. Click the Attribute drop-down arrow and click the AU_PPB attribute.
4. Click Kriging in the Methods list box.
5. Click Next. By default, Ordinary Kriging and Prediction Map will be selected on the Geostatistical Method Selection dialog box.
6. Click Next. On the Geostatistical Method Selection dia- log box.

Note that, having selected the method to map the Au_ppb surface, you could click Finish to create a surface using the default parameters. However, steps 6 to 10 will expose to different dialog boxes. The semivariogram/covariance modeling dialog box allows you to examine spatial relationships between measured points. It assumed things that are close are more alike. The semivariogram allows you to explore this assumption.

7. Click next.

The crosshairs show a location that has no measured value. To predict a value at the crosshairs, you can use the values at the measured locations. The values of the closest measured locations are most like the value of the unmeasured location that is being predicted. Semivariogram/Covariance Modeling dialog box is used to predict a more

accurate value for the unmeasured locations.

8. Click Next.

The Cross Validation dialog box gives you an idea of how well the model predicts the values at the unknown locations.

9. Click Finish.

The Method SummarY DIALOG BOX SUMMARIZES INFORMAtion on the method (and its associated parameters) that will be used to create the output surface.

10. Click OK. The predicted Au_ppb map will appear as the top layer in the table of contents.
11. Click the layer in the table of contents to select it, and then click again to change the layer name.
12. Click Save on the Arcmap Standard toolbar.

4.3.4 Leapfrog

The use of Leapfrog Geo Software to build complex wireframe models for resource domaining is becoming widely accepted and common amongst many large exploration and mining companies worldwide. Leapfrog provides significant advantages compared to most existing geological modeling software packages. Its innovative application of new interpolation and modeling techniques allows exploration and mine geologists to rapidly view, model and interpret lithology, alteration and assay data from drill holes. Leapfrog models highlight structural controls on the continuity of mineralization and can be used to improve near-mine and exploration drill targeting.

4.3.4.1 Steps in modeling using Leapfrog Geo

1. **Launch Leapfrog Geo,** the main window appears with the projects tab displayed. Leapfrog Geo main window is divided into three parts as shown in figure 4.3

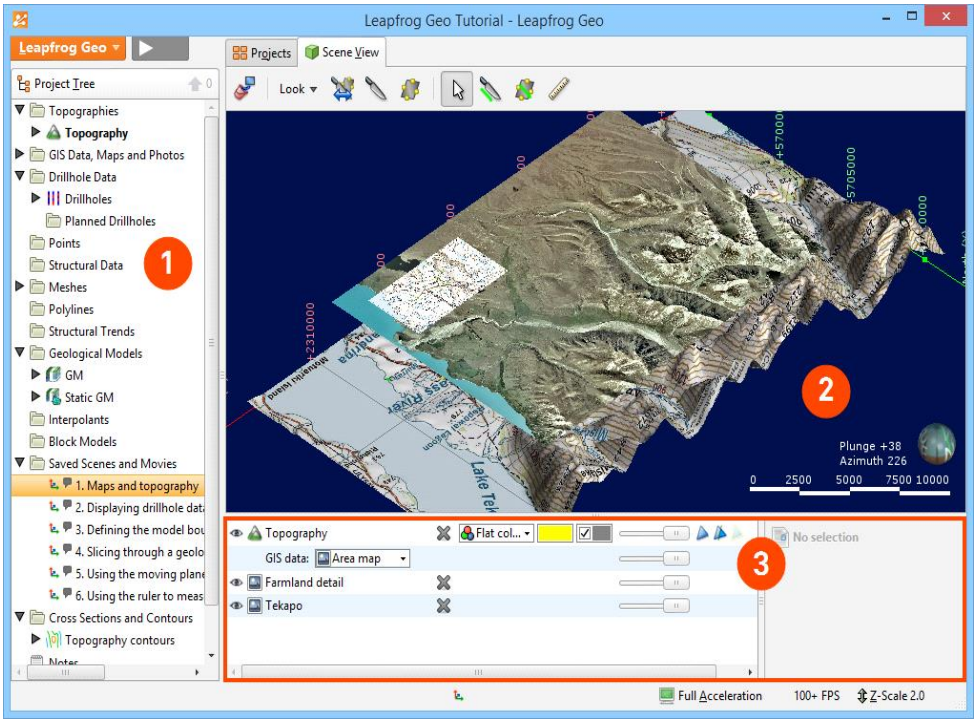

Figure 4.3: Three main window scenes of Leapfrog Geo (Aranz, 2014).

(1) The project tree contains all the data in the project and tools for working with that data.

(2) The scene view tab displays a 3d representation of selected

(3) Tools for changing the appearance of data in the scene window are available in the shape list and the shape properties panel.

4.3.4.2 Importing Drill HOLE Data

In Leapfrog Geo, drill hole data is managed using the drill hole data folder in the project tree. For this project the four data files, which are found in the drill HOLES' folder are Collar.csv, Survey.csv, Assay.csv and Geology.csv.

To start importing drill hole data:

1. Right-click on the drill hole data folder and select Import drill holes in the project tree and the Import drill hole data window is displayed.

2. For Collar, click on the Browse button to locate the file collar.csv

3. Click on the file, then click Open.

When a collar file is added to the Import drill hole data window, Leapfrog Geo looks for interval tables with names such as assay and lithology in the same location and will add them to the Interval tables list. If an interval table file is not automatically added to the list, click Add and browse for the required file.

4. Click on import to start the process of importing data.

First, the collar file is processed. Leapfrog Geo displays the data in the file and summarizes how each column will be imported. Leapfrog Geo expects four columns for the collar data and attempts to match imported data to these expected formats. For the collar file, Leapfrog Geo expects a drill hole identifier (Hole ID) and the location of the top of the drill hole, in X, Y and Z coordinates. The Hole ID is used to associate data in different tables with a single drill hole.

5. After Leapfrog Geo correctly mapped the data in the collar file to the expected format. Click Next to proceed to the next file (The survey file data is displayed). Leapfrog Geo expects four columns for the survey data, a Hole ID and deviation depth, azimuth and dip.

6. Click Next to proceed to the next file. (The interval table is displayed). The "lithology" column has been correctly mapped as lithology data, but the "veins" column has not been mapped.

7. In the Column Summary, click on the dropdown list for the "veins" column and select "Lithology". The Column Summary is updated to indicate that the "veins" column will

be imported as lithology data:

8. Click on Finish to complete the process. The data table is added to the PROJECT TREE AS PART OF A NEW Drill HOLES' object:

Leapfrog Geo automatically identifies and flags common drill hole data errors when drill hole data tables are imported. The three ways Leapfrog Geo marks tables that contain conflicts or errors are:

(a) Tables containing errors are marked with a red X ( ). These errors are fixed before the affected drill holes can be used for processing.

(b) Numeric data columns with non-numeric values are marked with a red X, which means that the rules that are used to handle non-numeric and negative values need to be reviewed.

(c) Tables containing warnings are marked with a yellow exclamation mark ( ). Affected drill holes can be used for further processing, but the information in the warning indicates that the data requires further attention. Until errors are corrected, the rows that contain those errors are excluded for all processing that uses the table, including viewing in the scene.

4.3.4.3 Creating Geological Model

1. Right-click on the Geological Models folder and select New Geological Model.

2. In the window that appears, change the following settings:

Set the Surface resolution to 50.

From the enclosed object dropdown, select the lithology table.

3. Click OK to create the geological model.

The new geological model is created in the Geological Models folder.

The **Boundary** object defines the limits of the geological model.

The **Lithology** object describes all the lithological units to be modeled in the geological model and the colors that are used to display them on the screen.

The **Surface** Chronology object describes the contact surfaces in the model, organized in chronological order, from youngest to oldest.

The **Output Volumes** folder contains all the volumes generated in building the geological model in chronological order, from youngest to oldest."

4. Clear the scene.

5. Display the geological model by dragging it into the scene or by right-clicking on it and selecting View Output Volumes.

At this point, the model is a single volume of lithology "Unknown". In order to divide this "Unknown" volume into volumes that represent known lithologies, the model's internal structure is defined. This involves:

1. Right-click on the Surface Chronology object and select New Deposit > From Base Lithology.

2. In the window that appears, select "Phyllite" from the Select primary lithology dropdown list.

3. Drag each of the vein lithologies to the Ignored lithologies list.

4. Click OK. The new contact surface will appear in the project tree under the Surface Chronology.

5. Add the new contact surface ( ) to the scene, together with the points ( ) and segments ( ) used to create it.

6. Display the legend ( ) for the segments.

The segments ( ) show how the lithologies in the drilled hole data have been handled in order to create the contact surfaces.

7. Double-click on the Surface Chronology and tick the box TO ENABLE THE CONTACT SURFACE.

8. Click OK.

9. Once the changes have been processed, drag the model ( ) into the scene to view.

CHAPTER FIVE

RESULTS AND DISCUSSION

5.1 GEOSTATISTICAL ANALYSIS

5.1.1 KUNSU VARIOGRAM ANALYSIS

A good model is a representation of quality data. The concept of garbage-in, garbage-out is very much applicable in the field of ore modeling and geostatistics. Model will always be a product of data used. The concept of variography or the modeling of the spatial relationships between samples is an important aspect in the kriging algorithm. It is therefore imperative to make sure that the data is

i. Well cleaned

ii. Well understood

iii. Well analyzed.

5.1.2 Exploratory Data Analysis (EDA)

The concept of EDA is to explore the sample data for possible spatial trend. Trends may be directional in which case it can expect an anisotropic variogram model. This may be achieved by initially plotting the data in a 2-dimension space for a quick check of the distribution and basically an idea of how the samples plot including the limits of the dataset.

Through the EDA, the nominal sample spacing is also known. This will enable us to correctly set lag distances for variogram calculation. This is because the lag spacing or the drill spacing will always have an effect on the quality of the variogram model.

Another important aspect of the EDA is the issue of outliers or extreme values. Although in most cases, only a small percentage of the overall data constitute extreme values, they can have a significant impact; it is therefore a good idea always to get rid of outliers before variogram calculations either by cutting back extreme values or entirely removing them from the dataset.

The Kunsu dataset has therefore been subjected through these processes before desirable variogram model was obtained. The unedited raw dataset consists of 1,957 samples in 3 dimensional spaces. The data for each drill hole consists of (x, y, z) coordinates and Au grade associated with each sample space. Figure 5.1 shows the basic statistics of the Kunsu dataset.

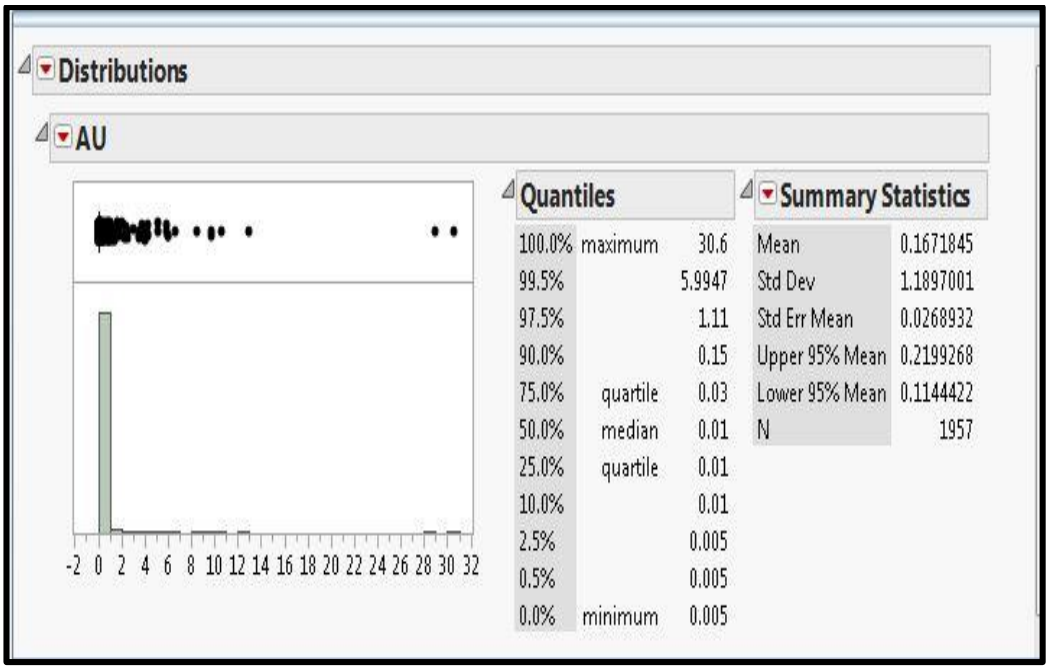

Figure 5.1: Basic statistics of the Kunsu raw dataset.

Figure 5.1 shows the number of samples, mean, median, the quartiles, maximum and minimum values. It can be deduced that, the coefficient of variation (cov) have the mean and the standard deviation. From the distribution, a cov value of 7.12 shows very high variability and obviously not much could be done with such a high cov. Again, such a high cov suggests that we have a very highly skewed distribution which is going to have a serious effect on calculating sample variograms. A mean value of 0.167 and a maximum value of 30.6 g/t presents a very high variability.

The figure 5.1 further shows that 97.5% → 1.11 g/t Au, which implies that only 2.5% of the samples have their grade ≥ 1.11 g/t Au; and these are outliers, although they constitute only 2.5% of the data, they create so much noise by skewing the dataset. If not dealt with appropriately, the final variograms will be a poor representation of the spatial continuity of the model.

For the Kunsu dataset, a cut back of the 2.5% extreme values have been applied and all such values have been brought to 1.11 g/t Au according to the statistical presentation. Another consideration taken with regards to the dataset for the variogram modeling was to deal with those below detection values. Values recorded as 0.005g/t (below detection values) were removed from the dataset. After the removal, the total number of samples came to 1,896 as shown in the histogram distribution in Figure 5.2.

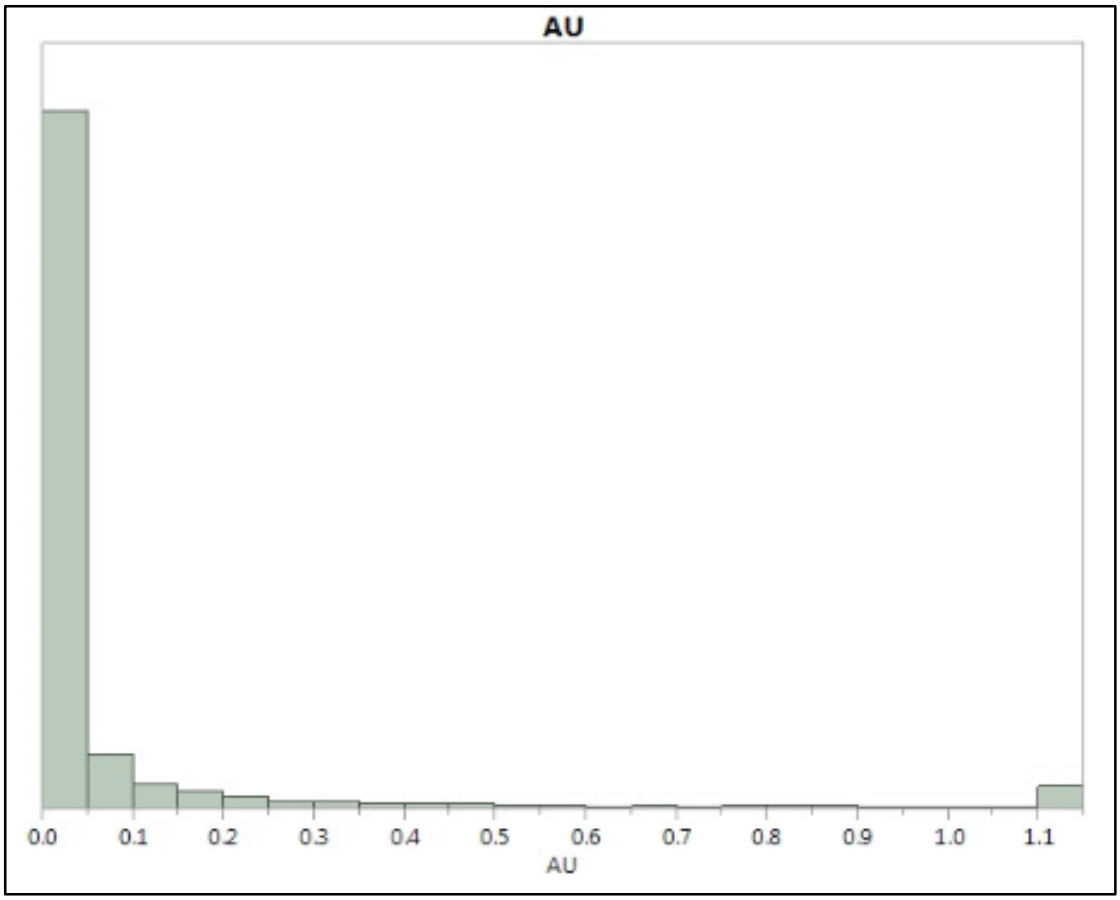

Figure 5.2: Data distribution after top cutting the extreme values from the dataset.

A 2 meter 3-dimension composite has been generated for the variogram analysis. In Figure 5.3a, and 5.3b, the presentation of the various drilling types has been plotted against the assay distribution. This highlights the skewed nature and the need for a top-cut of the outlier values to enhance the variography analysis of the Kunsu property.

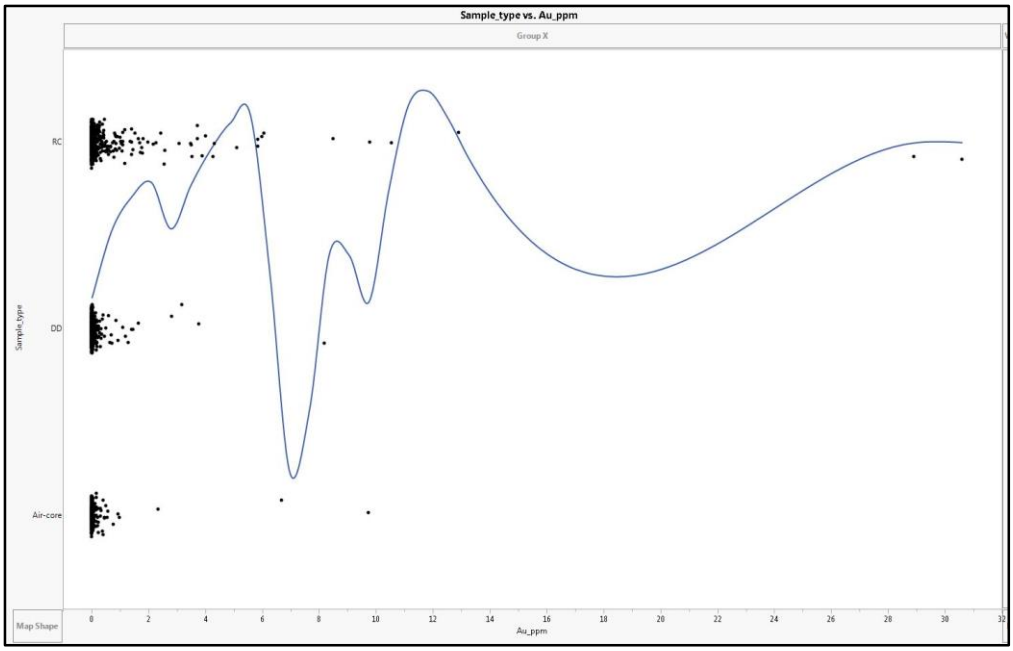

Figure 5.3a: Drill type and assay distribution 1.

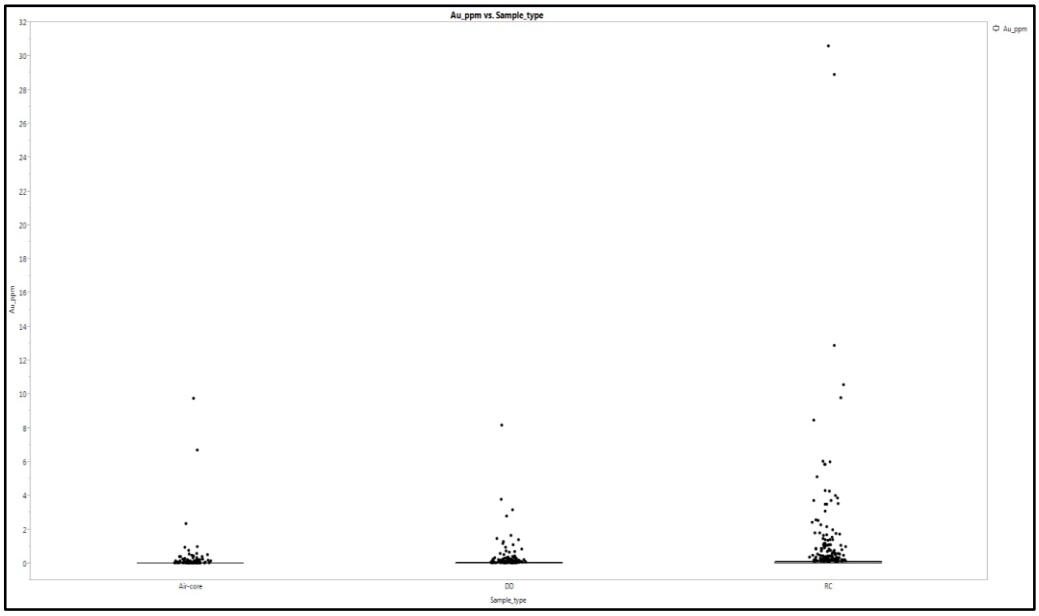

Figure 5.3b Drill type and assay distribution 2.

5.1.3 VARIOGRAPHY

There are a number of ways in securing the nugget effect of a deposit during such analysis. Firstly, one could borrow the nugget effect of established nearby mines. The need to analyze and secure nugget effect of the composite data was first done through modeling downhole variograms. This was achieved by going through a number of iterations using the composite length of 2 m and making the variogram look down the hole through the various drill holes in the dataset.

After a number of iterations, a nugget value of 0.44 was produced as being the level of variability between global composite pairs. Gold is usually erratic and at the exploration level where only few drill holes have been drilled, a nugget effect of 0.44 is rather impressive and could be better when drill spacing is closed in with time.

5.1.4 DIRECTIONAL VARIOGRAM MODELING

In all 37 directional sample variogram models have been produced around the clock along the directions (azimuths) and the angular tolerances (APPENDIX 1, 1XA). The dip, the lag and the lag tolerance are also given for each of the directional sample variograms. The summary statistics of each of the directional variograms are given in Table 5.1. The statistics in table 5:1 is used when considering the lag statistics of the various sample variograms. The lag statistics presentation in Table 5:2 shows the various statistics summaries of the data. Mean head tells the average of all the samples that were found at the head of the separation vector. Same applies to the mean tail, standard deviation head and standard deviation tail statistics.

So if pairing of data is representative of sample dataset, then the values at the individual azimuths and dips of the directional variograms (Table 5:2) must be pretty close to the

global averages (Table 5:1). These statistics are the reason why our sample variograms appear the way they are.

The model selected is presented in Figure 5:4. Prior to the modeling of the variograms the following mode modeling approach of the 3D orebody were adopted. The data was visualized in 3D space and outlier values were accordingly cutback to reflect a single geostatistical domain. Analysis of the high grades then commenced to spot possible trends. And this informed the structure position of a strike of $N45^{o}$ and a dip of 50^{o} W.

Global rough Ellipsoid parameters were defined in 3D space.

Downhole variograms were computed to calculate the nugget effect using the 2m composite samples. Directional sample variograms were computed and $N45^{o}$ was confirmed as the strike direction of the orebody with the dip varying between 50^{o} -55^{o}. The shortest range of the variogram is around 125, although this will greatly improve when more drilling is done. The variogram type used is the correlogram where the sill is fixed at 1.

The rest of the variogram and all the 37 directional variograms with their lag statistics and ellipsoids of the various direcTIONAL SLICES THROUGH THE MODEL are presented in the appendices.

SETUP

Variogram type = Correlogram,

No of Samples: 1,896

Horizontal Band Width ==> 250.00

Vertical Band Width ==> 250.00

Table 5.1: Summary Statistics of Directional Sample Variograms

GLOBAL SUMMARY STATISTICS:

Maximum → 1.100000

Minimum → 0.010000

Mean → **0.076458**

Variance → 0.042509

Std. Dev. → **0.206177**

Table 5.2: Lag Statistics of Directional Sample Variograms (Azimuth 45.0 deg dip)

SAMPLE VARIOGRAMS FOR AZIMUTH 45.0 and DIP = 0.0

LAG	NPAIRS	DIST	DRIFT	GCORR	MEAN HEAD	MEAN TAIL	STD. HEAD	STD. TAIL
1	708	41.8	-0.0162	0.85699	0.0654	0.0816	0.2062	0.2005
2	86060	254.2	0.0387	1.04337	0.1014	0.0627	0.2391	0.1897
3	52516	502.3	0.0358	1.02259	0.0549	0.0191	0.1494	0.0680

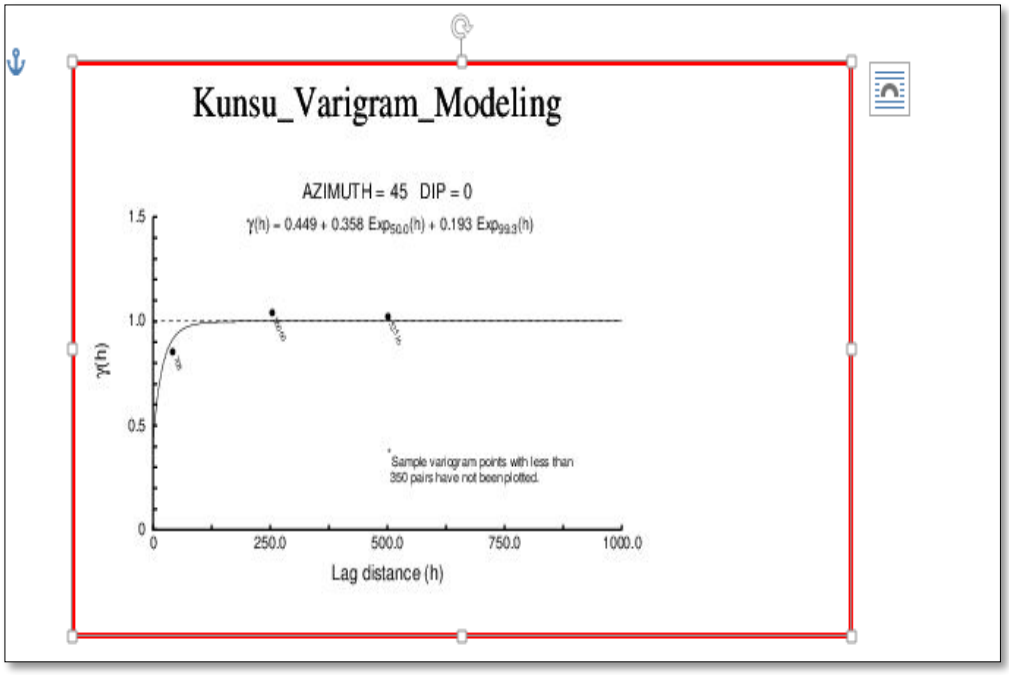

Figure 5.4: Preferred variogram model with consistent continuity and the shortest range.

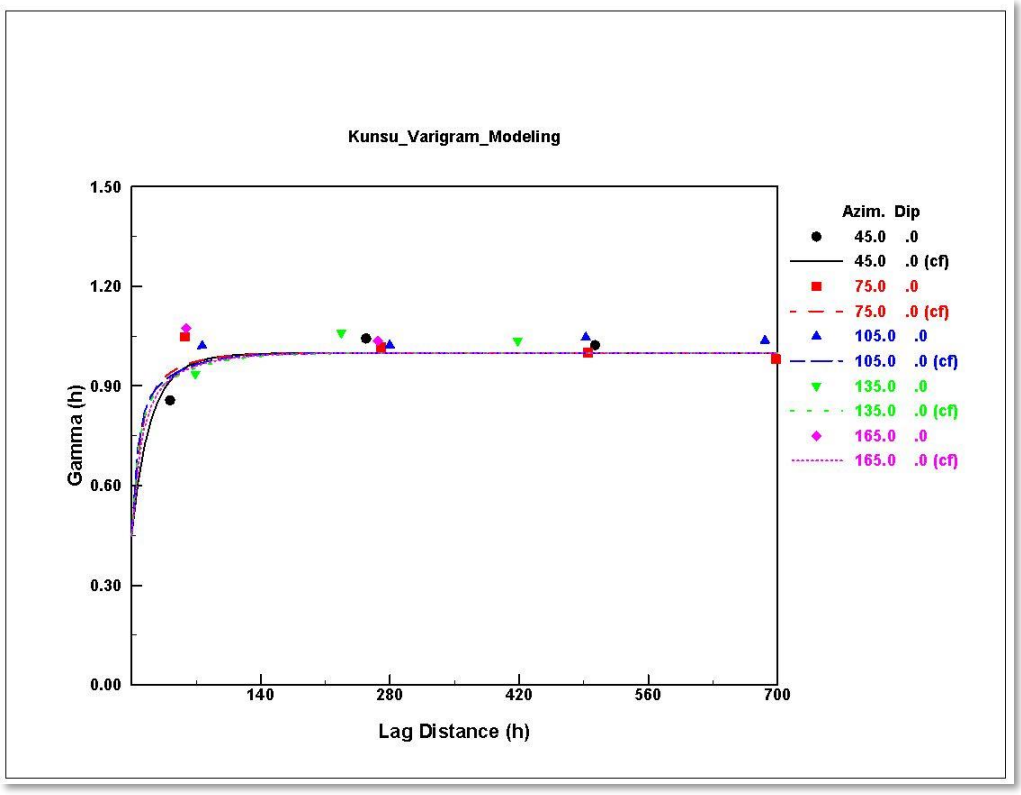

Figure5.5: Variogram model showing all three model directions, major, minor and vertical directions.

5.2 MINERALIZATION WITHIN TRENCHES

Gold concentrations within the mineralized zones from the retrenches are presented in Table 5.3.

Table 5.3: Trench Assay Results for two different fences (Trench TR07 and TR01).

Project	Trench number	From (m)	To (m)	Width (m)	Grade (g/t)
Kunsu	TR01-B1	0	3.8	3.8	0.75
Kunsu	TR01-B2	3.8	7.8	4	0.19
Kunsu	TR01-B3	7.8	12.1	4.3	0.13
Kunsu	TR01-B4	12.1	17.1	5	0.11
Kunsu	TR01-B5	17.1	21.5	4.4	0.21
Kunsu	TR07-B1	0	3.7	3.7	0.54
Kunsu	TR07-B2	3.7	7.7	4	1.05
Kunsu	TR07-B3	7.7	11.6	3.9	0.1
Kunsu	TR07-B4	11.6	15.6	4	0.78
Kunsu	TR07-B5	15.6	18.6	3	0.11

Concentration of the gold within the study area varies from mineralized zones of gold assay values greater than 0.1g/t above background values of less than 0.01 g/t. Due to the thickness of the regolith of the area, dispersion halos are significantly in less concentration as compared to the areas where the regolith is thin. Mineralization occurred in saprolite and mottled zones with quartz veins also mineralized as shown in figure 5.6.

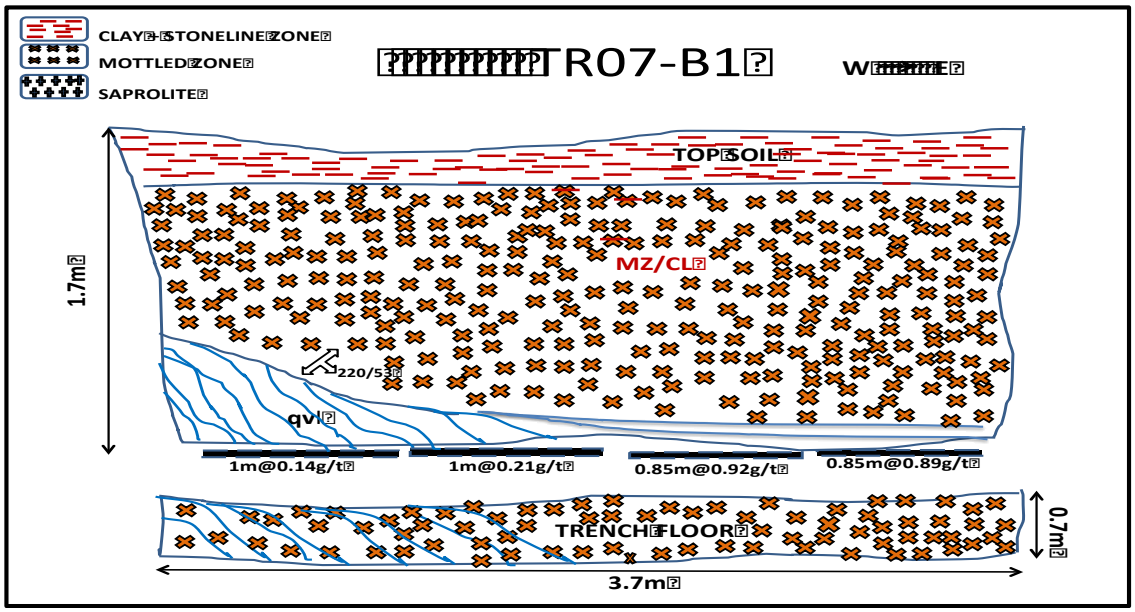

Figure 5.6: Soil profile of trench TR07-B1 showing mineralized zones with respect to gold content in grams per ton.

Figure 5.7: Pictorial soil profile of trench TR07- B1 shows mineralized quartz veining.

Two trenches KUTR007 and KUTR001 previously recorded 0.4 grams per tonnage and 0.18 grams per tonnage of mineralization at 8.7 and 60.5 metre respectively as shown in figure 5.8. Whiles figure 5.9 shows the results of re-trenching of the same two trenches KUTR07 and KUTR01 confirming mineralized zones within these trenches.

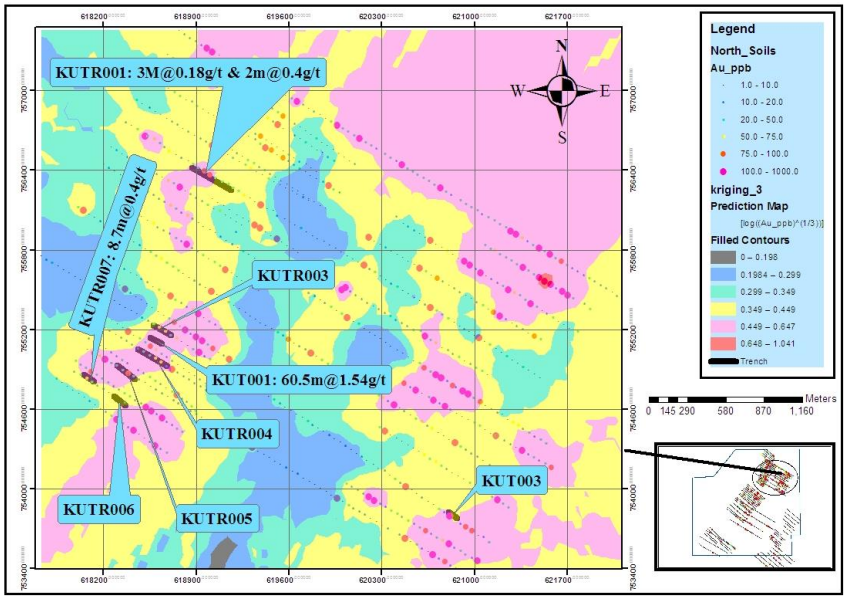

Figure 5.8: Gold concentration within previous mineralized trenches.

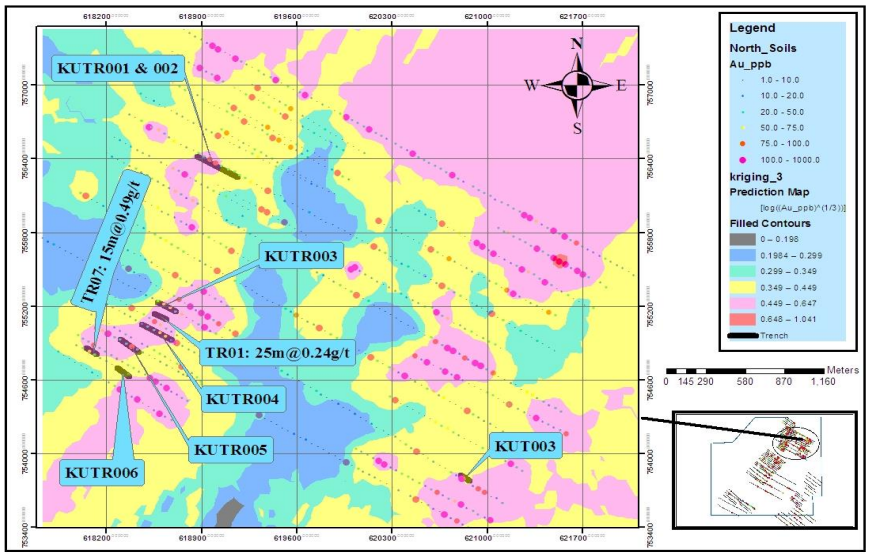

Figure 5.9: Gold concentration within retrenched of previous mineralized trenches.

5.4 SOIL GEOCHEMICAL TRENDS

The northeastern section of the study area is divided into zones as shown in figure 5.10 on the basis of the areas with high soil anomalies showing trends of mineralization in the northeast southwest direction. The main ZONE is one where much exploration works was done, ZONE 2 is where less drilling was conducted and ZONE 3 is the area where no drilling was conducted at all.

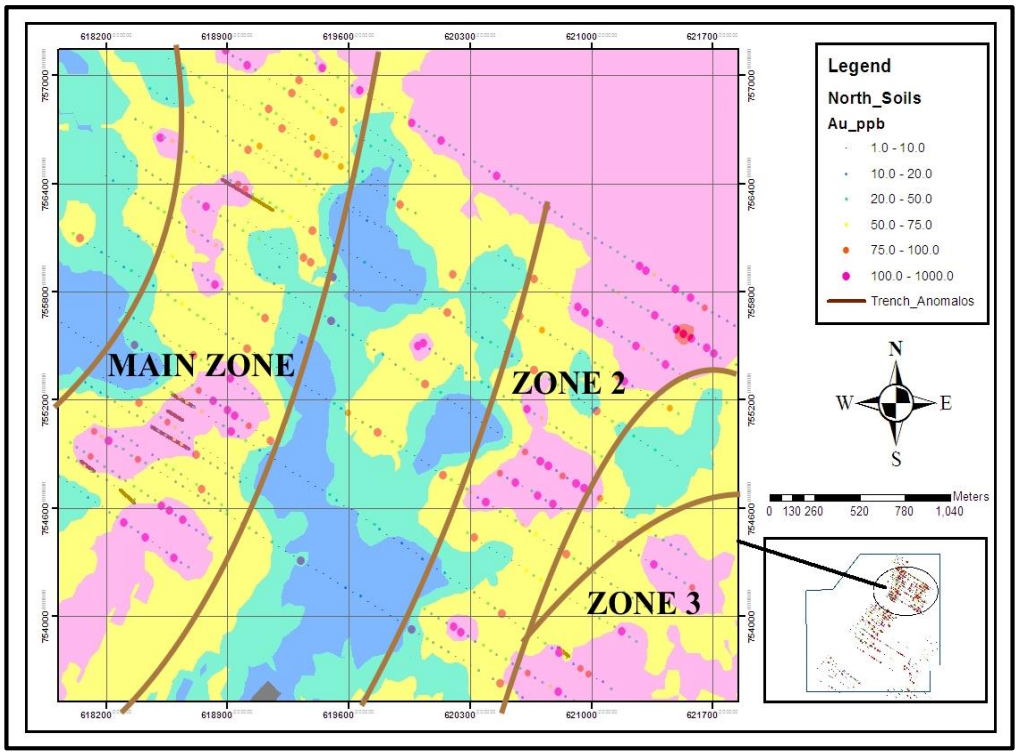

Figure 5.10: 2D model of soil geochemical survey outlining trend of mineralization overlaid by trench locations.

Results gathered from the retrenching fieldwork carried out in this study shows that trench with ID KUTR007 (or TR07 as it was renamed in this study) has shown an extension in mineralization across strike within mottled clay zone.

5.5 3D MODELS OF ORE BODY

Drill-hole sections were generated from the drill-hole database to check data and secondly to draw interpreted geological limits for the ore body or rock types. Three-dimensional enclosed solid surfaces are generated using wireframing strings of points on plan, or by triangulation of a series of points and strings into a digital terrain model, more commonly termed as surface.

Targets evaluation was based on three stages; development of geology and grade scenarios, geology modeling to build 3D representations of stationary domains (volume models) and grade modeling to populate volumes with the relevant grade estimates. The results are presented in an Isosurfaces format from an interpolation of probability values for visualization purposes. Representations of ore bodies in volume and grade variations were constructed using wireframe to delineate the ore bodies.

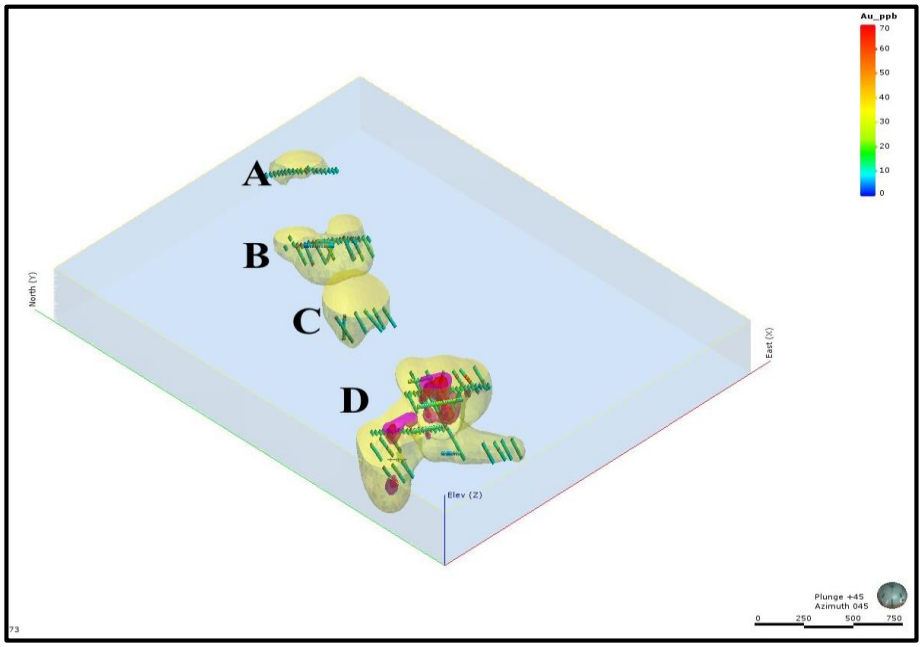

Figure 5.11: 3D model of gold prospect with drill holes' assay, showing NE-SW trending.

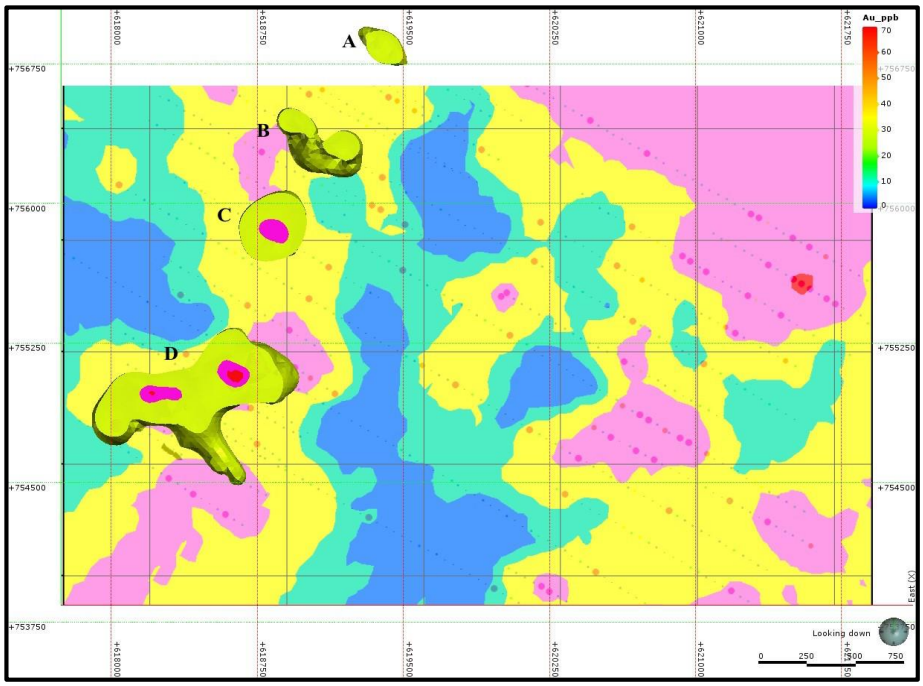

Figure 5.12: Plan view (viewing downward) of 3D model and drill holes' assay.

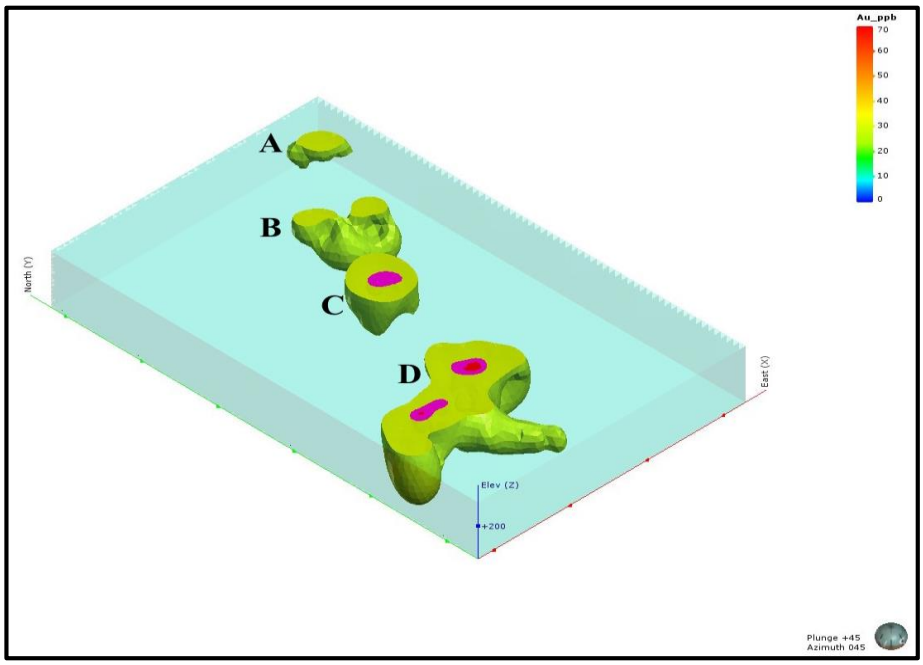

Figure 5.13: Solid 3D model of the gold deposit within a transparent background model.

The ore bodies are widely separated due to the spacing of drill holes. However, each drill fence generated a separate ore body namely A, B, C and D. Ore body D is trending more to nearly NE-SW direction. Orientation of the ore body D suggests or indicates a possible display, which could be as a result of tectonic event causing that display. Ore bodies A, B and C trends in northeast southwest slightly different from the main ore body D.

The extension of the ore body D requires reorientation of drilling direction and possibly the angle of drilling.

As shown in figure 5.12 below, the 3D model of gold deposit superimposed on to 2D soil model shows an indication of the soil anomalies matching with the 3D model of the gold deposit affirming that, the anomalies indicated by the soil geochemical survey continues downward. This is also an indication of the gold deposit being in-situ. Both the 3D and the 2D models are trending northeast southwest with an indication of displacement in structure ore bodies C and D. Ore bodies B and C are observed to be much toward the east of the 2D soil geochemical model suggesting that more detail works needs to be conducted within ore bodies B and C. The nature of the orientations of the ore bodies call for reconsidering the azimuth of the drill holes for future drilling program.

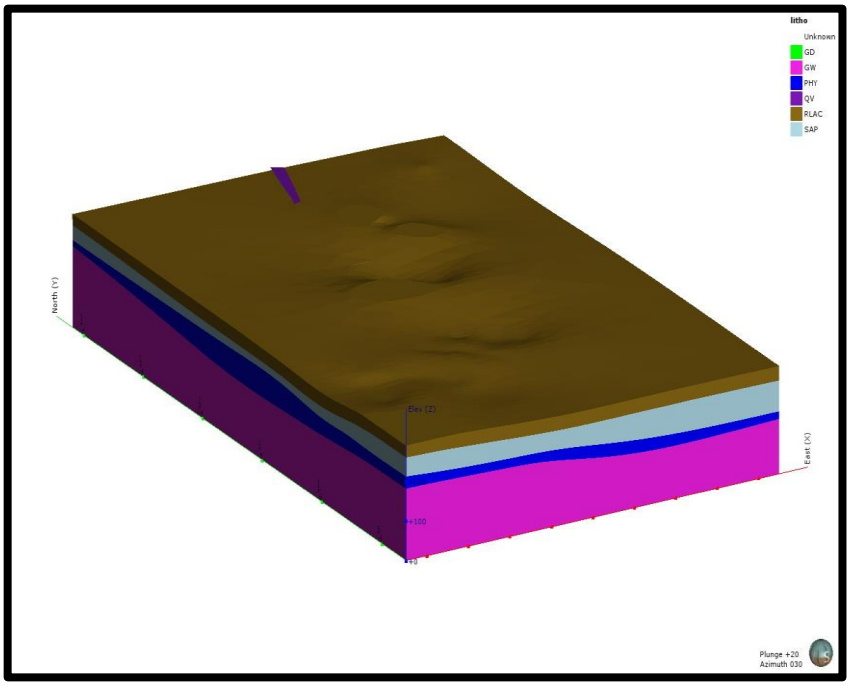

Figure 5.14: 3D lithological model of study area.

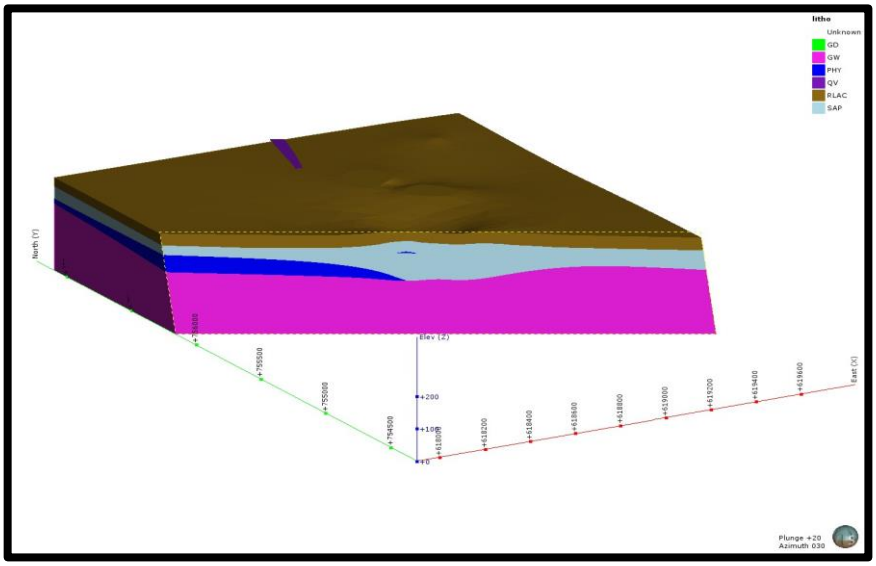

Figure 5.15: Cross sectional view of the 3D lithological model

5.6 DISCUSSIONS

5.6.1 Soil Geochemical Survey

The purpose of applying soil geochemical techniques in mineral exploration is to help define trends of mineralization. The study has revealed that the soil geochemical survey outlined the trends of mineralization within the study area. The areas with defined high soil anomalies are within the central and northeastern corner of the study area. The soil geochemical anomalies are observed trending generally in NE-SW.

The area has a very thick overburden averaging 45m that has been a factor for low concentration of gold within the oxides. The thickness of the overburden has contributed in subsidence of the dispersion halos of the minerals deposits within the area which as a result has made it difficult to encounter high grades of mineralization. Soils geochemical results from the southern portion of the study area show weak soil anomalies (ONE-POINT soil anomalies). Thickness of the regolith can be as a result of this observation in the southern part of the study area.

5.6.1.1 Trenches

Trenching is conducted in mineral exploration to further test or investigate mineralization extent from the topsoil. The reason is that; the high soil geochemical anomalies could be a transported material. Retrenching of mineralized zones from the previous trenches confirms the trend and extent of mineralization beyond topsoil or the B-horizon.

Almost all the trenches never exceeded 3m depth but recorded significant grades. Mineralization within trenches were recorded in the mottled and saprolitic regolith

regimes and mineralized quartz veins were noted in the trenches as a confirmation of stockworks style of mineralization within the area.

The trenches were sited based on soil geochemical anomalies without the consideration of geological structures mapped out by the geophysical investigations. Much information on the geological structures can be obtained by putting up more trenches between the existing ones or by digging deeper than 3 m depth as it was done in the current ones.

5.6.3 3D model

Interpolation/Kriging technique was used to model the ore bodies and this has helped to reveal the characteristics of the mineral deposits. The quantity of data used to model the ore bodies shows clearly from the study that the mineral deposits are controlled by the geological structures which were observed to be trending in a northeast southwest direction. This is shown from the alteration of the quartz veins tested for mineralization from the re-trenching geochemical results and the drill cores assays.

The 2D and 3D models constructed stipulate that the orientation of the main ore body in the NEE-SWW implies tectonic displacement of the mineral deposits within the adjoining deposits. The stretch of the strike of the ore bodies is about 1km long (deposits A, B, C and D) and covers a total area of about 113, 473m^2 and about 1,008,272 m^3 in volume.

CHAPTER SIX

CONCLUSIONS AND RECOMMENDATIONS

6.1 CONCLUSIONS

Soil and drill hole geochemical data were used to generate 2D and 3D models using Interpolation/Kriging techniques to delineate the Kunsu ore body. The ore bodies or deposits are observed trending along NE-SW direction.

It is clear from both the 2D and 3D models that the main ore body has been displaced slightly from the general NE-SW trend position to NEE-SWW trend. The 2D and 3D models were observed to match when the two models were compared indicating that the soil geochemical anomalies are of residual source and insitu. It was also deduced that the area has a very thick overburden and contributed to the low concentration of dispersion halos of the deposit within the oxides.

The re-trenching investigation within the mineralized zones of the previous trenches returned good assay results confirming the mineralization of the area and quartz veins. However, an extension of one of the trenches confirms continual mineralization. Due to the thickness of the overburden and the depth at which the trenches were dug much geological structural information could not be recorded and few quartz veins were encountered in the trenches.

Even though, the southern section of the study area has been neglected for further exploration works because, the area did not record high soil geochemical anomalies. The soil geochemical data could suggest possible high soil geochemical anomalies recorded in the area and this could be on an ore body hidden by the thickness of the regolith.

6.2 RECOMMENDATION

- A holistic geological mapping should be conducted to aid the understanding of the geological setting of the area and to aid in selecting of azimuth and angle to drill FOR FUTURE DRILLING PROGRAM.
- Infill diamond drilling parallel to RC holes KURC020, KURC021, KURC023 and KURC029 should be conducted to test to confirm the intercepts of these drill holes.
- New and infill trenches PROGRAM should be conducted to test for the mineralization of the geological structures outlined from the geophysical investigation.
- Infill soil geochemical sampling should be conducted on the southern portion of the area to test for the one-point soil geochemical anomalies.
- Careful re-logging of the drill cores should be done to map out and measure alterations and geological structures respectively.
- Geophysical investigation should be extended to the southern portion of the area to test for geological structures that could be comparable to the probable soil geochemical anomalies.

REFERENCES:

Abouchami, W., Boher, M., Michard A. and Albarede, F. (1990). A major 2.1 Ga event of mantle magmatism in West Africa: an early stage crustal accretion. J. Geophysics Research. 95, pp. 17605-17629.

Afzal, P., Fadakar, A. Y., Khakzad, A., Moarefvand, P., RashidnejadOmran, N. (2011). Delineation of mineralization zones in Porphyry Cu deposits by Fractal Concentration-Volume modeling. Journal of Geochemical Exploration, Vol. 108, pp. 220 – 232.

Agyei D. J., Loh, G. K., Boamah, K. O., Baba, M., Hirdes, W., Toloczki, M., and Davis, D. W., 2009, Geological map of Ghana 1: 1,000,000; Geological Survey of Ghana.

Allibone, A., Hayden, P., Cameron, G., Duku, F. (2004). Paleoproterozoic Gold Deposits Hosted by Albite-and-Carbonate-Altered Tonalite in the Chirano District, Ghana, West Africa. Economic Geology, 99: pp. 479 - 497.

Allibone, A., Teasdale, J., Cameron, G., Etheridge, M., Uttley, P., Soboh, A., Appiah-Kubi, J., and Lamb, E. (2002). Timing and structural controls on gold mineralization at the Bogoso Gold Mine, Ghana, West Africa. Econ. Geol. 97, pp. 949-969.

Amponsah P.O., Stefano S., Didier B., Luc S., Lenka B. and Mark W. J., (2015). Geology and Geochemistry of the Shear-hosted Julie Gold Deposit NW Ghana, Journal of African Earth Sciences 112 (2015) pp.505-523. Retrieved from https//www.elsevier.com/locate/jafrearsci

Appiah, H., (1991). Geology and Mine Exploration Trends of Prestea Goldfields, Ghana. Journal of African Earth Science. (Middle East) 13, pp.235–241.

Arhin, E. (2013). Use of Regolith Geochemistry to Delineate Gold Mineralisation Under Cover: A Case Study in The Lawra Belt, NW Ghana (Doctoral Dissertation, University of Leicester, Leicester, England). Available at http://lra.le.ac.Uk (2013arhinephd).

Aseidu, D.K., Kutu, J.M., Manu, J., Hayford, E.K., (2009). Geochemistry and Province of Metagreywakes from The Konongo Area, Southwestern Ghana. African Journal of Science and Technology (AJST), Science and Engineering Series Vol. 10, No 1, pp. 37-44.

Bancroft, B.A., and Hobbs, G.R. (1986). Distribution of Kriging Error and Stationarity of the Variogram in a Coal Property. Mathematical Geology 8(7): pp. 635-651.

Bernard, W.P., Dee. D. T, RICHARD, H., JAMES, S.M. and Reed, W. (2005). Physical Geology: Exploring The Earth. Mason, Ohio: Cengage Learning. P. 559.

Bertrand-Sarfati, J., Moussine-Pouchkine, A., Affaton, P., Trompette, R., and Y. Bellion, (1990). Cover Sequences of the West African Craton: in Dallmeyer, R. D., and J. P. Lecorche (eds), The West African Orogens and Circum-Atlantic Correlatives, pp. 65-84.

Bayraktar H., Turalioglu F.S. (2005). A kriging-based approach for locating a sampling site in the assessment of air quality. Stochastic Environmental Research and Risk Assessment 19 (4), pp. 301-305.

Blenkinsop, T.G., Schmidt-Mumm, A., Kumi, R., Sangmor, S., (1994). Structural geology of the Ashanti Gold Mine. Geol. Jahrb., D 100, pp. 131-153.

Boher, M., Abouchami, W., Michard A., Albarede, F and Arudt, N.T (1992). Crustal growth in West Africa at 2.1 Ga. J. Geophysics Research. 97, pp. 345-369.

Burrough, P.A., and Mcdonnell R.A. (1998). Principles of Geographical Information Systems. New York, NY: Oxford University Press. p.190, pp. 17-34

Clark Labs, (2000). Idrisi32 I32.01 Software. Clark University, Ma. Esri. Environmental Science Research Institute, Inc. 1999. Arc/Info 8.0.1 Software.

Chudasama, B., Porwal A., Kreuzer, O.P., Kris Butera K., (2015). Geology, Geodynamics and Orogenic Gold Prospectivity Modelling of the Paleoproterozoic Kumasi Basin, Ghana, West Africa. Journal for comprehensive studies of ore genesis and ore exploration, pp. 1-20. Retrieved from http://dx.doi.org/10.1016/j.oregeorev.2015.08.012

Davis, D., Hirdes, W., Schallegger, E., and Nunoo, E.A. (1994). U/Pb age constrains on deposition and provenance of Birimian and gold bearing Tarkwaian sediments in Ghana, West Africa. Precambrian Res. 130, 113-137.

Duke, J.H. and Hanna, P.J. (2001). Geological Interpretation for Resource Modelling and Estimation. pp. 147–156.

Duodu, A. J., Loh, G.K., Boamah, K.O., Baba, M., Hirdes, W., Toloczyki, M., and Davis, D.W., (2009). Geological map of Ghana 1:1000000, Geological Survey Department of Ghana (GSD). Accra, Ghana.

Eisenlohr, B. N., and Hirdes, W. (1991). The structural development of the earl Proterozoic Birimian and Tarkwaian rocks of southwest Ghana, West Africa. Journal of Earth Sci., vol. 14, No. 3, pp. 313-325.

Emery X. and Ortiz J. M. (2005). Estimation of Mineral Resources Using Grade Domains: Critical Analysis and A Suggested Methodology. The Journal of the South African Institute of Mining and Metallurgy, Vol. 105, pp. 247 – 256.

Emery, X. (2005). Simple and Ordinary Kriging; Multi-Gaussian Kriging for estimating recoverable reserves. Mathematical Geology, Vol. 37, pp. 295-319.

Emery X. and Ortiz J. M. (2005). Estimation of mineral resources using grade domains: critical analysis and a suggested methodology, The Journal of the South African Institute of Mining and Metallurgy, vol. 105 pp. 247 – 255.

Esri. Environmental Science Research Institute, Inc. (1999). Arcview 3.2 Software.

Feybesse, J.L., Billa M., Guerrot C., Duguey, E., Lescuyer, J., MiléSi, J.P., and Bouchot, V. (2006). The Paleoproterozoic Ghanaian Province: Geodynamic Model and Ore Controls, Including Regional Stress Modeling. Precambrian Research 149, pp. 149-196.

Feybesse, J. L., and MiléSi, J.P. (1994). The Archean/ Proterozoic Contact Zone In West Africa: A Mountain Belt Dé Collement Thrusting and Folding on Continental Margin Related to 2.1 Ga. Convergence of Archean Cratons? Precambrian Research 69, pp. 199- 227.

Gasquet, D., Barbey, P., Adou, M., Paquette, J. L. (2003). Structure, Sr–Nd isotope geochemistry and zircon U–Pb geochronology of the granitoids of the Dabakala area (Côte d'Ivoire): evidence for a 2.3 Ga crustal growth event in the Paleoproterozoic of West Africa? Precambrian Research, 127: pp. 329–354.

Garrett, R.G. and Grunsky, E.C., 2001. Weighted sums - knowledge based empirical indices for use in exploration geochemistry. Geochemistry: Exploration, Environment, Analysis, 1 (2): pp. 135-141.

Glacken, I. M. and Snowden, D. V. (2001). Mineral Resource Estimation, In Mineral Resource and Ore Reserve Estimation – The Ausimm Guide to Good Practice (Ed: A C Edwards), pp. 189-198.

Goodchild, M., F. Guoqing, and Shiren Y. (1992). Development and Test of an Error Model for Categorical Data. International Journal of Geographical Information Systems 6(2) pp. 87-104.

Griffis, R.J., Kwasi B., Agezo F. L. and. Akosah F. K. (2002). Gold Deposits of Ghana.Ontario: Gandalf Graphic. p. 438.

Groves, D.I., Goldfarb, R.J., Robert, F. and Hart, C. (2003). Gold deposits in Metamorphic Belts: Economic Geology 98. pp. 29.

Gubanov A.P. and Mooney W.D., (2009) new global Geological maps of crustal basement age.os transactions, AGU 90: Fall Meet. pp.53-153. Available at https://scholar.google.com/scholar_lookup?

Heuvelink, G.B.M., and. Burrough P.A. (1989). Propagation of Errors in Spatial Modeling with GIS, International Journal of Geographical Information Systems 3(4), pp. 303-322.

Hill E. J., Nicholas H.S. O., Fisher L, James S. C. and Michael J. N. (2014). Using Geochemical Proxies to Model Nuggety Gold Deposits: An Example from Sunrise Dam, Western Australia. Journal of Geochemical Exploration 145 (2014) pp. 12–24. Available at http:// www.elsevier.com/locate/jgeoexp

Hirdes, W., Davis, D.W., Lüdtke, and G., Konan, G. (1996). Two generations of Birimian (Paleoproterozoic) volcanic belts in the northeast Côte D'Ivore (West Africa): Consequence for Birimian controversy. Precambrian Research 80, pp. 173-191.

Hirdes, W., Davis, D.W., and Eisenlohr, B.N. (1992). Reassessment of Proterozoic granitoids ages in Ghana on the basis of U/Pb Zircons and Monazite dating. Precambrian Research, 56 pp. 889-96.

Hodkiewicz, P., (2015). New Software for faster and better 3d geological modelling, SRK Consulting, Australia. pp. 1-9.

Howarth, R. J. (1984). Statistical applications in geochemical prospecting: A survey of recent developments. Journal of Geochemical Exploration, Vol. 21, pp. 41-61.

Ioannis K. K. (1999). Application of Artificial Neural Network Systems To Grade Estimation From Exploration Data, (Doctoral Dissertation, University of Nottingham, Nottingham, England) retrieved from http://www.citeeerx.ist.psu.edu, doi=10.1.1.146.297&rep=rep1&type=pdf

John, T., Klemd, R., Hirdes, W. and Loh, G. (1999). The metamorphic evolution of the Paleoproterozoic (Birimian) Volcanic Ashanti Belt (Ghana, West Africa). Precambrian Research, 98: pp. 11-30.

Jon, B. (2011). 2D and 3D Block Models, Gemcom Software International Inc.

Juha, V., (2008). Sample Preparation and Analytical Methods: Geochemistry, Exploration and Mining. p. 32.

Junner, N. R. (1940). Geology of the Gold Coast and Western Togoland (with revised geological map). Bull. Gold Coast Geological Survey 11, pp. 40.

Junner, N.R., (1935). Gold in the gold coast. Gold Coast Geol. Surv., Mem. 4, pp.1-67.

Junner, N.R., 1932. Geology of the Obuasi goldfield. Gold Coast Geol. Surv., Mem. 2, pp.1-71.

Juvonen R., Kallio E. and Lakomaa T. (1994). Determination of piorecious metals in rocks by inductively coupled plasma mass spectrometry using nickel sulphide concentration. Comparison with other pre-treatment methods. Analyst 119 (1994), pp. 617 - 621.

Juvonen R. and Kontas E. (1999). Comparison of three analytical methods in the determination of gold in six Finnish gold ores, including a study of sample preparation and sampling, Journal of Geochemical Exploration 65 (1999) pp. 219 - 229.

Kontas E., Niskavaara H. and Virtasalo J., (1990). Gold, palladium and tellurium in South African, Chines and Japanese geochemical reference samples, Geostandards Newsletter, 14(1990), pp. 477 - 478.

Kontas E. ed. (1993). Analytical methods for determining gold in geological samples, Geological Survey of Finland, Report of Investigations 114 (1993), p. 41.

Krige, D G, (1978). South African Institute of Mining and Metallurgy Monography Series: Geostatistics I, Lognormal–De Wijsian Geostatistics for Ore Evaluation, Johannesburg. South African Institute of Mining and Metallurgy. p. 51

Lam, N.S. (1983). Spatial Interpolation Method: A Review. American Cartographer 10: pp.129-220.

Lefohn A.S., Knudsen H.P., Shadwick, D.S., (2005). Using Ordinary Kriging to Estimate the Seasonal W126, and N100 24-h Concentrations for the Year 2000 and 2003. A.S.L. and Associates, Montana. p. 10

Leube, A., Hirdes, W., Mauer, R., and Keese, G.O. (1990). The Early Proterozoic Birimian Supergroup of Ghana and Some Aspects of Its Associated Gold Mineralisation. Precambrian Research 46: pp. 46 -165.

Mandel, J. (1984). The Statistical Analysis of Experimental Data. New York, Dover Publications. p. 410.

Maurice O.A. (2015). 3D Block Modeling and Reserve Estimation of a Garnet Deposit (Master thesis, Montana Tech. of the University of Montana). p. 39. Available at http://digitalcommons.mtech.edu/grad_rsch.

Newmont Ghana Gold Limited, (2013). Kunsu Prospecting License Terminal Report. Unpubl.

Newmont Ghana Gold Limited, (2012). Kunsu Prospecting License Terminal Report. Unpubl.

Miller, A.V.M., Partington G.A., Kreuzer, O., Butera, K., Buckingham, A. and Ainoo, S. (2015). Regional Prospectivity Modelling in Data-Poor Areas: The Kumasi Basin, Ghana. p. 10. Available at http://www.kenex.com.au

Min, Q., Bao-Lin, Z., Guang-He, L., Jie W., and Xin-Ping C. (2007). 3D Modeling and Visualization of Geology Volume Based On Geophysical Field Data, Division of Solid Mineral Resource, Institute of Geology and Geophysics, Chinese Academy of Sciences, Beijing 100029, China. Data Science Journal, Vol. 6, Supplement.

Niskavaara H. (1990). Reductive Coprecipitation as a separation method for the determination of gold, palladium, platinum, rhodium, silver, selenium and tellurium in geological samples by graphite furnace atomic absorption spectrometry, Analytica Chimica Acta, 231(1990), pp. 273 - 282.

Nurmi P.A., Lestinen, P. and Niskavaara, H. (1991). Geochemical Characteristics of mesothermal gold deposits in Fennoscandian Shield and a comparison with selected Canadian and Australian deposits. Geological Survey of Finland, Bulletin 351, Espoo 1991, p. 101.

Oberthür, T., Vetter, U., Davis, D. W. and Amanor, J.A. (1998). Age constrains on gold mineralization and Paleoproterozoic crustal evolution in the Ashanti belt of Southern Ghana. Precambrian Research 89, pp. 129-143.

Osterholt V, Herod, O and Arvidson, H. (2009). Regional Three-Dimensional Modelling of Iron Ore Exploration Targets, Ore body Modelling and Strategic Mine Planning, pp. 35-41, Available at hppt://www.intrepid-geophysics.com

Perrouty, S., Ailleres, L., Jessell, M.W., Baratoux, L., Bourassa, Y. and Crawford, B., (2012). Revised Eburnearn geodynamic evolution of the gold-rich southern Ashanti Belt, Ghana, with new field and geophysical evidence of the pre-Tarkwaian deformations. Precambrian Res. Pp. 204 -205, pp. 12-39.

Pouclet, A., Doumbia, S. and Vidal, M. (2006). Geodynamic setting of the Birimian volcanism in Central Ivory Coast (Western Africa) and its place in the evolution of the Palaeoproterozoic of the Man Shield Bulletin. Geological Society France 177 (2), pp.195-121.

Pride, D. E. (2014). Geochemical prospecting. In AccessScience. McGraw-Hill Education. Available at http://www.accessscience.com, doi 10.1036/1097-8542.285700.

Qi, M., Zhang B., Liang G., Wang j. and Cai X. (2007). 3d Modeling and Visualization of Geology Volume Based on Geophysical field data, Data Science Journal, vol.6, pp. 652 – 657.

Reedman J. H., (1979). Techniques in Mineral Exploration, London, Applied Science. P. 533. Available at DOI 10.107/978-94-009-9227-6

Roddaz, M., Debat, P. and Nikiéma, S. (2007). Geochemistry of upper Birimian sediments and Implications for weathering and tectonic setting of the Late Paleoproterozoic crust. Precambrian Research, 159: pp. 197–211.

Rouhani, S.R., Srivastava M., Desbarats, A. J., Cromer M. V., Johnson A.L., (1996). Geostatistics for ENVIRONMENTAL and Statistical Applications. Ann Arbor, Michigan: ASTM. p. 277.

Roger, M., (2010). Geological Methods in Mineral Exploration and Mining retrieved from http://www.mining-eng.

Sample Preparation and Analytical Methods Geochemistry, Exploration and Mining, http://www.infomine.com

Sarma, V.S., (2014). ELECTRICAL RESISTIVITY (ER), SELF POTENTIAL (SP), INDUCED POLARIZATION (IP), SPECTRAL INDUCED POLARIZATION (SIP) and Electrical Resistivity Tomography (ERT) Prospection, available at http://www.igu.in/18-2/7paper.

Schofield, N.A., (2011). Geological Domaining and Resource Estimation, Proceedings of the 35th APCOM Symposium, Wollongong, NSW. Australasian Institute of Mining and Metallurgy, Melbourne.

SGS Minerals Services, (2013). Ore body Modeling and Resource Estimation available at http://www.sgs.com/mining

Stewart, M and Dunham, S., ed. (2014). QG Australia Pty Ltd (QG): Trans-Siberian Gold Asacha Mineral Resource Estimate, Kamchatka. pp. 11-71.

Sylvester, P.J. and Attoh, K. (1992). Lithostratigraphy and Composition OF 2.1 Ga. Greenstone Belts OF West Africa Craton and Their Bearing On Crustal Evolution and The Archean-Proterozoic Boundary. Journal of Geology. 100, pp. 377-393.

Tapsoba, B., Lo, C. H., Jahn, B. M., Chunga, S. L., Wenmenga, U., and Iizuka, Y. (2013). Chemical and Sr–Nd isotopic compositions and zircon U–Pb ages of the Birimian granitoids from NE Burkina Faso, West African Craton: Implications on the geodynamic setting and crustal evolution. Precambrian Research 224: pp. 364-396.

Taylor, G., and Eggleton, R. A., (2001). Regolith Geology and Geomorphology: John Wiley & Sons. London. Cambridge University Press. Geol. Mag. 138, pp. 727-731. Available at doi: 10.1017/S0016756801216239

Taylor, N. P., Moorbath, S., Leube, A. and Hirdes, W. (1992). Early Proterozoic crustal evolution in the Birimian of Ghana: constraints from geochronology and isotope geochemistry. Precambrian Research 56: pp. 97–111.

Van Loon, J.C. and Barefoot, R.R., (1989). Analytical Methods for Geochemical Exploration. San Diego, Academic Press, p. 344.

Vidal, M., Delor, C., Pouclet, A., Siméon, Y., and Alric, G. (1996). Evolution géodynamique de l'Afrique de l'Ouest entre 2,2 Ga et 2 Ga: le style -archéen‖ des ceintures vertes etdes ensembles sédimentaires birimiens du nord-est de la Côte- d'Ivoire. Bulletin. Geological Society France 167 (3), pp. 307–319.

Wang G, Zhu Y., Zhang S., Yan C., Song Y., Ma Z, Hong D. and Chen T. (2012) 3D geological modeling based on gravitational and magnetic data inversion in the Luanchuan ore region, Henan Province, China, Journal of Applied Geophysics 80 (2012) pp.1–11. Retrieved from http://www.elsevier.com/locate/jappgeo

Wright, J., Hastings, D., Jones, W. and Williams, H., (1985). Geology and Mineral Resources of West Africa. London.

Yamamoto, J.K. (2005). Comparing Ordinary Kriging Interpolation Variance and Indicator Kriging Conditional Variance for Assessing Uncertainties at Unsampled Locations, pp.265–269. Retrieved at doi:1201/9781439833407.ch34

Yan-lin S, Ai-ling Z., You-bin H. and Ke-yan X. (2011). 3D Geological Modeling and Its Application under Complex Geological Conditions, Journal of Procedia Engineering 12 (2011) pp. 41–46. Retrieved from www.sciencedirect.com

Zhang R., Zeng M., Chen J. (2011). Study on Geological Structural Interpretation Based on Worldview-2 Remote Sensing Image and Its Implementation, journal of Procedia Environmental Science Volume 10, Part A, (2011) pp. 653–659. Retrieved from www.sciencedirect.com

Zhu Y., Fang A. and Juanjuan T. (2011). Geochemistry of Hydrothermal Gold Deposits: A review, Journal of Geoscience Frontiers 2(3) pp. 367-374. Retrieved from www.sciencedirect.com.

Zitzmann, A., Kiessling, R., and Loh, G., (1997). Geology of the Bui Belt Area in Ghana; in A. Zitzmann (ed), Geological, Geophysical and Geochemical Investigation in the Bui Belt Area in Ghana. Geol. Jb. Reihe B, Heft 88, p. 269.

APPENDIX ONE

RE-TRENCHING ASSAY RESULTS

PROJECT	TRENCH_ID	SAMPLE_ID	FROM	TO	Au_ppm	Au_ppb
KUNSU	TR01-B1	TR01_B1_1	0	1	0.12	120
KUNSU	TR01-B1	TR01_B1_2	1	2	0.21	210
KUNSU	TR01-B1	TR01_B1_3	2	3	0.16	160
KUNSU	TR01-B1	TR01_B1_4	3	3.8	2.52	2520
KUNSU	TR01-B2	TR01-B2_1	0	1	0.13	130
KUNSU	TR01-B2	TR01-B2_2	1	2	0.18	180
KUNSU	TR01-B2	TR01-B2_3	2	3	0.3	300
KUNSU	TR01-B2	TR01-B2_4	3	4	0.16	160
KUNSU	TR01-B3	TR01-B3_1	0	1	0.08	80
KUNSU	TR01-B3	TR01-B3_2	1	2	0.15	150
KUNSU	TR01-B3	TR01-B3_3	2	3	0.19	190
KUNSU	TR01-B3	TR01-B3_4	3	3.7	0.1	100
KUNSU	TR01-B3	TR01-B3_5	3.7	4.3	0.12	120
KUNSU	TR01-B4	TR01-B4_1	0	1	0.12	120
KUNSU	TR01-B4	TR01-B4_2	1	2	0.12	120
KUNSU	TR01-B4	TR01-B4_3	2	3	0.11	110
KUNSU	TR01-B4	TR01-B4_4	3	4	0.08	80
KUNSU	TR01-B4	TR01-B4_5	4	5	0.14	140
KUNSU	TR01-B5	TR01-B5_1	0	1	0.13	130
KUNSU	TR01-B5	TR01-B5_2	1	2	0.23	230
KUNSU	TR01-B5	TR01-B5_3	2	3	0.13	130
KUNSU	TR01-B5	TR01-B5_4	2	3	0.1	100
KUNSU	TR01-B5	TR01-B5_5	3	3.7	0.18	180
KUNSU	TR01-B5	TR01-B5_6	3.7	4.4	0.4	400
KUNSU	TR07-B1	TR07-B1_1	0	1	0.14	140
KUNSU	TR07-B1	TR07-B1_2	1	2	0.21	210
KUNSU	TR07-B1	TR07-B1_3	2	2.85	0.92	920
KUNSU	TR07-B1	TR07-B1_4	2.85	3.7	0.89	890
KUNSU	TR07-B1	TR07-B1_5	Grab sample		0.12	120
KUNSU	TR07-B2	TR07-B2_1	0	1	0.18	180
KUNSU	TR07-B2	TR07-B2_2	1	2	1.74	1740
KUNSU	TR07-B2	TR07-B2_3	2	3	2.1	2100
KUNSU	TR07-B2	TR07-B2_4	3	4	0.19	190
KUNSU	TR07-B3	TR07-B3_1	0	1	0.11	110
KUNSU	TR07-B3	TR07-B3_2	1	2	0.1	100
KUNSU	TR07-B3	TR07-B3_3	2	3	0.1	100
KUNSU	TR07-B3	TR07-B3_4	3	3.85	0.1	100
KUNSU	TR07-B3	TR07-B3_5	3.75	4.7	0.08	80
KUNSU	TR07-B4	TR07-B4_1	0	1	0.07	70
KUNSU	TR07-B4	TR07-B4_2	1	2	0.07	70

KUNSU	TR07-B4	TR07-B4_3	2	3	0.07	70
KUNSU	TR07-B4	TR07-B4_4	3	4	0.1	100
KUNSU	TR07-B5	TR07-B5_1	0	1	0.19	190
KUNSU	TR07-B5	TR07-B5_2	1	2	0.06	60
KUNSU	TR07-B5	TR07-B5_3	2	3	0.07	70
KUNSU	TR07-B5	TR07-B5_4	3	3.75	0.06	60
KUNSU	TR07-B5	TR07-B5_5	3.75	4.55	0.03	30

APPENDIX TWO

MINERALIZED ZONES OF TRENCHES

Trench ID	FIELD ID	From (m)	To (m)	Sample ID	Au_ppm	Au_ppb
KUT001	KUT001/1	0	1	1016001	0.153	153
KUT001	KUT001/1	1	2	1016002	0.122	122
KUT001	KUT001/1	2	3	1016003	0.138	138
KUT001	KUT001/1	3	4.1	1016004	0.183	183
KUT001	KUT001/2	6.1	7.1	1016005	0.115	115
KUT001	KUT001/2	7.1	8.1	1016006	0.104	104
KUT001	KUT001/2	8.1	9.1	1016007	0.093	93
KUT001	KUT001/2	9.1	9.7	1016008	0.113	113
KUT001	KUT001/2	9.7	10.3	1016009	0.494	494
KUT001	KUT001/3	11.3	12.3	1016010	0.194	194
KUT001	KUT001/3	12.3	13.3	1016012	0.163	163
KUT001	KUT001/3	13.3	14.3	1016013	0.194	194
KUT001	KUT001/3	14.3	15	1016014	0.131	131
KUT001	KUT001/3	15	17.6	1016015	0.179	179
KUT001	KUT001/4	17.6	18.6	1016017	0.234	234
KUT001	KUT001/4	18.6	19.6	1016018	0.165	165
KUT001	KUT001/4	19.6	20.6	1016019	0.132	132
KUT001	KUT001/4	20.6	21.2	1016020	0.508	508
KUT001	KUT001/4	21.2	22.3	1016021	0.127	127
KUT001	KUT001/5	22.3	22.3	1016022	0.197	197
KUT001	KUT001/5	22.3	23.3	1016023	0.501	501
KUT001	KUT001/5	23.3	24.3	1016024	0.23	230
KUT001	KUT001/5	24.3	25.3	1016025	0.15	150
KUT001	KUT001/5	25.3	26.1	1016026	0.125	125
KUT001	KUT001/5	26.1	27.9	1016027	0.135	135
KUT001	KUT001/6	27.9	28.9	1016028	0.171	171
KUT001	KUT001/6	28.9	30.9	1016029	0.121	121
KUT001	KUT001/6	30.9	31.9	1016030	0.123	123
KUT001	KUT001/6	31.9	32.8	1016031	0.092	92
KUT001	KUT001/6	32.8	34.1	1016032	0.118	118
KUT001	KUT001/7	34.1	35.1	1016033	0.21	210
KUT001	KUT001/7	35.1	36.1	1016034	0.13	130
KUT001	KUT001/7	36.1	37.1	1016035	0.294	294
KUT001	KUT001/7	37.1	38	1016036	0.147	147
KUT001	KUT001/7	38	39.3	1016037	0.107	107
KUT001	KUT001/8	39.3	40.3	1016038	0.11	110
KUT001	KUT001/8	40.3	41.3	1016039	0.144	144
KUT001	KUT001/8	41.3	42.3	1016040	0.211	211
KUT001	KUT001/8	42.3	43	1016041	0.2	200
KUT001	KUT001/8	43	44.1	1016042	0.177	177
KUT001	KUT001/9	44.1	45.1	1016044	0.166	166
KUT001	KUT001/9	45.1	46.1	1016045	0.277	277

KUT001	KUT001/9	46.1	47.1	1016046	0.189	189
KUT001	KUT001/9	47.1	47.9	1016047	0.134	134
KUT001	KUT001/9	47.9	51.7	1016048	0.236	236
KUT001	KUT001/10	51.7	52.7	1016049	0.279	279
KUT001	KUT001/10	52.7	53.7	1016050	0.182	182
KUT001	KUT001/10	53.7	54.7	1016051	0.176	176
KUT001	KUT001/10	54.7	55.3	1016052	0.35	350
KUT001	KUT001/10	55.3	55.9	1016053	0.124	124
KUT001	KUT001/11	56.9	57.9	1016055	0.264	264
KUT001	KUT001/11	57.9	58.9	1016056	0.258	258
KUT001	KUT001/11	58.9	59.9	1016057	0.351	351
KUT001	KUT001/11	59.9	59.9	1016058	0.17	170
KUT001	KUT001/11	59.9	61.9	1016059	0.138	138
KUT001	KUT001/12	61.9	62.9	1016060	0.163	163
KUT001	KUT001/12	62.9	63.9	1016061	0.137	137
KUT001	KUT001/12	63.9	64.9	1016062	0.119	119
KUT001	KUT001/12	64.9	65.5	1016063	0.097	97
KUT001	KUT001/12	65.5	67	1016064	0.084	84
KUT001	KUT001/13	67	68	1016065	0.074	74
KUT001	KUT001/13	68	69	1016066	0.082	82
KUT001	KUT001/13	69	70	1016067	0.091	91
KUT001	KUT001/13	70	70.8	1016068	0.09	90
KUT001	KUT001/13	70.8	72.6	1016069	0.085	85
KUT001	KUT001/14	72.6	73.6	1016070	0.063	63
KUT001	KUT001/14	73.6	74.6	1016071	1.805	1805
KUT001	KUT001/15	82.3	84	1016079	0.383	383
KUTR007	KUTR007/1	0	1	KUTR007000000001	0.314	314
KUTR007	KUTR007/1	1	2	KUTR007000000002	0.531	531
KUTR007	KUTR007/1	2	3	KUTR007000000003	1.84	1840
KUTR007	KUTR007/1	3	3.6	KUTR007000000004	0.247	247
KUTR007	KUTR007/1	3.6	4.3	KUTR007000000005	0.144	144
KUTR007	KUTR007/2	5.3	6.3	KUTR007000000006	0.126	126
KUTR007	KUTR007/2	6.3	7.3	KUTR007000000007	0.11	110
KUTR007	KUTR007/2	7.3	8.3	KUTR007000000008	0.093	93
KUTR007	KUTR007/2	8.3	9	KUTR007000000009	0.086	86
KUTR007	KUTR007/2	9	9.7	KUTR007000000011	0.087	87
KUTR007	KUTR007/3	11	12	KUTR007000000012	0.085	85
KUTR007	KUTR007/3	12	13	KUTR007000000013	0.073	73
KUTR007	KUTR007/3	13	14	KUTR007000000014	0.062	62
KUTR007	KUTR007/3	14	14.7	KUTR007000000015	0.06	60
KUTR007	KUTR007/3	14.7	15.2	KUTR007000000016	0.096	96
KUTR007	KUTR007/4	16	17	KUTR007000000017	0.127	127

APPENDIX THREE

KUNSU: THREE DIMENSIONAL VARIOGRAM PROGRAM
Project Title -- Kunsu Sample Variograms
Program started at 10/20/17 12:10:00
DATA SELECTION

	MINIMUM	MAXIMUM	FIELD
Attribute	0.010	1.100	4
X coord	617994.2	618956.7	1
Y coord	754775.3	755296.4	2
Z coord	-1.0	249.2	3

1XA:
DIRECTIONS IN WHICH TO COMPUTE VARIOGRAMS

AZIMUTH	ANGTOL	DIP	LAG	LAG TOL
45.00	15.00	0.00	250.00	112.50
75.00	15.00	0.00	250.00	112.50
105.00	15.00	0.00	250.00	112.50
135.00	15.00	0.00	250.00	112.50
165.00	15.00	0.00	250.00	112.50
195.00	15.00	0.00	250.00	112.50
225.00	15.00	0.00	250.00	112.50
255.00	15.00	0.00	250.00	112.50
285.00	15.00	0.00	250.00	112.50
315.00	15.00	0.00	250.00	112.50
345.00	15.00	0.00	250.00	112.50
15.00	15.00	0.00	250.00	112.50
45.00	15.00	-30.00	250.00	112.50
75.00	15.00	-30.00	250.00	112.50
105.00	15.00	-30.00	250.00	112.50
135.00	15.00	-30.00	250.00	112.50
165.00	15.00	-30.00	250.00	112.50
195.00	15.00	-30.00	250.00	112.50
225.00	15.00	-30.00	250.00	112.50
255.00	15.00	-30.00	250.00	112.50
285.00	15.00	-30.00	250.00	112.50
315.00	15.00	-30.00	250.00	112.50
345.00	15.00	-30.00	250.00	112.50
15.00	15.00	-30.00	250.00	112.50
45.00	15.00	-50.00	250.00	112.50
75.00	15.00	-50.00	250.00	112.50
105.00	15.00	-50.00	250.00	112.50
135.00	15.00	-50.00	250.00	112.50
165.00	15.00	-50.00	250.00	112.50
195.00	15.00	-50.00	250.00	112.50
225.00	15.00	-50.00	250.00	112.50
255.00	15.00	-50.00	250.00	112.50
285.00	15.00	-50.00	250.00	112.50
315.00	15.00	-50.00	250.00	112.50
345.00	15.00	-50.00	250.00	112.50
15.00	15.00	-50.00	250.00	112.50
45.00	15.00	-90.00	250.00	112.50

SAMPLE VARIOGRAMS FOR AZIMUTH 45.0 and DIP = 0.0

LAG	NPAIRS	DISTANCE	DRIFT	GCORR	MEAN HEAD	MEAN TAIL	STD. HEAD	STD. TAIL
1	708	41.8	-0.0162	0.85699	0.0654	0.0816	0.2062	0.2005
2	86060	254.2	0.0387	1.04337	0.1014	0.0627	0.2391	0.1897
3	52516	502.3	0.0358	1.02259	0.0549	0.0191	0.1494	0.0680

SAMPLE VARIOGRAMS FOR AZIMUTH 75.0 and DIP = 0.0

LAG	NPAIRS	DISTANCE	DRIFT	GCORR	MEAN HEAD	MEAN TAIL	STD. HEAD	STD. TAIL
1	1594	57.5	-0.0492	1.04845	0.0830	0.1321	0.1918	0.2757
2	102434	270.7	-0.0218	1.01632	0.0824	0.1042	0.1962	0.2504
3	151150	494.3	0.0599	1.00137	0.0985	0.0386	0.2215	0.1145
4	105720	697.9	0.0640	0.98122	0.1226	0.0586	0.2710	0.1305

SAMPLE VARIOGRAMS FOR AZIMUTH 105.0 and DIP = 0.0

LAG	NPAIRS	DISTANCE	DRIFT	GCORR	MEAN HEAD	MEAN TAIL	STD. HEAD	STD. TAIL
1	16197	76.6	-0.0323	1.02119	0.0695	0.1018	0.1668	0.2272
2	33079	279.8	-0.0146	1.02255	0.0570	0.0716	0.1511	0.1867
3	30099	492.2	0.0230	1.04671	0.0600	0.0371	0.1964	0.1147
4	5299	686.2	0.0265	1.03744	0.0502	0.0237	0.1773	0.0692

SAMPLE VARIOGRAMS FOR AZIMUTH 135.0 and DIP = 0.0

LAG	NPAIRS	DISTANCE	DRIFT	GCORR	MEAN HEAD	MEAN TAIL	STD. HEAD	STD. TAIL
1	40443	69.2	0.0227	0.93552	0.0809	0.0582	0.2163	0.1618
2	76839	227.3	-0.0046	1.05935	0.0524	0.0570	0.1529	0.1612
3	4767	418.4	-0.0091	1.03566	0.0121	0.0212	0.0083	0.0426

SAMPLE VARIOGRAMS FOR AZIMUTH 165.0 and DIP = 0.0

LAG	NPAIRS	DISTANCE	DRIFT	GCORR	MEAN HEAD	MEAN TAIL	STD. HEAD	STD. TAIL
1	2125	59.3	0.1291	1.07290	0.2116	0.0824	0.3461	0.1848
2	15593	267.1	0.1037	1.03633	0.1224	0.0187	0.3114	0.0640
3	125	393.6	0.0010	1.05365	0.0142	0.0132	0.0124	0.0074

SAMPLE VARIOGRAMS FOR AZIMUTH 195.0 and DIP = 0.0

LAG	NPAIRS	DISTANCE	DRIFT	GCORR	MEAN HEAD	MEAN TAIL	STD. HEAD	STD. TAIL
1	851	38.8	0.1591	0.70882	0.2670	0.1078	0.4105	0.2225
2	55593	245.6	0.0240	1.05001	0.0733	0.0493	0.2123	0.1508
3	399	465.1	-0.0185	1.02464	0.0114	0.0299	0.0046	0.0545

SAMPLE VARIOGRAMS FOR AZIMUTH 225.0 and DIP = 0.0

LAG	NPAIRS	DISTANCE	DRIFT	GCORR	MEAN HEAD	MEAN TAIL	STD. HEAD	STD. TAIL
1	708	41.8	0.0162	0.85699	0.0816	0.0654	0.2005	0.1424
2	86060	254.2	-0.0387	1.04337	0.0627	0.1014	0.1897	0.2391
3	52516	502.3	-0.0358	1.02259	0.0191	0.0549	0.0680	0.1494

SAMPLE VARIOGRAMS FOR AZIMUTH 255.0 and DIP = 0.0

LAG	NPAIRS	DISTANCE	DRIFT	GCORR	MEAN HEAD	MEAN TAIL	STD. HEAD	STD. TAIL
1	1594	57.5	0.0492	1.04845	0.1321	0.0830	0.2757	0.1918
2	102434	270.7	0.0218	1.01632	0.1042	0.0824	0.2504	0.1962
3	151150	494.3	-0.0599	1.00137	0.0386	0.0985	0.1145	0.2215
4	105720	697.9	-0.0640	0.98122	0.0586	0.1226	0.1305	0.2710

SAMPLE VARIOGRAMS FOR AZIMUTH 285.0 and DIP = 0.0

LAG	NPAIRS	DISTANCE	DRIFT	GCORR	MEAN HEAD	MEAN TAIL	STD. HEAD	STD. TAIL
1	16197	76.6	0.0323	1.02119	0.1018	0.0695	0.2272	0.1668
2	33079	279.8	0.0146	1.02255	0.0716	0.0570	0.1867	0.1511
3	30099	492.2	-0.0230	1.04671	0.0371	0.0600	0.1147	0.1964
4	5299	686.2	-0.0265	1.03744	0.0237	0.0502	0.0692	0.1773

SAMPLE VARIOGRAMS FOR AZIMUTH 315.0 and DIP = 0.0

LAG	NPAIRS	DISTANCE	DRIFT	GCORR	MEAN HEAD	MEAN TAIL	STD. HEAD	STD. TAIL
1	40443	69.2	-0.0227	0.93552	0.0582	0.0809	0.1618	0.2163
2	76839	227.3	0.0046	1.05935	0.0570	0.0524	0.1612	0.1529
3	4767	418.4	0.0091	1.03566	0.0212	0.0121	0.0426	0.0083

SAMPLE VARIOGRAMS FOR AZIMUTH 345.0 and DIP = 0.0

LAG	NPAIRS	DISTANCE	DRIFT	GCORR	MEAN HEAD	MEAN TAIL	STD. HEAD	STD. TAIL
1	2125	59.3	-0.1291	1.07290	0.0824	0.2116	0.1848	0.3461
2	15593	267.1	-0.1037	1.03633	0.0187	0.1224	0.0640	0.3114
3	125	393.6	-0.0010	1.05365	0.0132	0.0142	0.0074	0.0124

SAMPLE VARIOGRAMS FOR AZIMUTH 15.0 and DIP = 0.0

LAG	NPAIRS	DISTANCE	DRIFT	GCORR	MEAN HEAD	MEAN TAIL	STD. HEAD	STD. TAIL
1	851	38.8	-0.1591	0.70882	0.1078	0.2670	0.2225	0.4105
2	55593	245.6	-0.0240	1.05001	0.0493	0.0733	0.1508	0.2123
3	399	465.1	0.0185	1.02464	0.0299	0.0114	0.0545	0.0046

SAMPLE VARIOGRAMS FOR AZIMUTH 45.0 and DIP = -30.0

LAG	NPAIRS	DISTANCE	DRIFT	GCORR	MEAN HEAD	MEAN TAIL	STD. HEAD	STD. TAIL
1	1185	46.9	0.0088	0.92851	0.0886	0.0798	0.1849	0.1881
2	25285	207.1	-0.1378	1.10135	0.0473	0.1851	0.1387	0.3503
3	6175	495.6	-0.0029	0.98632	0.0100	0.0129	0.0001	0.0094

SAMPLE VARIOGRAMS FOR AZIMUTH 75.0 and DIP = -30.0

LAG	NPAIRS	DISTANCE	DRIFT	GCORR	MEAN HEAD	MEAN TAIL	STD. HEAD	STD. TAIL
1	1017	60.4	-0.0134	1.01091	0.0953	0.1087	0.2094	0.2242
2	43161	249.0	-0.1065	1.07119	0.0502	0.1567	0.1661	0.3206
3	4561	486.2	0.1005	0.98355	0.1293	0.0288	0.3058	0.1064

SAMPLE VARIOGRAMS FOR AZIMUTH 105.0 and DIP = -30.0

LAG	NPAIRS	DISTANCE	DRIFT	GCORR	MEAN HEAD	MEAN TAIL	STD. HEAD	STD. TAIL
1	7974	69.1	-0.0441	0.75825	0.0985	0.1426	0.2476	0.2909
2	22499	272.6	-0.0425	1.02740	0.0525	0.0950	0.1803	0.2412
3	2113	421.3	-0.0323	1.02464	0.0107	0.0431	0.0071	0.1361

SAMPLE VARIOGRAMS FOR AZIMUTH 135.0 and DIP = -30.0

LAG	NPAIRS	DISTANCE	DRIFT	GCORR	MEAN HEAD	MEAN TAIL	STD. HEAD	STD. TAIL
1	18507	75.4	0.0147	0.94751	0.1178	0.1032	0.2791	0.2214
2	42053	225.3	0.1612	0.86272	0.2198	0.0587	0.4054	0.1673
3	981	412.3	0.0002	0.10055	0.0102	0.0100	0.0011	0.0000

SAMPLE VARIOGRAMS FOR AZIMUTH 165.0 and DIP = -30.0

LAG	NPAIRS	DISTANCE	DRIFT	GCORR	MEAN HEAD	MEAN TAIL	STD. HEAD	STD. TAIL
1	3716	61.6	0.0415	1.04046	0.1319	0.0904	0.2799	0.1943
2	1875	280.6	0.5633	0.99907	0.5755	0.0122	0.4878	0.0101

SAMPLE VARIOGRAMS FOR AZIMUTH 195.0 and DIP = -30.0

LAG	NPAIRS	DISTANCE	DRIFT	GCORR	MEAN HEAD	MEAN TAIL	STD. HEAD	STD. TAIL
1	1687	51.9	0.0217	0.95815	0.0930	0.0713	0.2451	0.1379
2	8660	246.4	0.1816	0.98803	0.2491	0.0675	0.4107	0.1697
3	95	391.7	-0.0913	0.97823	0.0105	0.1018	0.0015	0.0834

SAMPLE VARIOGRAMS FOR AZIMUTH 225.0 and DIP = -30.0

LAG	NPAIRS	DISTANCE	DRIFT	GCORR	MEAN HEAD	MEAN TAIL	STD. HEAD	STD. TAIL
1	1528	61.5	0.0698	0.90427	0.1071	0.0373	0.2664	0.0832
2	11374	239.1	0.2784	0.88214	0.3453	0.0669	0.4578	0.1754

SAMPLE VARIOGRAMS FOR AZIMUTH 255.0 and DIP = -30.0

LAG	NPAIRS	DISTANCE	DRIFT	GCORR	MEAN HEAD	MEAN TAIL	STD. HEAD	STD. TAIL
1	3305	63.8	0.0275	0.91074	0.0875	0.0600	0.2226	0.1378
2	7941	224.0	0.0855	1.10134	0.1651	0.0796	0.3306	0.1900
3	55	401.2	0.0479	1.04834	0.0632	0.0153	0.1583	0.0364

SAMPLE VARIOGRAMS FOR AZIMUTH 285.0 and DIP = -30.0

LAG	NPAIRS	DISTANCE	DRIFT	GCORR	MEAN HEAD	MEAN TAIL	STD. HEAD	STD. TAIL
1	14007	72.5	0.0131	1.05778	0.0982	0.0851	0.2315	0.1966
2	8065	186.2	0.0537	1.04431	0.0888	0.0352	0.2431	0.1214

SAMPLE VARIOGRAMS FOR AZIMUTH 315.0 and DIP = -30.0

LAG	NPAIRS	DISTANCE	DRIFT	GCORR	MEAN HEAD	MEAN TAIL	STD. HEAD	STD. TAIL
1	8254	75.0	-0.0349	1.00750	0.0730	0.1079	0.1839	0.2627
2	12255	191.2	0.0109	1.05847	0.0475	0.0366	0.1391	0.1138

SAMPLE VARIOGRAMS FOR AZIMUTH 345.0 and DIP = -30.0

LAG	NPAIRS	DISTANCE	DRIFT	GCORR	MEAN HEAD	MEAN TAIL	STD. HEAD	STD. TAIL
1	1865	62.0	-0.1934	0.99358	0.0706	0.2640	0.1504	0.3726
2	5201	265.4	0.0229	1.01242	0.0347	0.0118	0.1162	0.0078

SAMPLE VARIOGRAMS FOR AZIMUTH 15.0 and DIP = -30.0

LAG	NPAIRS	DISTANCE	DRIFT	GCORR	MEAN HEAD	MEAN TAIL	STD. HEAD	STD. TAIL
1	680	45.6	-0.1284	0.94202	0.1114	0.2398	0.2528	0.3640
2	14519	198.3	-0.0803	1.09438	0.0380	0.1183	0.1072	0.2679

SAMPLE VARIOGRAMS FOR AZIMUTH 45.0 and DIP = -50.0

LAG	NPAIRS	DISTANCE	DRIFT	GCORR	MEAN HEAD	MEAN TAIL	STD. HEAD	STD. TAIL
1	1023	52.5	-0.0333	0.86680	0.1109	0.1442	0.2453	0.2610
2	13494	229.5	-0.1792	1.03812	0.0104	0.1896	0.0049	0.3513

SAMPLE VARIOGRAMS FOR AZIMUTH 75.0 and DIP = -50.0

LAG	NPAIRS	DISTANCE	DRIFT	GCORR	MEAN HEAD	MEAN TAIL	STD. HEAD	STD. TAIL
1	3159	73.3	-0.0248	0.94222	0.0781	0.1029	0.1746	0.2075
2	20109	255.6	-0.1734	1.00122	0.0100	0.1834	0.0002	0.3426

SAMPLE VARIOGRAMS FOR AZIMUTH 105.0 and DIP = -50.0

LAG	NPAIRS	DISTANCE	DRIFT	GCORR	MEAN HEAD	MEAN TAIL	STD. HEAD	STD. TAIL
1	7658	78.8	0.0534	0.87359	0.1743	0.1208	0.3432	0.2449
2	7964	236.7	-0.0731	0.94712	0.0642	0.1373	0.2016	0.2806

SAMPLE VARIOGRAMS FOR AZIMUTH 135.0 and DIP = -50.0

LAG	NPAIRS	DISTANCE	DRIFT	GCORR	MEAN HEAD	MEAN TAIL	STD. HEAD	STD. TAIL
1	30846	51.7	0.0263	0.88053	0.1052	0.0789	0.2656	0.1893
2	23699	214.1	0.0559	0.79157	0.1339	0.0780	0.3241	0.1774

SAMPLE VARIOGRAMS FOR AZIMUTH 165.0 and DIP = -50.0

LAG	NPAIRS	DISTANCE	DRIFT	GCORR	MEAN HEAD	MEAN TAIL	STD. HEAD	STD. TAIL
1	12543	51.3	0.0276	0.78545	0.1163	0.0887	0.2622	0.1883
2	4659	212.7	-0.0699	1.02232	0.0102	0.0802	0.0053	0.1344

SAMPLE VARIOGRAMS FOR AZIMUTH 195.0 and DIP = -50.0

LAG	NPAIRS	DISTANCE	DRIFT	GCORR	MEAN HEAD	MEAN TAIL	STD. HEAD	STD. TAIL
1	3067	60.3	0.0292	0.72848	0.1044	0.0752	0.2623	0.1735
2	76	238.9	0.0533	0.99930	0.0633	0.0100	0.0684	0.0000

SAMPLE VARIOGRAMS FOR AZIMUTH 225.0 and DIP = -50.0

LAG	NPAIRS	DISTANCE	DRIFT	GCORR	MEAN HEAD	MEAN TAIL	STD. HEAD	STD. TAIL
1	3446	63.3	0.0748	0.92305	0.1407	0.0659	0.3121	0.1509
2	206	220.9	0.0148	1.01080	0.1112	0.0964	0.2438	0.2380

SAMPLE VARIOGRAMS FOR AZIMUTH 255.0 and DIP = -50.0

LAG	NPAIRS	DISTANCE	DRIFT	GCORR	MEAN HEAD	MEAN TAIL	STD. HEAD	STD. TAIL
1	6240	58.5	0.0512	1.03370	0.1324	0.0812	0.2871	0.1872
2	158	146.8	0.0063	0.64144	0.0201	0.0137	0.0186	0.0097

SAMPLE VARIOGRAMS FOR AZIMUTH 285.0 and DIP = -50.0

LAG	NPAIRS	DISTANCE	DRIFT	GCORR	MEAN HEAD	MEAN TAIL	STD. HEAD	STD. TAIL
1	10689	68.8	0.0193	1.05709	0.1003	0.0810	0.2367	0.1952
2	7081	183.4	0.1145	1.08500	0.1492	0.0346	0.3424	0.1047

SAMPLE VARIOGRAMS FOR AZIMUTH 315.0 and DIP = -50.0

LAG	NPAIRS	DISTANCE	DRIFT	GCORR	MEAN HEAD	MEAN TAIL	STD. HEAD	STD. TAIL
1	10379	55.9	0.0154	1.00466	0.0858	0.0703	0.2163	0.1879
2	8043	179.2	0.0643	1.07785	0.1015	0.0372	0.2748	0.1063

SAMPLE VARIOGRAMS FOR AZIMUTH 345.0 and DIP = -50.0

LAG	NPAIRS	DISTANCE	DRIFT	GCORR	MEAN HEAD	MEAN TAIL	STD. HEAD	STD. TAIL
1	5695	60.6	-0.0629	1.04837	0.0891	0.1521	0.2098	0.2920
2	1160	265.6	-0.0020	0.13890	0.0100	0.0120	0.0000	0.0086

SAMPLE VARIOGRAMS FOR AZIMUTH 15.0 and DIP = -50.0

LAG	NPAIRS	DISTANCE	DRIFT	GCORR	MEAN HEAD	MEAN TAIL	STD. HEAD	STD. TAIL
1	1461	67.0	-0.1845	1.06115	0.0949	0.2794	0.2197	0.3792
2	4129	235.7	-0.0059	1.00607	0.0105	0.0164	0.0058	0.0409

SAMPLE VARIOGRAMS FOR AZIMUTH 45.0 and DIP = -90.0

LAG	NPAIRS	DISTANCE	DRIFT	GCORR	MEAN HEAD	MEAN TAIL	STD. HEAD	STD. TAIL
1	14566	49.4	0.0635	0.80436	0.1657	0.1022	0.3358	0.2406
2	10913	169.9	-0.0653	1.04378	0.0305	0.0959	0.1269	0.1755

Appendix four

Directional Sample variograms

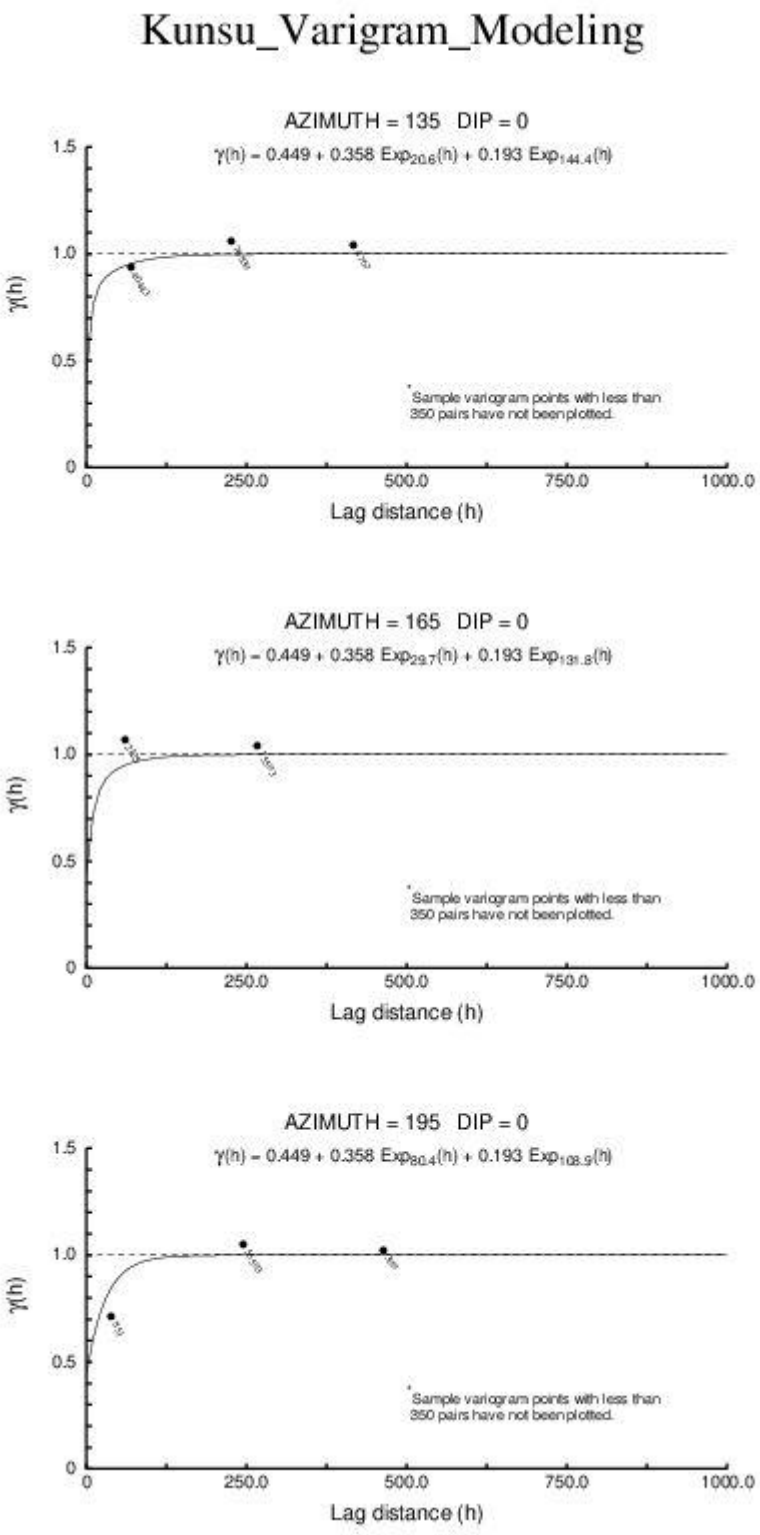

Kunsu_Varigram_Modeling

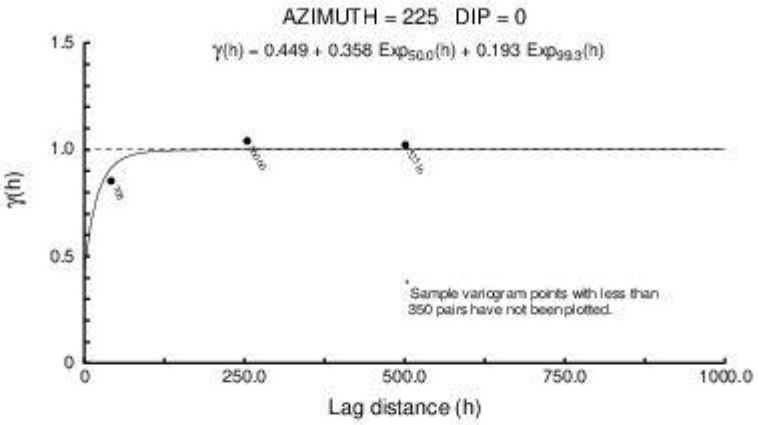

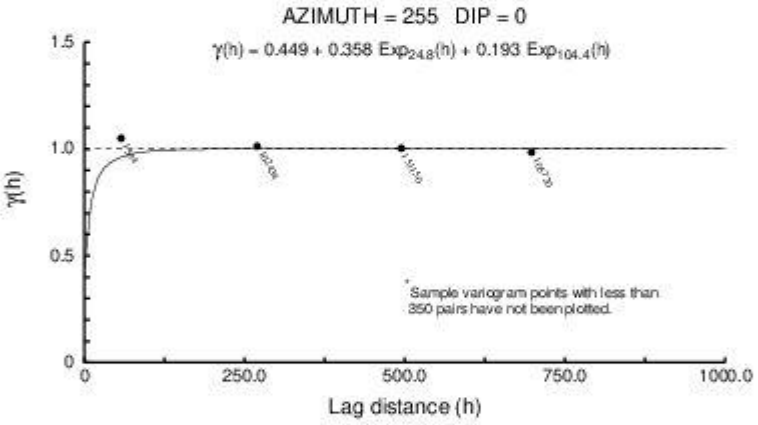

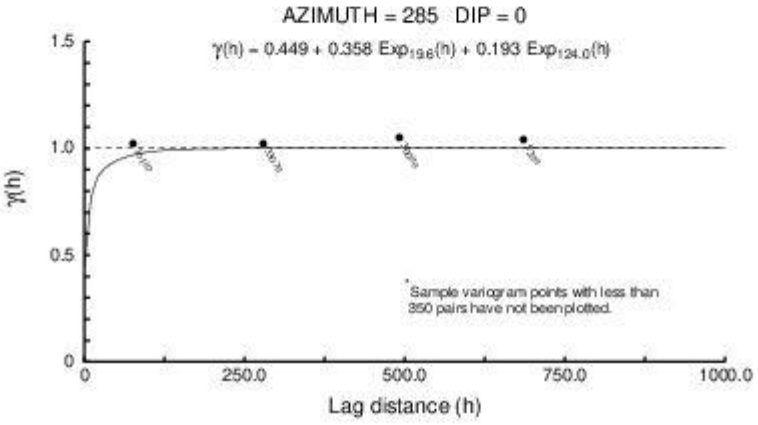

Kunsu_Varigram_Modeling

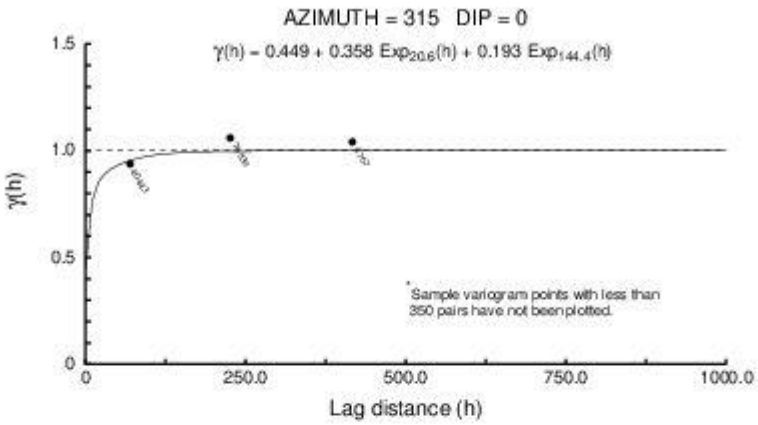

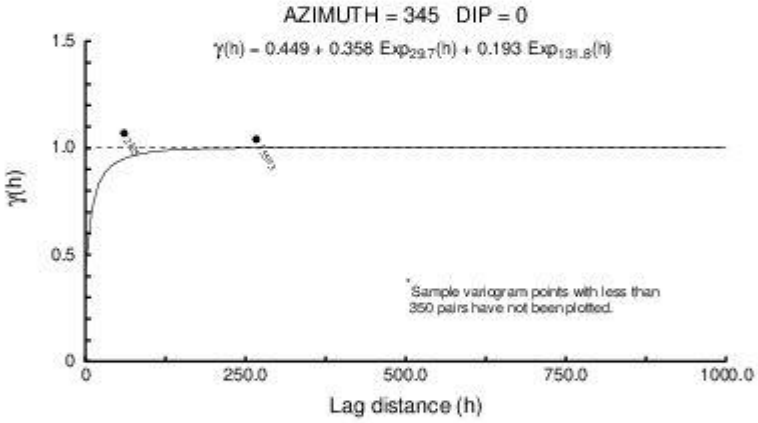

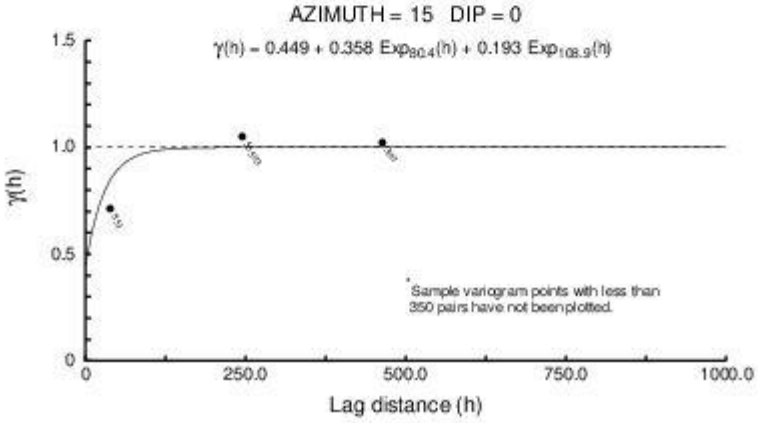

Kunsu_Varigram_Modeling

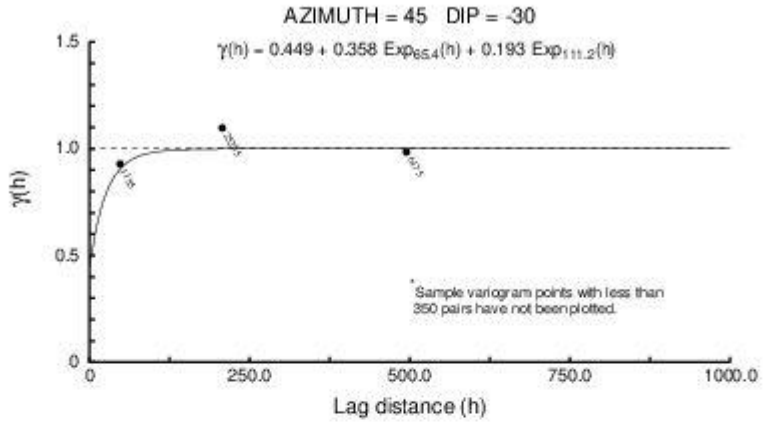

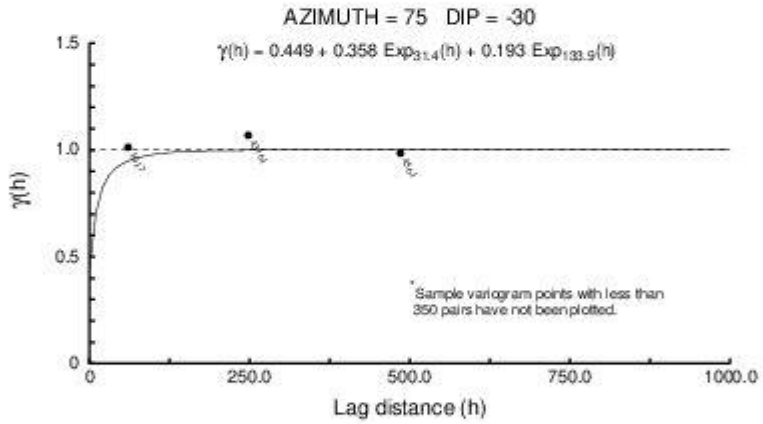

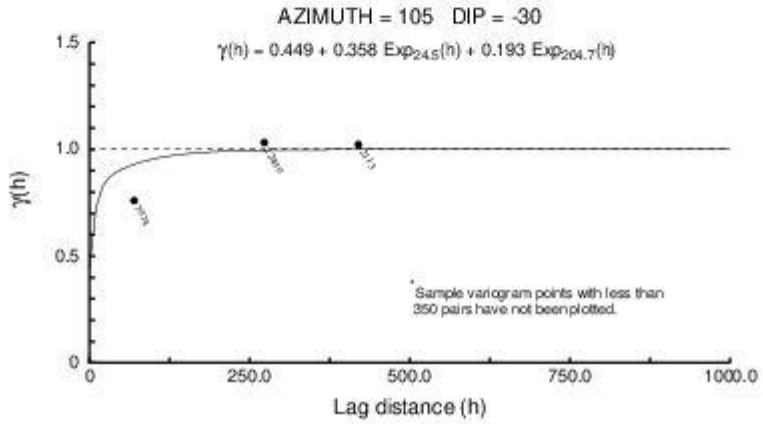

Kunsu_Varigram_Modeling

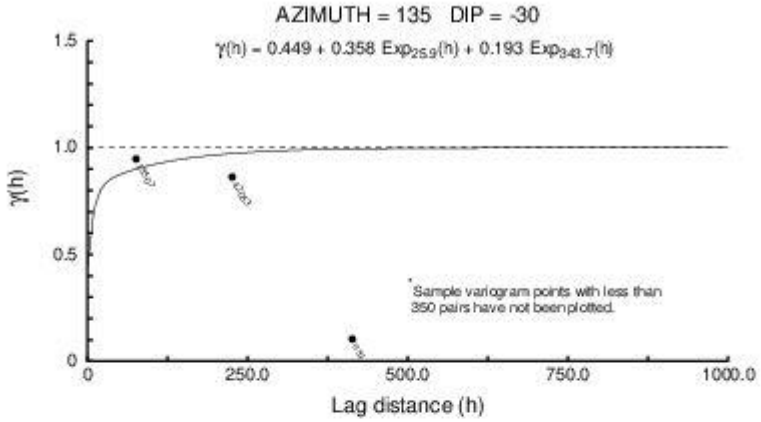

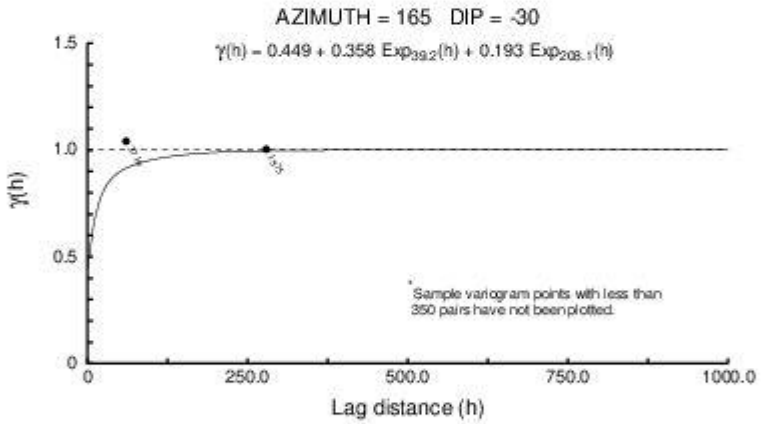

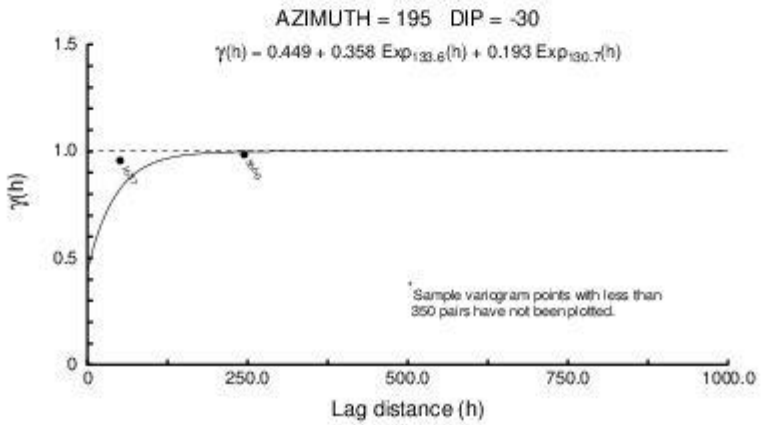

Kunsu_Varigram_Modeling

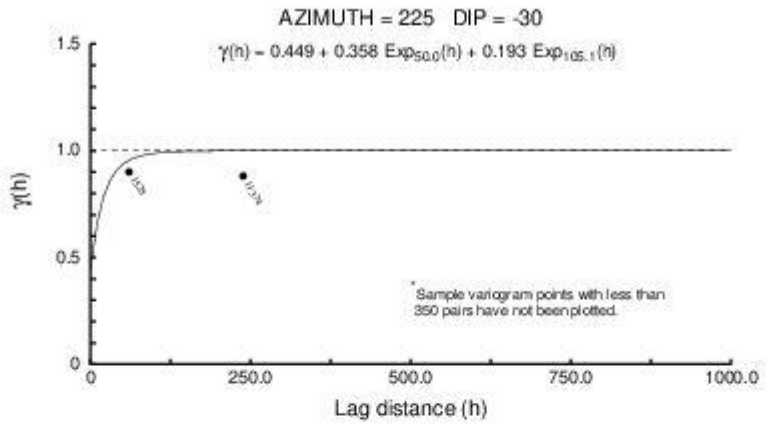

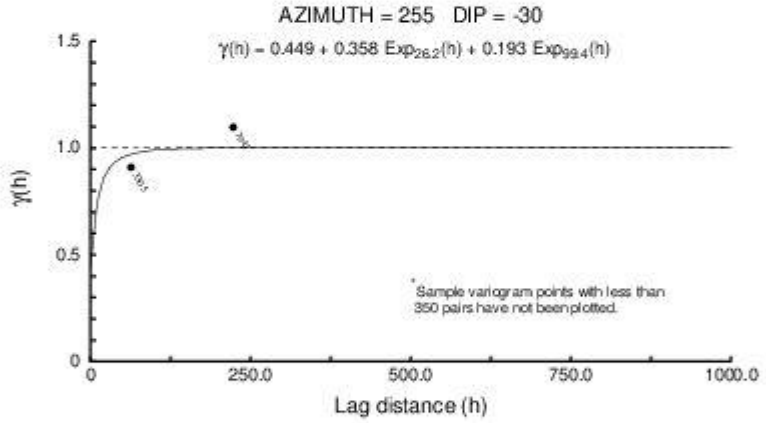

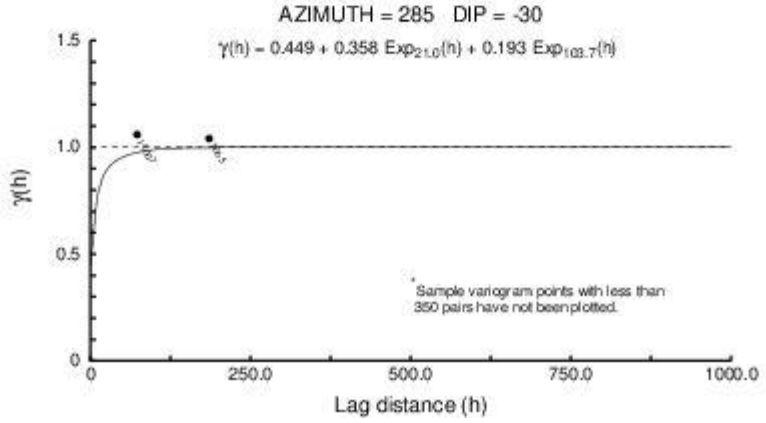

Kunsu_Varigram_Modeling

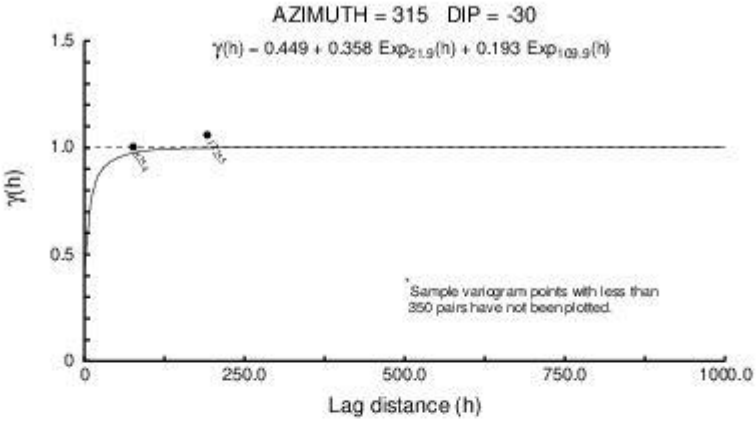

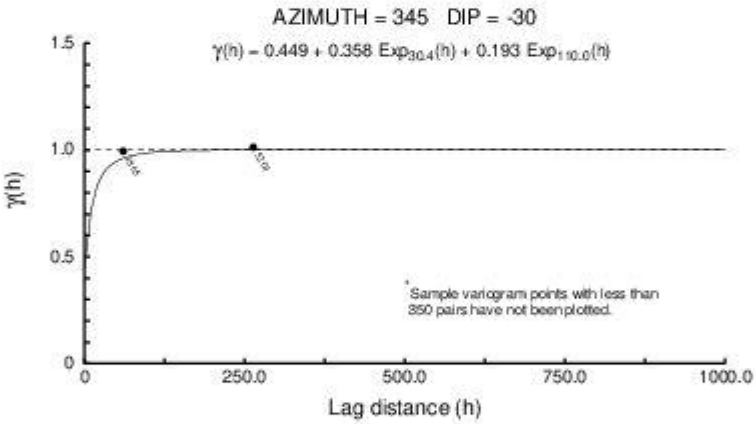

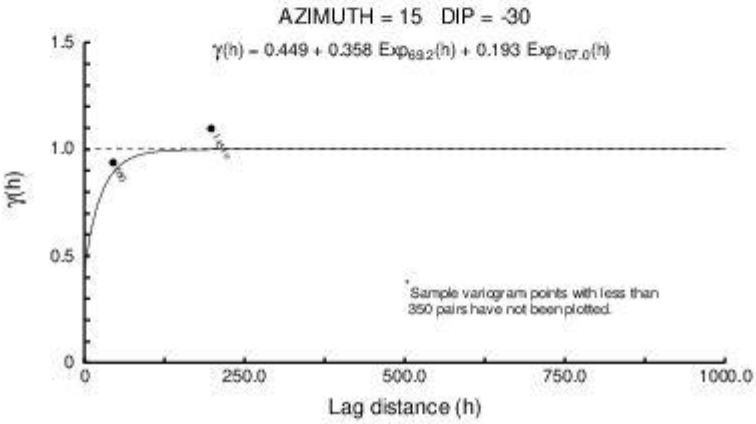

Kunsu_Varigram_Modeling

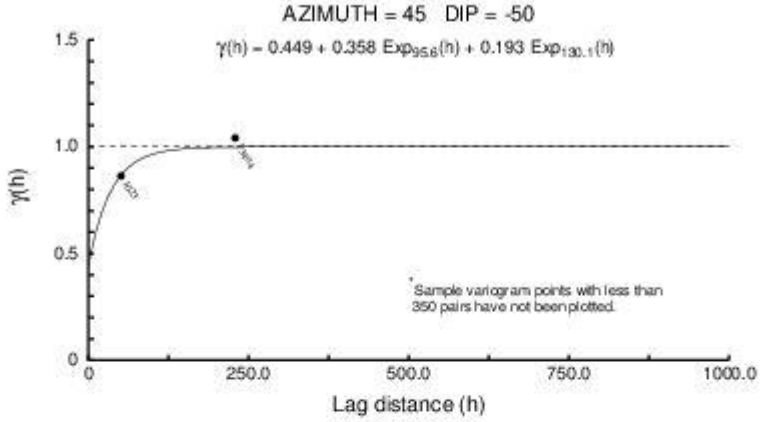

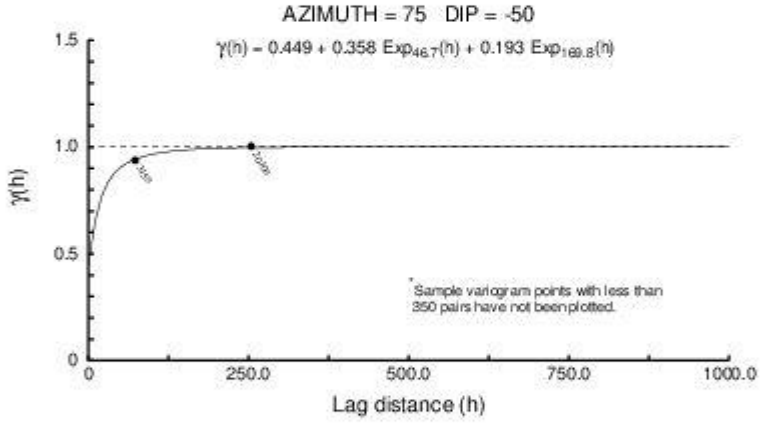

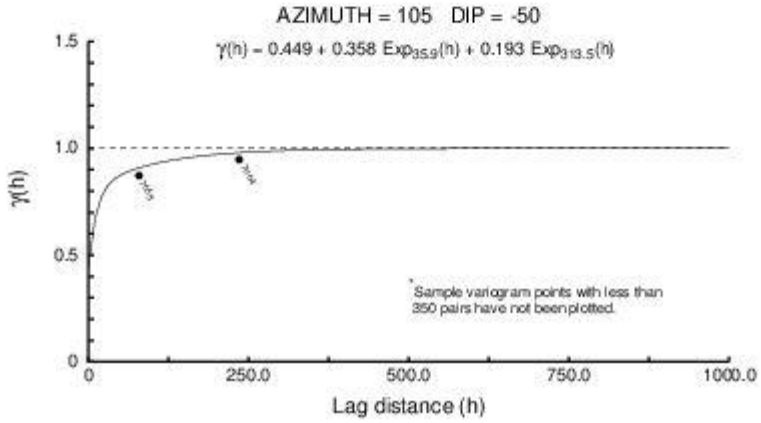

Kunsu_Varigram_Modeling

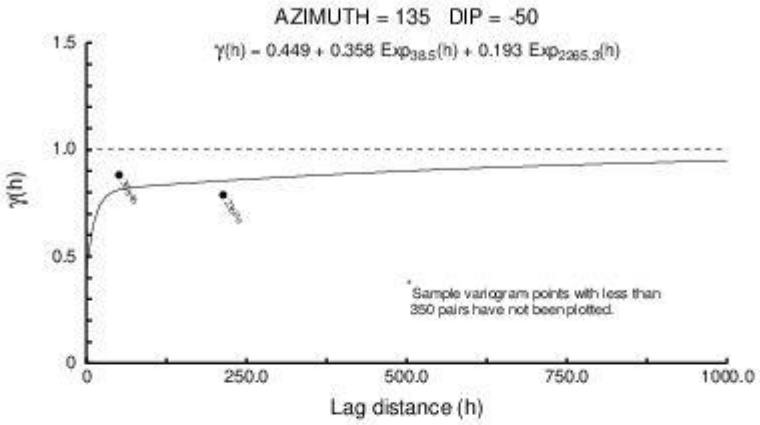

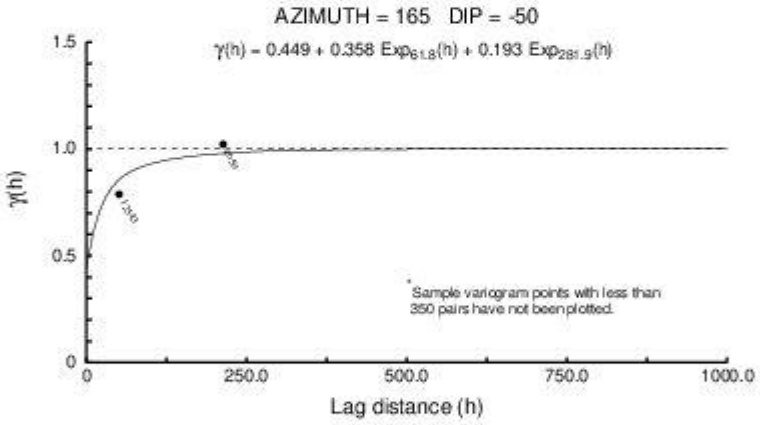

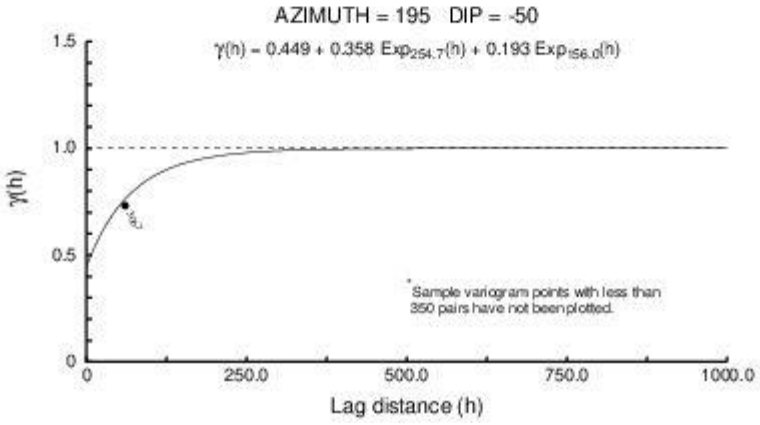

Kunsu_Varigram_Modeling

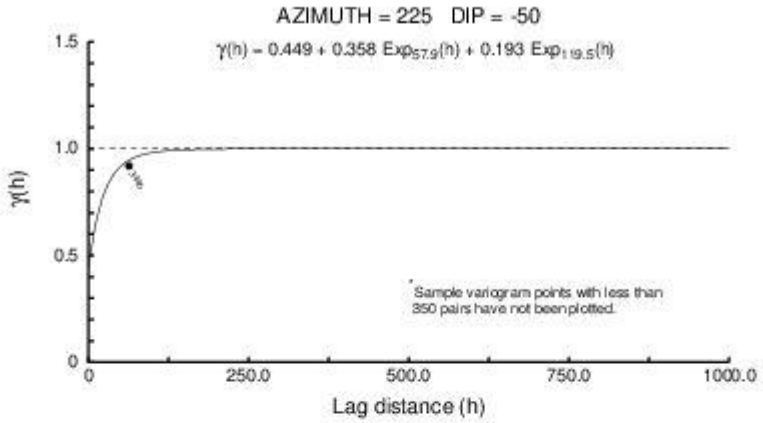

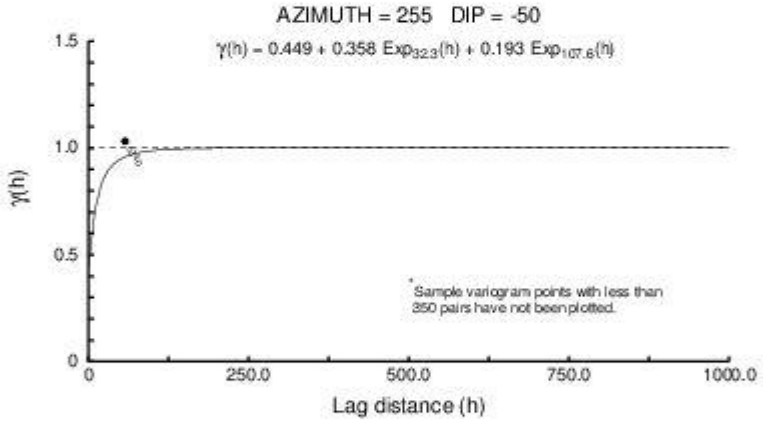

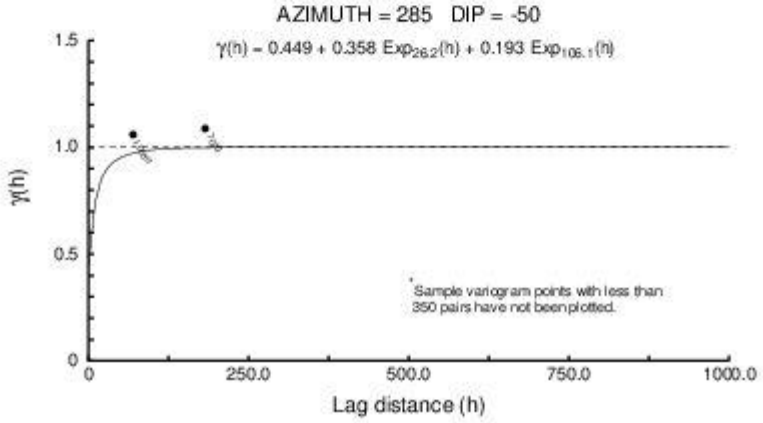

Kunsu_Varigram_Modeling

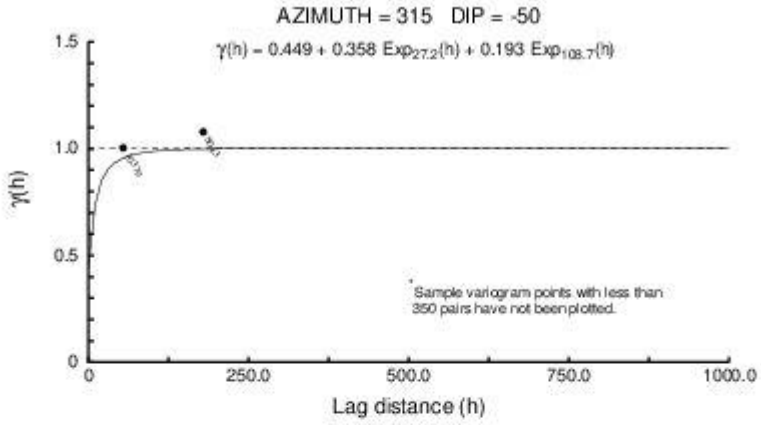

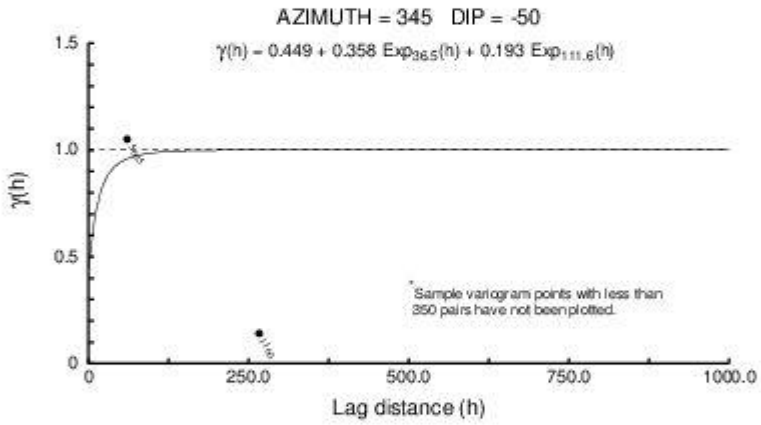

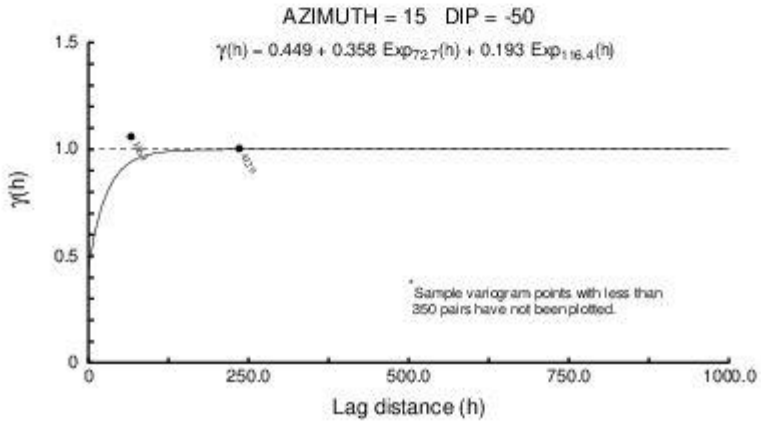

Kunsu_Varigram_Modeling

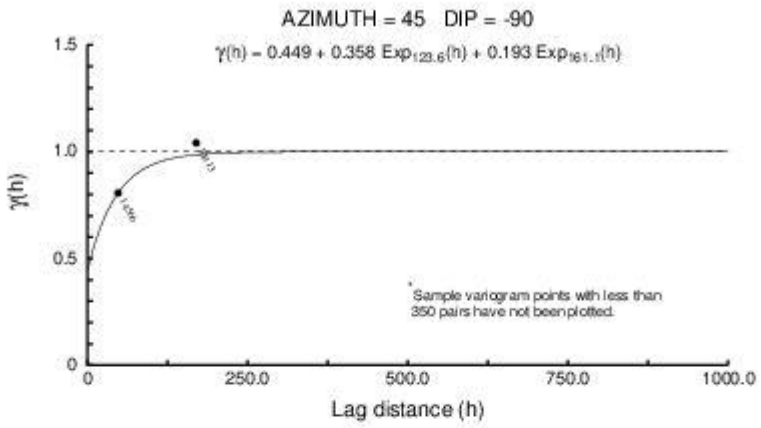

Co.

APPENDIX FIVE

ELLIPSOID PRESENTATION

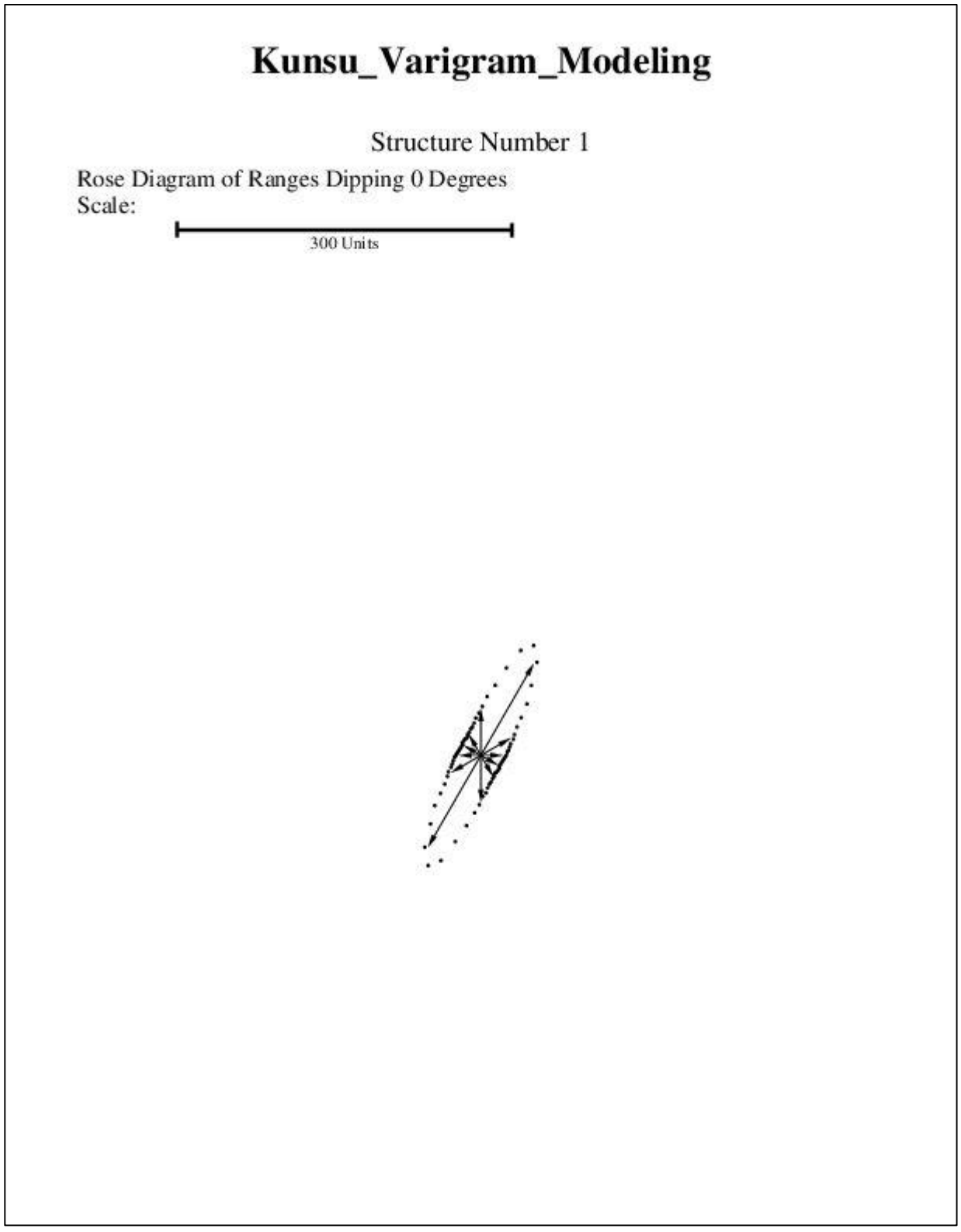

Horizontal Slices Through the Ellipsoids

Reference Cube

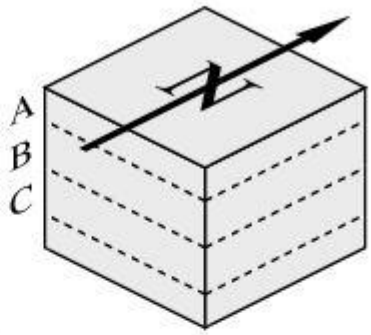

X-Y Planes Looking Down

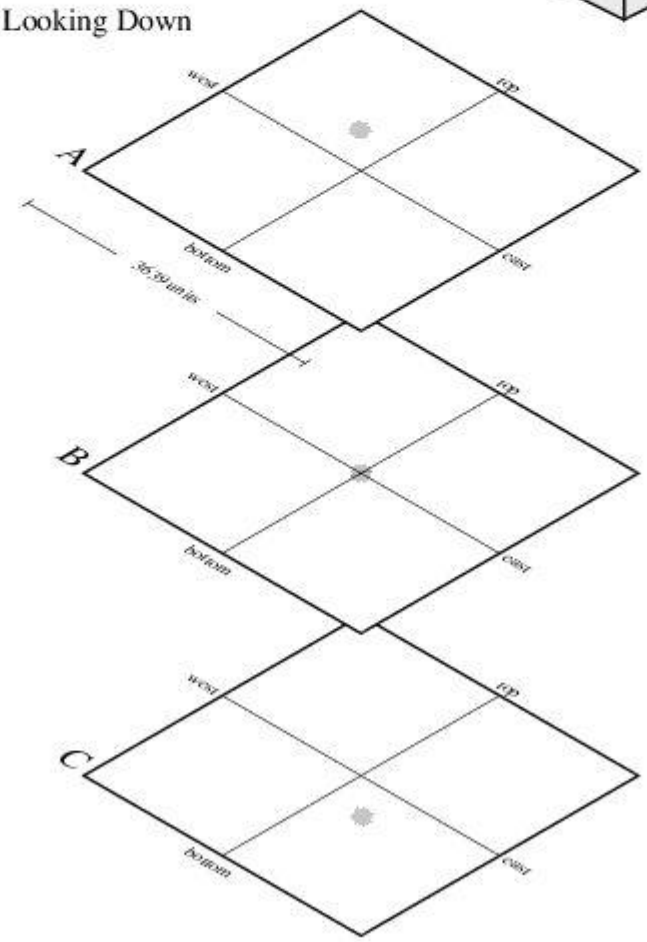

Note -- the orientation, dip and lengths of the ellipsoid axes in these figures may be "apparent" rather than "true".

Long Section Views Through the Ellipsoids

Reference Cube

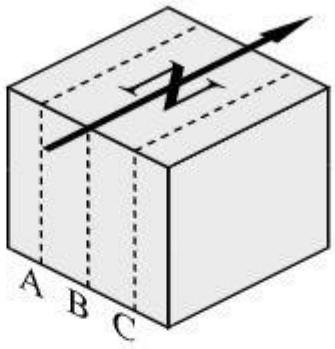

Y-Z Planes Looking West

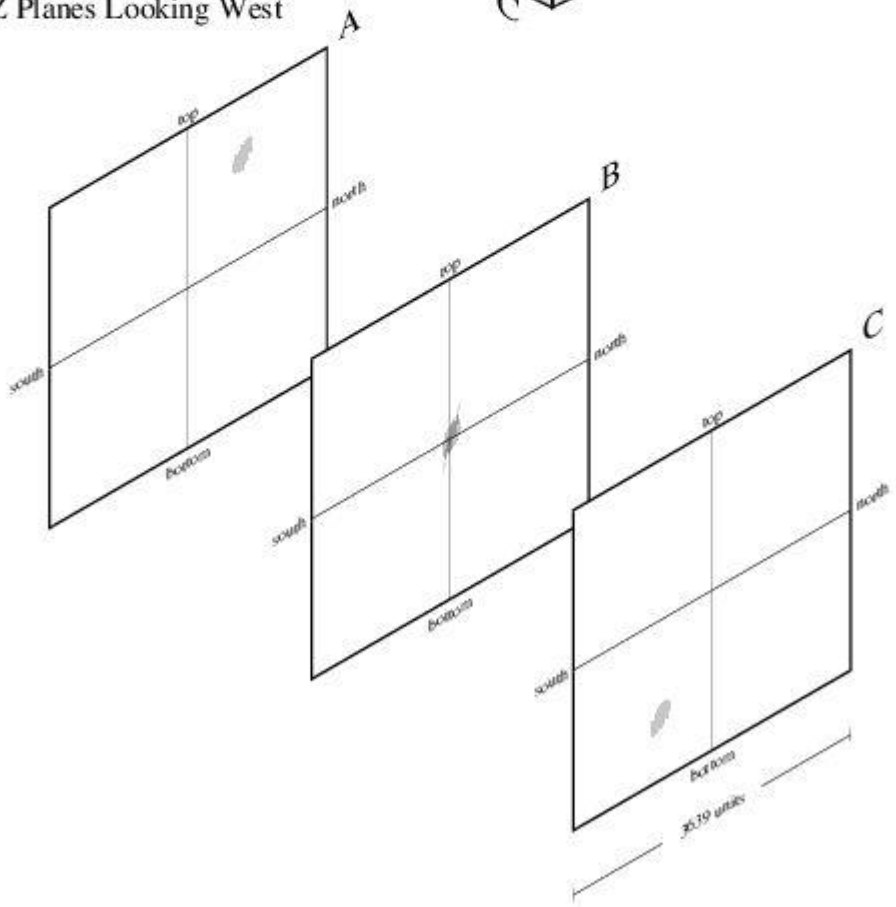

Note -- the orientation, dip and lengths of the ellipsoid axes in these figures may be "apparent" rather than "true".

Cross Section Views Through the Ellipsoids

Reference Cube

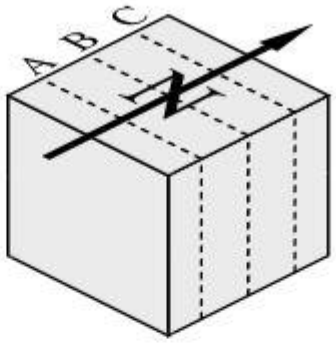

X-Z Planes Looking North

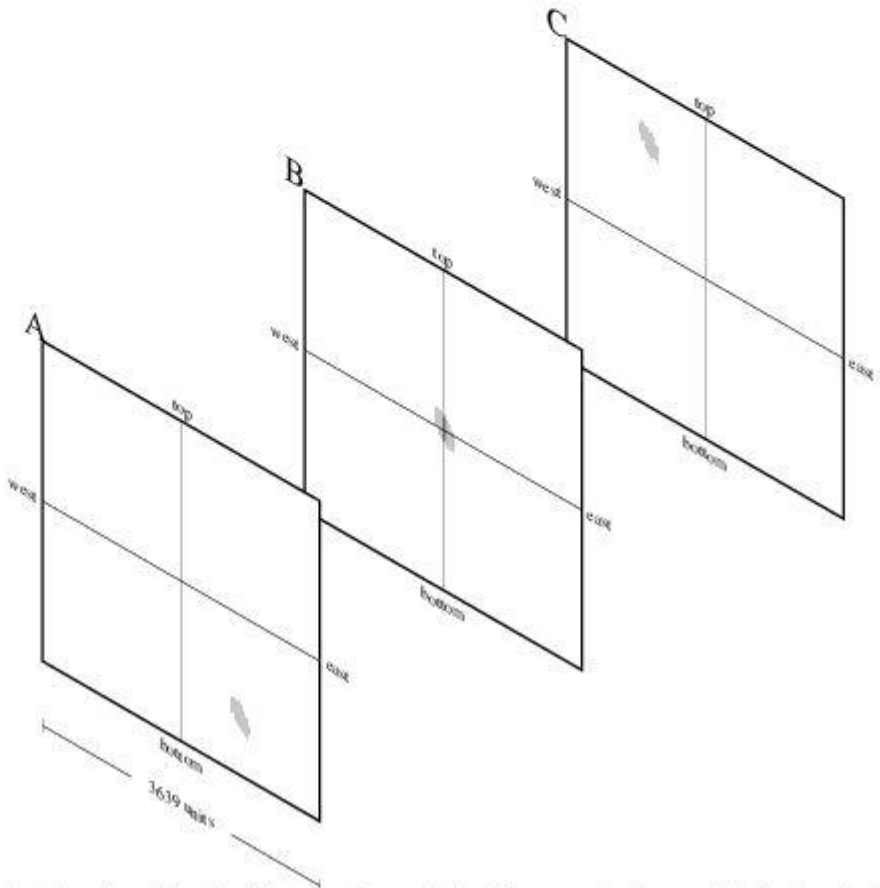

Note -- the orientation, dip and lengths of the ellipsoid axes in these figures may be "apparent" rather than "true".